THE UNIVERSITY OF CALGARY

Corrosion Generated Hydrogen Flux Measurements Using A Vacuum Gradient

by

Dinu Gheorghe Matei

A THESIS
SUBMITTED TO THE FACULTY OF GRADUATE STUDIES
IN PARTIAL FULFILLMENT OF THE REQUIREMENTS FOR THE
DEGREE OF MASTER OF SCIENCE
IN MECHANICAL ENGINEERING

DEPARTMENT OF MECHANICAL AND MANUFACTURING ENGINEERING

CALGARY, ALBERTA

JUNE, 1999

ABSTRACT

The purpose of this investigation is establishing the limits under which hydrogen flux measurements will work in some corrosive environments using the Hydrogen Vacuum Foil technique. It relies in capturing the hydrogen atoms that permeate through a steel specimen into a vacuum chamber where they recombine into pairs to form molecular hydrogen. The vacuum decay is proportional to the amount of hydrogen that permeates through the specimen.

Hydrogen permeation measurements are important because corrosion often generates hydrogen which leads to embrittlement causing delayed fracture in steel components.

Suitable for qualitative and quantitative analysis of hydrogen flux this technique should be used in deaerated conditions only. It has relatively short response times to changing corrosion conditions. Measurements are directly affected by the film formation. The hydrogen pick-up rate and permeation are a function of the environment, presence of poisons, and the material. For quantitative analysis the equipment needs to be calibrated.

This work describes the initial scientific investigation using this new technique and correlates the vacuum induced hydrogen flux measurements with electrochemical hydrogen flux measurements.

ACKNOWLEDGMENTS

I would like to thank Prof. W. J. D. Shaw for giving me the opportunity to work under his direct supervision on such an interesting research program. Thank you Dr. Shaw for letting me steal something from your experience, for finding the time to answer all my questions and uncertainties, for encouraging me throughout the whole program.

The generous financial support received from the NSERC during this program is very much appreciated and made this work possible. Thanks go also to the ASM International "Calgary Chapter" for the award I was offered in 1998.

Special thanks go to Maureen Fraser and Lynn Banach from the Department of Mechanical Engineering for taking care and helping me in solving all the administrative problems I was confronted with during my stay at The University of Calgary. The help received from Connie Busch and Jessie McColley from the Faculty of Graduate Studies is also very much appreciated.

Many thanks go to the members of staff and technicians from the Department of Mechanical Engineering for their support and kindness. Especially, I would like to thank Tracy Leblanc, Art Moehrle, Greg East, Brandon Fergusson and Dan Forre. Many thanks also go to Rob Scorey from the machine shop.

The foils and the datalogger were supplied by Corrosion Detection Systems, a Division of Diversity Corporation.

Least but not last, the unconditional support and understanding received from my wife, Anca, contributed to the finalization of this work. Thank you Anca!

DEDICATION

This work is entirely dedicated to the memory of my beloved Father, Prof. Dr. Ing. Gheorghe Matei (1934-1999) from the Department of Materials Science and Technology from The Technical University of Cluj-Napoca, Romania.

You first introduced me to this fascinating world of materials science, you helped me, you supported me, you understood me, you encouraged me, you believed in me throughout the years. You shared with me and offered me from the vast experience you accumulated during your life and you have always been with me when I needed you. I am extremely proud to be your son. Thank you, thank you Dad for everything you have done for me. God rest you in peace.

TABLE OF CONTENTS

LIST OF FIGURES

LIST OF TABLES

NOMENCLATURE

1-D- one-dimensional diffusion

3-D- three-dimensional diffusion

θ- steady-state surface hydrogen coverage

C- hydrogen concentration in the material, [mol/cm^3]

C_0- concentration of hydrogen dissolved in the metal at the surface, [mol/cm^3]

D- hydrogen diffusion coefficient in the material, [cm^2/sec]

E_c- applied cathodic potential, [V]

E_{corr}- corrosion potential, [V]

E_D- activation energy for diffusion, [kcal/mol]

E_p- activation energy for permeation, [kcal/mol]

F = 96,480 C/mol- Faraday's constant

ΔH- enthalpy, [J/mol]

H_{ads}- hydrogen adsorbed on the steel's surface.

H_{abs}- hydrogen absorbed within the bulk of the steel.

H_a'- hydrogen adsorbed on the surface

H_{ch}- hydrogen bound in chemical compounds

H_d- hydrogen fixed on dislocations

H_m- molecular hydrogen in the pores

H_s- hydrogen in the solid solution

H_v- hydrogen bound to vacancies

HA- hydrogen attack

HAR- hydrogen absorption reaction

HE- hydrogen embrittlement

HER- hydrogen evolution reaction

HIC- hydrogen-induced cracking

i_c- applied cathodic current, [μA]

i_{corr}- steady-state corrosion current, [μA]

I_∞- steady-state hydrogen permeation current density, [$\mu A/cm^2$]

J_∞- steady-state hydrogen permeation flux, [molH/m^2sec]

J- hydrogen permeation flux, [molH/m^2sec]

k- ratio of the rate constants for adsorption and desorption (k_{abs}/k_{des}).

k_{abs}- specific rate constant for adsorption process.

k_{des}- specific rate constant for desorption process.

k_d- rate constant for desorption from the precursor to the gas phase

k'- rate constant for adsorption from the precursor to the dissociated state

k"- rate constant for desorption from the dissociated state to the molecular state

$k_a p_{H2}$- rate of hydrogen adsorption from the gas phase

L- specimen thickness, [cm]

LEO- Low Earth Orbit

mpy- mills per year

n- number of fragments formed upon adsorption

NACE- National Association of Corrosion Engineers

p_{H2}- hydrogen gas pressure, [Pa]

p_0- temperature independent factor for permeability

p_r- permeability, permeation rate, [molH/cm^2]

R = 8.314 J/molK- universal gas constant

SCC- stress corrosion cracking

SCE- saturated calomel electrode

SOHIC- stress-oriented hydrogen-induced cracking

SSC- sulfide-stress cracking

t- time, [h]

T- absolute temperature, [^{0}K]

x- distance into the specimen, [cm]

z- number of electrons transferred

CHAPTER 1

INTRODUCTION

1.1. General Background

In every material used from deep space to deep sea, hydrogen presents a problem. Like high blood pressure [1] the problem exists and one may not be aware of it until it is too late! Just like blood pressure, the situation can be worsened by stress, residual and/or applied. The higher the stress, the less hydrogen required to make conditions critical. Hydrogen degradation of structural materials is a very serious problem that has received increasing attention for the past years. Researchers from disciplines ranging from thermodynamics, materials science, and fracture mechanics were and are involved in finding the explanation and the solution to the problem that is hydrogen degradation of materials.

Hydrogen has a bad influence on the properties of all metals: it reduces their ductility, without exception. Metals often come into contact with hydrogen gas or hydrogen-producing environments. Once hydrogen has entered the material it leads to problems at temperatures near room temperature, at which hydrogen embrittlement, HE, is observed, as well as at elevated temperatures, at which hydrogen attack, HA, can occur.

Hydrogen reacts to a certain extent with almost all metals and alloys and it is well established that hydrogen induces or promotes intergranular cracking in many metallic materials. Obviously, for intergranular cracking to occur, hydrogen has to arrive at the interior grain boundaries by diffusion through the lattice, grain boundaries, dislocation networks, or by dislocation transport as dislocation core atmospheres [2-7].

Hydrogen, in the atomic form, can enter the materials from steel making, heat-treatment, etching, pickling, corrosion, and cathodic protection. Atomic hydrogen can combine with impurities in steel or with other hydrogen atoms to cause serious blistering

and brittle fracture. Even small amounts of hydrogen can lead to the formation of cracks and to rapid failure in steels. Hydrogen in its stable molecular form, H_2, cannot penetrate the steel.

Hydrogen, the lightest element known, and its isotopes, may comprise the most studied element, from its cosmic role of being continually created in space, through its role in fission and fusion, in organic compounds including most fuels, to its ubiquitous presence in solution in solids. The unique aspects of hydrogen diffusion into metals is a topic of enormous interest having a high technological importance to electrochemistry, surface science, gas-phase physics, materials and corrosion science. Comprehension of the basics of hydrogen adsorption on the metal surfaces, followed by its interfacial transfer into the metal bulk is also of great important in recently developing metal-hydride science and technology. In corrosion science, knowledge of fundamental steps involved in hydrogen entry into the host metal is of vital significance in protecting metal structures from undergoing hydrogen embrittlement, a costly and often disastrous process. Undesirable entry of hydrogen into metal alloys limits its application as a fuel in space and aviation technology, as well as a fuel in internal combustion engines.

Hydrogen is a difficult species to measure. Since it has only one electron, it is incapable of an Auger transition and therefore escapes one of the most convenient detection methods, namely the Auger Electron Spectroscopy.

The low-temperature permeation of hydrogen through steels has been a subject of broad interest since Cailletet discovered in 1864 that a small amount of hydrogen liberated when an iron specimen was immersed in dilute H_2SO_4 was absorbed by the metal. In 1922 Bodenstein found that the quantity of atomic (nascent) hydrogen entering iron could be varied by the application of a cathodic current [8-9]. These two simple observations demonstrated that hydrogen atoms produced electrochemically may enter the metallic lattice and permeate through the metal. It is the entry of these hydrogen atoms into the lattice of the metal that causes embrittlement and, as a result, possibly catastrophic failure of structures in service environments. HE and stress corrosion cracking, SCC, are serious engineering problems, and hydrogen permeation is an

important aspect of these phenomena. Hydrogen embrittlement is defined as the hydrogen-induced loss in ductility and/or strength and can result from hydrogen effects on either initiation or propagation of fracture. Hydrogen-induced cracking, HIC, is the major form of HE and is a brittle mechanical failure caused by penetration and diffusion of atomic hydrogen into the crystal structure of a metal or alloy. HIC develops on nonmetallic inclusions, such as FeS, MnS, preferential sites for hydrogen accumulation, or at various traps. Molecular hydrogen formed at those sites builds-up pressure causing the rupture of the interatomic bonds, decreasing the cohesive strength, forming voids and blisters that will led to formation of cracks in the material. Stress corrosion cracking, SCC, is defined as initiation and propagation of cracks by simultaneous action of corrosion and tensile stress (applied and/or residual) that can result in failure or embritlement of steels at stresses below the normal materials yield strength.

The need for permeation data is based on the consideration that there is evidence that cracks initiate below the surface of the material in the presence of internal hydrogen. The first information needed for understanding the crack initiation and propagation mechanism is the rate at which hydrogen is transported in the material. A corollary to this would be to check the effect of microstructure on hydrogen transport, processes, and trapping.

Exhaustive statistical analysis of the large existent data on hydrogen permeation has shown that the most reliable results are those obtained by electrochemical methods using Pd-coated specimens [10]. All permeation techniques have in common the measurement of the time necessary for hydrogen introduced on one surface (input side) to enter into the metal, migrate through the thickness of the specimen, and then be detected on the exit surface (output side).

A new method for monitoring hydrogen permeation in metallic materials, called hydrogen vacuum foil (or Beta Foil) [11-14], relies on capturing the hydrogen atoms that permeates through a steel specimen in a vacuum chamber where they combine into pairs to form molecular hydrogen. The build-up of molecular hydrogen causes the vacuum decay in a ratio directly proportional to the amount of hydrogen that was permeating

through the specimen. Currently there is generally a total lack of scientific information with respect to understanding vacuum technology as placed on the outside of components undergoing corrosion. The Beta Foil can be welded, soldered, brazed, or sealed at the edges on the structure (pipeline or pressure vessel) to be monitored. There is a great deal of information required in order to understand and correctly apply this technology.

1.2. Why Measure Hydrogen Permeation?

Hydrogen in steel is never beneficial and the effect of hydrogen permeation on steel is widely documented. Atomic hydrogen can combine with impurities in steel or with other hydrogen atoms in steel to cause serious cracking, blistering, or degradation of other physical and mechanical properties. It is extremely important to accurately quantify this hydrogen permeation activity in an industrial environment.

If the hydrogen flux (i.e., flow rate per unit area) through the steel can be measured, the hydrogen concentration in that part can be determined, if hydrogen diffusivity is known. Several overviews regarding the hydrogen diffusivity in pure iron were published over the years [5,10,15-17,78]. The most recent one was completed in 1998 at The University of Calgary [18] and comprises no less than 250 sets of data regarding hydrogen diffusivity in pure iron, steel, stainless steel, and aluminum. It must be noted that hydrogen concentration in steel can be expressed in various units, depending on the measuring method and on the researcher. For a comparison between the results obtained by various authors, using the same material and the same experimental conditions, some correlation and equivalency factors exist. The most recent overview on this subject was done, again, at The University of Calgary in 1997 [19-21]. Both overviews were made available to some sponsors from industry that solicited those informations.

For many cracking mechanisms, there are published threshold hydrogen concentrations for various steel types, below which cracking will not occur. This is especially true for hydrogen-induced cracking, HIC, where considerable HIC testing was carried out. Combining the two, monitoring the hydrogen flux will determine when

hydrogen cracking is likely to occur, and the operating process can be changed (e.g., by inhibition) to get below the threshold hydrogen flux. This requires that the flux monitor be quantitative [13].

Alternatively, the flux monitor can be used simply as a quality device, changes in relative flux being used to control the operating process. Low hydrogen permeation activity might indicate a corrosion protection program's efficiency. High hydrogen activity could be used to develop guidelines whereby particular equipment could be scheduled for inspection to ensure its integrity [76].

Conversely, effective monitoring which indicates low hydrogen permeation activity could be used to justify forgoing costly inspections of equipment not likely to be experiencing hydrogen associated attack. Measurement can evaluate operating schemes and monitor hydrogen activity due to contaminant metals on cracking catalysts, quantify hydrogen activity in pipelines, power generation facilities, or other systems, which may be subject to hydrogen permeation activity.

There are several reasons for using a hydrogen flux monitor [14,22]. By monitoring hydrogen permeation flux, the potential situations that might lead to cracking can be tracked. This monitoring would typically be backed-up by periodic ultrasonic inspection for cracking to confirm the indications obtained by monitoring. The use of a flux monitor is a relatively low cost option compared with frequent non-destructive inspection. An important feature of hydrogen flux monitoring is that it is a real-time device, which can detect short-term upsets in the process, which may result in brief but high hydrogen fluxes. Such upsets cannot be addressed by non-destructive inspection techniques.

Hydrogen permeation (hydrogen flux) measurements are particularly important in refineries and gas plants, especially where sour service and hydrogen service are involved. Also, it is important in chemical and petro-chemical plants, where hydrogen service is involved and where stress-corrosion situations are expected. Hydrogen flux monitoring is useful in pulp and paper operations, again, where SCC is known to occur. Other applications include: start-ups in sour systems (including pipelines), before stable

operating conditions are achieved, in any vessel or component known or suspected to have suffered hydrogen damage, in any vessel or component going into service where hydrogen damage may be expected.

The main reason for corrosion and hydrogen-related damage is delayed detection. Dynamic systems are always changing. Therefore, corrosion types, rates, and location change. Despite best efforts, upset conditions will occur. These can be attributed to human error, weather changes, function changes, changes due to equipment failure and changes in products moving through the pipelines. The earlier the hydrogen flux is monitored, the better the chances of preventing damage. By getting near real-time data from an internal corrosion-monitoring program, operators can relate this data to events that caused the corrosion. Then they can lower corrosion rates by adjusting or eliminating corrosion-causing events.

1.3. Objectives of the Study

The objective of this investigation is directed at establishing the limits under which hydrogen vacuum flux measurement for some selected corrosive environments will work. A depth analysis on the common parameters that may affect the vacuum flux (presence of poisons, various corrosive environments that are representative to common industrial process conditions, various gases, extra amount of hydrogen other than that resulted due to the corrosion reaction, instrumentation volume) will be performed. The investigations are directed at establishing the sensitivity of the various parameters affecting these measurements, to firmly establish both the application and the limitation of the hydrogen vacuum foil system based on hard scientific information. In order to verify the behavior response of the hydrogen vacuum foil technique simultaneous hydrogen permeation measurements were performed using the already established electrochemical permeation technique called barnacle electrode.

In order to meet the objectives of this investigation the research was carried out in specific steps in order to isolate and control the different parameters that affect the hydrogen permeation measurement.

The tasks set out for this study were to:

- Investigate the sensitivity of the degree of vacuum on the hydrogen permeation through the system. In addition the degree of vacuum will be looked at with respect to regular permeation using the electrochemical permeation method.
- The presence of hydrogen gas in excess of what has formed from the reduction reaction will also be investigated. Surplus hydrogen gas generated from another remote location may dissociate at the measurement location and then end-up as atomic hydrogen diffusing into the material and may affect the vacuum foil measurement.
- The effect of various poisons, such as H_2S, As, and Se, on the hydrogen permeation will be investigated.
- Another problem to be solved is that of the deaerated vs. aerated condition.
- The alteration of hydrogen flux and corrosion rate is very much dependent upon film formation on the exposed surface. The vacuum decay rate change as time elapses for different charging solutions will be investigated.
- The influence of the capillary tubing length, which connects the vacuum foil with the datalogger, on the vacuum rate will be also investigated.
- The hydrogen quantity that permeates through the specimens will be determined.

CHAPTER 2

BACKGROUND AND LITERATURE REVIEW

2.1. Origin of Hydrogen

Hydrogen problems in metallic materials may arise from the pick-up of hydrogen in the atomic form from: steel making, heat-treatment, cleaning, etching, pickling, welding, excessive cathodic protection, and corrosion. In service, hydrogen may enter the metal from a hydrogenous environment, which is almost any environment one might imagine.

Hydrogen can be initially present either externally (in contact with an external surface) in the form of a molecule, a dissociated molecule or atom, or a component of a complex molecule, such as hydrogen sulfide, H_2S, H_2O, or methanol, CH_3OH, or internally (within the bulk of a structural alloy) in the form of an atom or molecule [4].

In steel, the total amount of hydrogen, H_{Fe}, can be considered as a summation of several terms, as follows [23]:

$$H_{Fe} = H_s + H_V + H_d + H_m + H'_a + H_{ch}. \qquad [1]$$

where:

H_s- hydrogen in the solid solution.

H_V- hydrogen bound to vacancies.

H_d- hydrogen fixed on dislocations.

H_m- molecular hydrogen in the pores.

H'_a- hydrogen adsorbed on the surfaces.

H_{ch}- hydrogen bound in chemical compounds (hydrides) or dissolved in chemical compounds (carbides, non-metallic inclusions, such as FeS, MnS, etc.).

H_m and H_{ch} are known not to cause hydrogen embrittlement.

The exact location and form of hydrogen are extremely important to the overall embrittlement process in that they establish the starting point for the hydrogen transport.

Both location and form of hydrogen will have an influence on the number and type of transport reaction steps required to bring the hydrogen to a location where the degrading hydrogen-metal interaction can occur [4]. However, it is the mobile (rather than the total) hydrogen with which we should be concerned. Hydrogen can migrate to areas of high triaxial stress, thereby magnifying its effect and causing delayed failure [24].

Since iron does not form a bulk hydride, any chemical interactions leading to hydrogen embrittlement of steel must occur at the surface [25]. Hydrogen can enter the metals from gas phase or from liquid phase.

2.1.1. Entry of Hydrogen into Iron-Base Alloys from the Gas Phase

The whole process of the take-up of gaseous hydrogen by metals and alloys can be divided into the following steps [26]: diffusion of the gas to the surface, adsorption on the surface (including dissociation), penetration through the surface, and diffusion into the bulk of material.

The hydrogen molecule can be taken-up only at those sites that are not already occupied by other adsorbed molecules. Only the molecules that possess certain requisite activation energy will be adsorbed and the adsorption is only effective if the activation energy can be dissipated sufficient quickly, otherwise the molecule will be desorbed again. Each molecule that strikes a vacant site is either adsorbed or returns to the gas phase. The adsorption process is strongly influenced by the presence of contaminants and/or layers of oxides, sulfides, on the surface. The roughness of the surface also has a strong influence on the adsorption process. On an ideally smooth surface a larger fraction of the impinding molecules will be reflected back into the gas phase than on a very rough surface.

At the entrance side of the material molecular hydrogen from the gas phase adsorbs and desorbs from an adsorbed molecular precursor state, H^* [27]. Dissociation and recombination occur between the precursor state (physisorbed) and the chemisorbed state, H. In the physisorption state the chemical bonds are not broken, the hydrogen

molecule being intact. Van der Waals force couples the molecule to the surface which does not dissociate. In the chemisorbed state the adsorbate shares electrons with the substrate. There is a chemical bond between the adsorbate and the surface. Chemisorption is not always a spontaneous process. From the chemisorbed state, hydrogen can reversibly go into the bulk of material establishing a subsurface hydrogen concentration, C_H. This hydrogen diffuses to the other side of the specimen (output surface) where the surface reaction is reversed. The surface reaction step is clearly the controlling step in the penetration of hydrogen into the bulk phase [28]. A schematic of the reactions involved in hydrogen absorption from the gas phase is depicted in Figure 1.

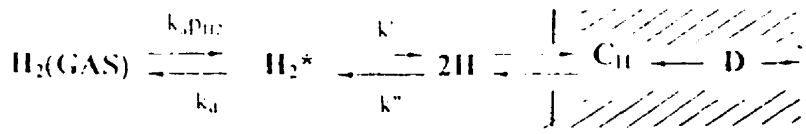

Fig.1: Schematic of the surface reaction of hydrogen in iron.
(after Shanabarger et.al. [27]).

The reaction steps for the dissociative chemisorption process can be described as follows [4,27]:

$$H_2(gas) \underset{K_s}{\overset{k_s p_{H_2}}{\longleftrightarrow}} H + \underset{k'}{\overset{k''}{\longleftrightarrow}} 2(H-Fe) \qquad [2]$$

where:

$k_s p_{H2}$- rate of adsorption from the gas phase to the molecular precursor, H*.

p_{H2}- hydrogen gas pressure.

k_d- rate constant for desorption from the precursor to the gas phase.

k'- rate constant for adsorption from the precursor to the dissociated chemisorbed state.

k"- rate constant for desorption from the dissociated chemisorbed state to the molecular state.

Jerkiewicz and Zolfaghari [30] proposed the following scheme for the two steps that occur during chemisorption:

$$H_2 = 2H^*. \qquad [3]$$

$$2H^* + 2M = 2M\text{-}H_{chem}. \qquad [4]$$

where: H*- energetically rich, atomic hydrogen prior to adsorption.

Considering the equilibrium situation at the surface, one may use the Langmuir approach to adsorption at an interface, where θ represents the fractional number of surface sites that are covered by adsorbed species [25,29]. The Langmuir isotherm is based on an equilibrium adsorption for an ideally uniform surface with no lateral interactions between neighboring adsorbed species. The fraction, θ, of the surface covered by adsorbate is given by:

$$\theta = \frac{k_a p_{H_2}}{1 + X p_{H_2}^{1/n}} \qquad [5]$$

where:

X- ratio of the rate constants for adsorption and desorption.

n- number of fragments formed upon adsorption.

However, the ideal condition of no lateral interactions between the adsorbed species may not be completely true for many real situations. The adsorption process is then followed by three-dimensional diffusion into the metal bulk.

2.1.2. Entry of Hydrogen into Iron-Base Alloys from the Liquid Phase

There are many instances in which metals may occlude considerable amounts of hydrogen derived from aqueous environments. In principle, hydrogen electroadsorption (electrosorption) can be accomplished from either acidic or basic aqueous solutions or from non-aqueous solutions that are capable of dissolving hydrogen-containing acids [30-31]. The solid metal/aqueous electrolyte interface is more complicated than the metal/gas one because the presence of a dense network of water dipoles in the electrolyte, and by the competitive adsorption of different species on the metal surface.

2.1.2.1. Mechanisms of the Cathodic Evolution of Hydrogen from Aqueous Electrolytes

Electrochemically adsorbed hydrogen originates from hydrogen atoms discharged from H_2O or H_3O^+ ions at the host metal surface. The adsorption process is driven by the chemical potential gradient associated at the surface with the fractional surface coverage, θ, and in the bulk by fractional site occupancy [32].

The processes that may take place during electrochemical hydrogen adsorption are illustrated in Figure 2.

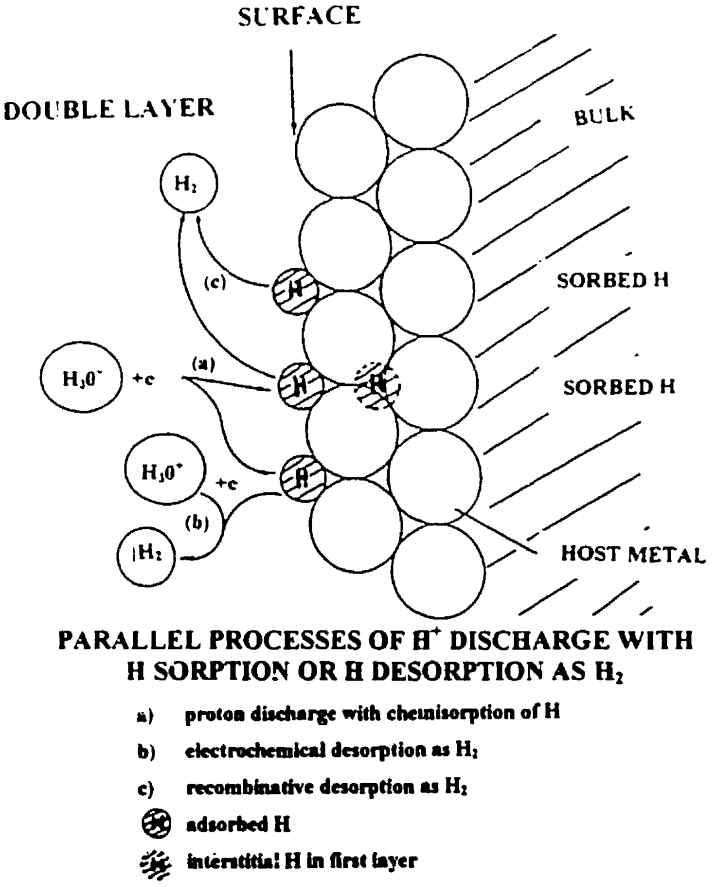

Fig.2: Paths for hydrogen adsorption into the metal and desorption by electrochemical or chemical combination to hydrogen gas at the metal-electrolyte interface. (after Gao and Conway,[32]).

The sequences presented in Figure 2 may be summarized as follows [32]:

- Proton discharge with chemisorption of hydrogen.
- Phase transfer of hydrogen from the surface to interstitial sites in the host lattice, just below the surface.
- Transfer of hydrogen from the previous state into the bulk by 3-D diffusion along the chemical potential gradient.
- Parallel processes of desorption of the adsorbed hydrogen from the surface as hydrogen by electrochemical step or the hydrogen recombination.

Wilde and Kim [33] have shown that the absorption reaction may be treated as a simple first order process:

$$H_{ads} = H_{abs}. \qquad [6]$$

In which the absorption, or permeation flux, J, can be expressed as:

$$J = k_{abs}\theta - k_{des}C_0. \qquad [7]$$

where:

k_{abs}, k_{des}- specific rate constants for adsorption and desorption processes.

C_0- concentration of hydrogen dissolved in the metal at the surface.

Determination of θ on a corroding metal surface is very difficult due to complications derived from accelerated anodic dissolution of the metal. Wilde and Kim [33] suggested the following equation for the surface coverage, θ, of a corroding metal:

$$\theta = \frac{1 - \frac{i_c}{i_{corr}} \exp\frac{F\Delta E}{2RT}}{\exp\frac{-F\Delta E}{4RT} - \frac{i_c}{i_{corr}} \exp\frac{F\Delta E}{2RT}} \qquad [8]$$

where:

i_c- applied cathodic current.

i_{corr}- steady-state corrosion current.

θ- steady-state coverage at i_{corr}.

F = 96,480 C/mol- Faraday's constant.

R = 8.314 J/molK-universal gas constant.

T- absolute temperature.

$\Delta E = E_c - E_{corr}$.

Solution of equation 7 requires data that can be obtained from cathodic polarization curves for a corroding metal in any environment.

It was found that the evolution and adsorption of hydrogen in any metal/electrolyte interface occurs by two or more of the following steps [30-31,33-34]:

$H^+ + e^- = H_{ads}$	(charge transfer reaction)	[8]
$H_{ads} + H_{ads} = H_2$	(Tafel recombination reaction)	[9]
$H_{ads} + H^+ + e^- = H_2$	(Volmer-Heyrowsky reaction)	[10]
$H_{ads} = H_{abs}$	(hydrogen-absorption reaction, HAR)	[11]

The first three equations represent the pathways of the hydrogen evolution reaction, HER. Equation 8 is the electron transfer reaction for HER, so-called because electrical charge passes through the electrical double layer at the metal/electrolyte interface. Following this reaction, the recombination of adsorbed atoms to form adsorbed molecular hydrogen occurs, as shown by equation 9. The step from equation 8 to equation 9 is depicted in Figure 3a. The Volmer-Heyrowsky reaction, equation 10, differs from the previous mechanism by the fact that in addition to the chemical recombination, equation 9, an elecrochemical recombination occurs, by which the already available atomic hydrogen reacts with H^+ ions to form adsorbed molecular hydrogen [34]. This mechanism is depicted in Figure 3b.

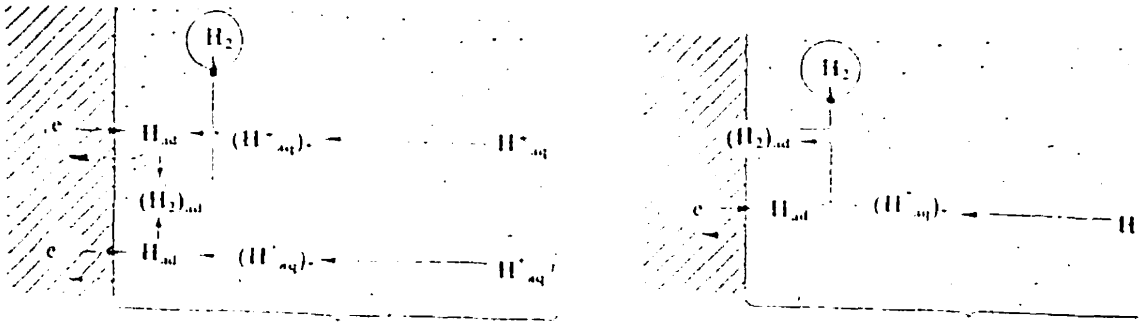

a. METAL BOUNDARY LAYER SOLUTION b. METAL BOUNDARY LAYER SOLUTION

Fig.3: Reaction scheme for cathodic hydrogen evolution. (after Kaesche,[34]).

The HAR reaction, equation 11, describes the interfacial hydrogen transfer from the adsorbed state to the absorbed state and it is followed by 3-D hydrogen diffusion into the bulk of the host metal. The 3-D diffusion of atomic hydrogen into the host metal, causing HE, is a parallel reaction to hydrogen recombination [34]. The 3-D hydrogen diffusion into the metal's bulk is often the rate-determining step in hydrogen absorption and it limits the charging/discharging kinetics [30].

It must be noted that, as in the case of chemisorption, the interfacial hydrogen transfer from the adsorbed state to the absorbed state may be strongly affected by the presence of small amounts of surface impurities [30].

Depending on the electrolyte, the overall HER can be written as:

$2H_3O^+ + 2e^- = H_2 + 2H_2O$. (in acid solutions) [12]

$2H_2O + 2e^- = H_2 + 2OH^-$. (in alkaline solutions) [13]

In acid solutions, HER mechanism takes place in two steps:

$H_3O^+ + M + e^- = MH_{ads} + OH^-$ (discharge of hydrated protons) [14]

$MH_{ads} + H_3O^+ + e^- = H_2 + H_2O + M$ (detachment of hydrogen atoms from the metal surface by electrochemical desorption) [15]

Similar, in alkaline solutions:

$H_2O + M + e^- = MH_{ads} + OH^-$ (electrolysis of water) [16]

$MH_{ads} + H_2O + e^- = H_2 + OH^- + M$ (electrochemical desorption) [17]

Usually, only a small portion of the hydrogen liberated at the cathode enters the metal lattice. The rate of hydrogen entry is very much influenced by many variables, such as [31]: the nature of the metal or alloy, its composition and thermal-mechanical history, surface conditions, composition of the electrolyte, temperature, pressure, etc.

With the exception of noble metals (such as Pt, Au, Ir) and Hg, most metals in aqueous solutions are covered by corrosion film products. Under freely corroding conditions, in deaerated-neutral or near-neutral solutions, iron and iron-base alloys are normally covered with films containing $Fe(OH)_2$, Fe_3O_4, FeOOH, in addition to oxides containing alloying elements (such as Cr_2O_3, $FeCr_2O_4$), depending on the existing conditions at the interface. In sulfide-containing aqueous environments, which are known to promote the hydrogen entry into the metal phase, the corrosion products may consist of iron sulfides, such as mackinawite, $Fe_{1-x}S$, troilite, FeS, pyrrholite, $Fe_{1-x}S$ and pyrite, FeS_2 [35].

It is important to mention that only very rarely does hydrogen evolution occur on a "clean" iron surface. The real interface is not that between iron and the electrolyte, but that between corrosion products and the aqueous phase. Many oxides and sulfides of iron are good electric conductors, thus representing a highly catalytic surface for the HER to occur.

2.1.2.2. Entry of Hydrogen into Steel from Sulfide Solutions

Hydrogen sulfide, H_2S, is encountered in a large number of environments and it is known to accelerate general corrosion and also the SCC of steels. The embrittlement observed in H_2S-containing media is termed sulfide stress cracking, SSC [36-40]. It is now generally accepted that this type of failure is a result of HE, i.e. enhanced hydrogen entry into steel.

The metal-water-H_2S system is very complex. H_2S can be absorbed on the metal surface as H_2S or HS^- in competition with H_2S, OH^- and possibly O_2 that is often present in the electrolyte. The difficulty of measuring H_2S in the aqueous phase contributes to the uncertainty [31].

H_2S is a classic example of a diprotic acid and in water dissociates into HS^- and S^{2-} [31,41-43]:

$$H_2O + H_2S = H_3O^+ + HS^- \quad [18]$$

and

$$HS^- + H_2O = H_3O^+ + S^{2-} \quad [19]$$

In the presence of H_2S, HER may be represented by the overall reaction [31]:

$$2H_2S + 2e^- = H_2 + 2HS^- \quad [20]$$

It is well known that H_2S accelerates the anodic dissolution of iron and acts as a cathodic depolarizer. H_2S accelerates the discharge of hydrogen ions on a steel surface according to the following reaction, which is a model of H_2S adsorption on Fe [31,42]:

$$H_2S = H_2S^* = H\text{-}Fe + HS\text{-}Fe \quad [21]$$

where: H_2S^*- molecular precursor.

The dissolution of Fe in aqueous H_2S solution is usually given by the conversion of the base metal, Fe, to its soluble divalent cation state, Fe^{2+}, or iron sulfide, which depends on the environmental conditions. The corrosion process of metal surface in the absence of oxygen is [31]:

$$Fe + H_2S_{(aq)} = FeS + H_{2(gas)} \quad [22]$$

The dissolution of steels in H_2S-containing environments would result in the formation of corrosion products, which may be either protective or non-protective. FeS precipitates and usually forms an adherent protective coating at low and moderate temperatures as long as the film is not mechanically disturbed [41].

Atomic hydrogen produced by the sulfide corrosion reaction diffuses into the steel and can either diffuse through the full thickness of the specimen and exit on the other side or recombine to form molecular hydrogen at inclusions or other microstructural discontinuities leading to the formation of hydrogen blisters, HIC, SSC, or SOHIC.

H_2S-containing environments vary significantly in their ability to promote hydrogen absorption. The most important variables are [31,43]: pH, H_2S concentration, temperature, and surface conditions.

Solubility of hydrogen in steels increases with increasing sulfide concentration. The pH range of high hydrogen activity and embrittlement of steel corresponds to the stable domain of molecular H_2S.The embrittling effect decreases with increasing pH and once the solution pH is >7 the effect of sulfides becomes insignificant [43].

Other sulfide solutions that are known to promote hydrogen entry into steels are ammonium sulfide, $(NH_4)_2S$, and ammonium bisulfide, NH_4HS [44].

It must be noted that only the aqueous dissolved part of the sulfides will contribute to embrittlement and cracking of metals and alloys.

In conclusion, it can be said that sulfides poison the hydrogen recombination reaction on metal and alloy surfaces, thereby permitting a large fraction of hydrogen atoms to enter the metal, further accelerating the iron dissolution reaction.

2.1.2.3. Entry of Hydrogen into Steels from Molten Salts

Hydrogen absorption reaction, HAR, and hydrogen degradation effects at higher temperatures can be studied by using molten salts for hydrogen charging. Molten salt baths consisting of neutral acid and acid sulfates of sodium and potassium, with or without addition of small amounts of water, are commonly used. Such examples are [31]: $KHSO_4$, $NaHSO_4$, and $NaHSO_4$-$KHSO_4$.

The test specimens can be rapidly charged to a high concentration of hydrogen because both the solubility and diffusivity of hydrogen increase with increasing temperature.

2.1.2.4. Entry of Hydrogen into Steels from Non-Aqueous Liquids

There is no mechanism to date to explain how the hydrogen can be transferred from non-aqueous liquids into the metals. However, it is clear that such a transfer exists [31].

Hydrogen can be introduced into steels by decomposition of lubricants. It was suggested that hydrogen can evolve as a results of the thermal decomposition of polymer macromolecules in lubricants and cooling liquids.

2.1.3. Promoters of Hydrogen Entry into Steels

It has been established that the rate of hydrogen entry in a metal is affected by the potential of the metal, nature of the electrolyte, presence of surface layers, temperature, and/or presence of impurities.

Some elements, "poisons", when present in relatively small concentrations have a marked effect in increasing hydrogen entry into metals and alloys. The mechanisms of effects of poisons in promoting hydrogen absorption is often proposed that poisons block the hydrogen-hydrogen, H-H, recombination reaction and thus favor entry of the adsorbed hydrogen into the metal or alloy [32]. Some authors [45] have suggested that the poisons actually deposit on active sites on the surface, resulting in mechanical blockage of hydrogen entry. However, there is no practical evidence nor theoretical background supporting this theory.

It has been demonstrated that promoters of hydrogen entry into metals show their full effect at relatively very low concentration [31].

Among the species found to promote hydrogen entry into steels are [28,31,43,45]:

- Compounds of P, As, Sb, Bi, belonging to the V-A periodic Group, and S, Se, Te, belonging to the VI-A periodic Group.
- Following compounds of carbon: carbon sulfite, CS_2, carbon monoxide, CO, urea, CON_2H_4, thiourea, CSN_2H_4, and carbon dioxide, CO_2.
- Active ions, such as: cyanide, CN^-, chloride, Cl^-, iodide, I^-, rhodanide, CNS^-, bromide, Br^-, and fluoride, F^-.

There are also reported in the literature, but are inconsistent indications or assumptions, as to the promoting hydrogen entry effect of Hg, Pb, tin salts, and napthalene derivates [31]. Recently, Zachroczymski [46] found that addition of ethylenediaminetetraacetic acid to electrolyte solution strongly accelerated the hydrogen entry into steels mainly due to the effectively removal of oxides and other scales.

In one of the very few studies available on the effect of poisons in promoting hydrogen entry into metals and alloys Radhakrishnan and Shreir [45] classified the effect of poisons according to their effectiveness in promoting hydrogen entry as follows:

$$As > Se > Te > S > Pb > Bi$$

They also concluded that addition of Hg and Sn resulted in deposition of these metals to the cathode, thus decreasing the hydrogen entry rate.

2.1.4. Inhibitors of Hydrogen Entry into Steels

It was suggested [47] that all three states of hydrogen in steels (mobile, reversibly trapped, and irreversibly trapped) can be minimized in quantity when specially designed inhibitors are used.

Inhibitors of hydrogen entry into metals and alloys function by [48]:

- Adsorption as a thin protective film onto the surface of the metal.

- Changing characteristics of the environment either by producing protective precipitates or removing or inactivating an aggressive constituent so that it does not attack the metal.

There is the possibility of controlling the hydrogen entry into metals and alloys by the use of inhibitors that strongly adsorb and are not embrittlers themselves. The inhibition effect is due to the kinetic limitations of the hydrogen discharge reaction and suppression of the hydrogen absorption. By changing the chemical properties of the substrate, the hydrogen coverage on the surface is decreased, thus the degree of hydrogen entry is drastically reduced.

An alloy surface with deposited metals (Zn, Bi, Pb) will inhibit the hydrogen discharge reaction and reduces drastically the degree of hydrogen entry [49-51].

Diamines with long carbon chains are most effective in reducing the corrosion rate and hydrogen absorption [48-49,52]. Phenylpropyonil and pyridylnonadiene are the most common ones and they reduce the permeation rate by lowering the amount of hydrogen that discharges at the metal surface. Ethylene and ethane are also known to reduce the rate of hydrogen entry into metals, while methane is known to have no effect.

Other effective inhibitors of hydrogen entry into metals are calcium bicarbonate, phosphates, and $NaSiO_3$ that protect the metals by forming protective carbonate, phosphate, and silicate films that act as barriers to hydrogen entry [52].

$K_2Cr_2O_7$ is effective as an anodic inhibitor. It converts the metal into a passive state, thus decreasing the hydrogen entry rate [52].

As in the case of hydrogen promoters, hydrogen inhibitors show their full effect at relatively very low concentrations.

Certainly, there are more inhibitors to be discovered.

2.2. Permeation of Hydrogen

In addition to its diffusion through the bulk metal, the permeation of hydrogen through steels involves its entrance at one surface and its exit at the other surface of the specimen. There are seven steps that take place before the hydrogen is detected on the

output side of the specimen [53-54]. Figure 4 shows the seven steps that take place in the permeation of a hydrogen isotope through a metallic membrane.

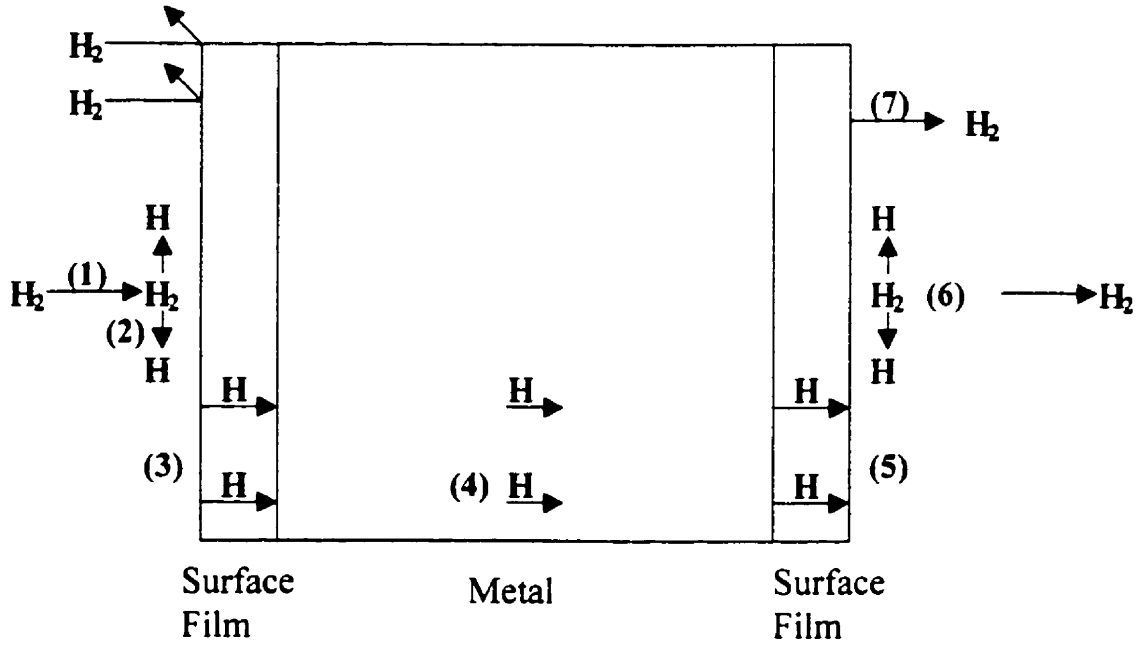

Fig.4: Seven steps of hydrogen permeation. (after Stone,[53]).

This model takes into account the presence of surface films on both input and output side of the specimen. The seven steps are:

1. Adsorption of hydrogen molecule on the surface.
2. Dissociation of the adsorbed molecule on the surface.
3. Permeation of dissociated atoms through the surface film (oxide).
4. Permeation of atoms through the metal.
5. Permeation of atoms through the film on the output side.
6. Reassociation of atoms to form H_2 molecule.
7. Desorption of the reassociated H_2 molecule.

The permeation rate is a consequence of the relative restraining contribution of the seven steps. Sorting out these steps and learning to control and to use them is of considerable practical importance. While it is desirable to prevent hydrogen from permeating through the metals, it is more desirable to prevent hydrogen entering the metal in the first place. Electrochemical corrosion, mechanical behavior, and general material/environmental interaction depend upon the level of mobile and trapped hydrogen absorbed in the material.

The permeation rate at which hydrogen passes through a specimen will be established by the diffusivity and the difference between the hydrogen concentration at the input side and the output side.

Under the assumption that there are no surface effects on both sides of the specimen the hydrogen surface concentration will be equal to the solubility limit for hydrogen in that metal [53]. As time passes, the hydrogen permeates through the metal and when the steady-state condition is reached, the concentration gradient of hydrogen through the specimen will be linear. Then, the following definition applies [53]:

$$\text{permeability} = \text{diffusivity} \times \text{solubility}.$$

However, if the permeability is reduced by a surface defect, then the solubility term changes:

$$\text{permeability} = \text{diffusivity} \times \text{surface concentration}.$$

The steady-state situation may be associated with the passage of hydrogen through a membrane. If conditions are maintained constant, the rate of passage (permeation) usually becomes constant (stationary) after sufficient time. This state is described by the permeability, p_r, which is the quantity of hydrogen transferred in one second through a specimen 1 mm thick and 1 cm^2 in cross-section. The non-stationary state (non-steady-state) is associated with the rate at which a specimen absorbs or loses hydrogen. The boundary conditions and the diffusion coefficient, D, usually describe the non-steady-state situation.

The process that leads to the deterioration of properties by the hydrogen presence begins in the first instant at the input side (surface facing the hydrogen). This begins long before breakthrough. The hydrogen concentration at the input side of the specimen will always be the highest of any place in the system [53].

In all models dealing with hydrogen permeation it is assumed that the hydrogen concentration at the output side is zero and that the imposed physical parameter is the hydrogen concentration just under the input surface.

In the case of steady-state permeation, the diffusion is not inhibited by trapping either at higher or at lower temperatures and local equilibrium between the dissolved and trapped hydrogen is established [2]. Hydrogen transport is carried out mainly by the mobile hydrogen atoms on normal interstitial positions and it is developed by impurities and substitute elements blocking interstitials, by precipitates decreasing the diffusion cross-section and by compressive elastic stress fields. Hydrogen trapping itself may decrease the permeability of a material. Before the traps are filled the measured permeation rates are at first anomalously low, increasing with time as the traps become filled. When they are completely filled, steady-state permeation occurs at a rate controlled by the interstitial concentration gradient. The time for equilibrium hydrogen absorption in a material varies from material to material and from environment to environment.

The measurement of hydrogen within a material and the correlation of HE with various parameters is complex. The amount of hydrogen permeating through the membrane is usually determined by a very sensitive electrochemical method, which will be presented later, in Section 2.3. Another method for measuring permeable hydrogen through metallic samples has been developed recently [11]. It is called hydrogen vacuum foil (Beta Foil) and will be presented in detail in Section 2.4.

There are three controlled variables that have a strong influence on the hydrogen permeation rate: temperature, specimen thickness, and the pressure at the input side of the specimen [37,54].

The effect of temperature on the hydrogen permeability through the metals can be described by an Arrhenius type equation as follows:

$$p_r = p_0 \exp(-E_p/RT). \quad [23]$$

where:

p_r- permeability, permeation rate.

p_0- temperature independent factor for permeability.

E_p- activation energy for permeation.

R- universal gas constant.

T-absolute temperature.

The activation energy for permeation, E_p, can be described as follows:

$$E_p = E_D + \Delta H. \quad [24]$$

where:

E_D- activation energy for diffusion.

ΔH- enthalpy.

The activation energy for diffusion, E_D, corresponds to the energy surplus necessary to enable the diffusing atom to overcome the potential barrier for diffusion.

In general, the steady-state permeation flux is inversely proportional to thickness for large membrane thickness. As the thickness is reduced the steady-state flux becomes thickness independent. However, there are several important deviations. Oxide films, usually present on a metal surface, lower the degree of hydrogen dissociation and the permeation flux is lowered. Thicker oxide films lower the flux even further and the apparent diffusivity in the layer gets lower than that in the metal. However, significant reductions in the hydrogen permeation rate are achieved even with very thin films, as thin as 50 nm [51,53,55].

Metallic coatings deposited on a metallic substrate can effectively reduce hydrogen entry, permeation, and embrittlement providing they satisfy a number of criteria, such as adhesion and cohesion. It was found that Sn, Cd, Pb, Ni, Al, and Zn coatings decrease the hydrogen absorption in iron because they have lower diffusion coefficients compared with the substrates [49-51,56-61].

Erratic permeation measurements that may occur can be attributed to the alteration of materials that may take place during aging, hydriding, and cracking. Other uphill effects can be produced by development of asymmetrical lattice deformation across the specimen thickness, which can be produced either by external mechanical forces or by internal non-uniform lattice volume changes induced by concentration gradients of the diffusing species. Due to those effects the period of time required to establish the steady-state condition for hydrogen permeation can be substantially prolonged [51,55].

2.3. Electrochemical Hydrogen Permeation Measurements

Most methods for determining hydrogen in metals are destructive and cumbersome and their greatest drawback is that they measure total hydrogen. However, it is the mobile (rather than total) hydrogen with which we should be concerned. It is therefore important to have a method of determining mobile, or damaging, hydrogen which can then be related to actual service condition.

Electrochemical methods for investigation of metal-hydrogen systems are superior to other techniques because of their simple procedure and their flexibility towards variation of experimental conditions. Moreover, these techniques allow measurements at very low hydrogen equilibrium pressures. The analysis of the permeation curves is based largely on the application of Fick's laws and on the theory of McNabb and Foster [62]. An important assumption in these analyses is that the movement of atoms through the material can be described by 1-D transport equations. The premise is that lateral diffusion of hydrogen can be neglected. Obviously, this is intuitively true if the membrane thickness is very much less than the radius of the monitoring area [63]. However, no specific recommendation for an acceptable ratio of area to thickness is available when designing appropriate test systems. To date, there is no general agreement on the experimental conditions used in the hydrogen electrochemical permeation methods.

The electrochemical permeation of hydrogen consists in creating a hydrogen concentration gradient in a metallic sample to achieve diffusion through the metal. This technique was first developed by Devanathan and Stachurski in 1962 on Pd [64-65] and it relies on the entrance and exit of hydrogen atoms at metallic surfaces.

The removal of the surface layers that retard the hydrogen passage from the specimen is a necessary condition for the electrochemical methods to be applicable. It is common practice to electroplate a thin film of Pd on the output (detection) side to prevent corrosion of the iron or iron-base alloy specimens. Pd is inert and permeable to hydrogen and the diffusion resistance of the Pd layer is so small it does not affect or show-up in the results.

Since electrochemical methods rely on the transport of atomic hydrogen through the lattice, alloys that form hydrides and irreversible traps are not recommended for study with these methods. This is true for metals like V, Nb, Ta, or Ti [66].

A necessary requirement of studying the electrolytic hydrogen permeation through metallic samples is that the hydrogen permeation rate be controlled by diffusion in the material of the specimen [64-65].

2.3.1. Devanathan-Stachurski Method

The so-called Devanathan-Stachurski method is a very sensitive electrochemical technique that permits the recording of instantaneous rate of electrolytic hydrogen through a metallic sample. A schematic of the Devanathan-Stachurski cell is depicted in Figure 5.

The cell is composed of two compartments separated by the specimen to be measured, which is cathodically charged with hydrogen or exposed one side to a corrosive environment. Each compartment carries an auxiliary electrode, a Luggin-capillary-saturated calomel reference electrode system, SCE, and facilities for nitrogen bubbling.

Solutions from both compartments should be deoxygenated in order to reduce background current arising from the reduction of oxygen.

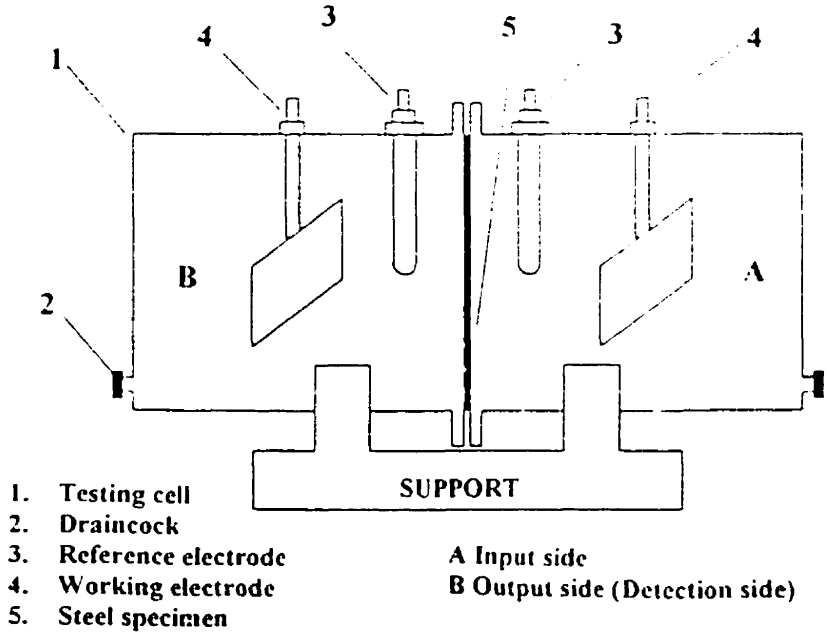

Fig.5: Schematic of a Devanathan-Stachurski cell. (after Casanova, Crousier,[67-68]).

In the anodic compartment (output side of the specimen) the solution employed is NaOH. Controversy exists regarding the normality of the NaOH solutions to be used. It is obvious that the conductivity of various NaOH solutions is not identical and the solution resistivity varies considerably for various concentrations. The effect of solution resistance should not be great since the current measured through the cell is very small. It was suggested [69-73] that the proper solution to be used should be 0.2N NaOH.

Diffusion theory required that coverage of the specimen with adsorbed atomic hydrogen on one side be maintained at a certain fixed level, while on the opposite side it should be always zero. Cathodic polarization of one side and anodic polarization of the opposite side easily satisfies these conditions, by the use of a potentiostatic circuit [64-65]. The output side of the specimen must be polarized at a potential high enough to oxidize all the hydrogen atoms that are emerging before they recombine, which would give hydrogen bubbles.

The anodic potential has to be chosen to ensure oxidation of all the hydrogen coming out of the specimen. Any potential above (more negative than) the reference potential of hydrogen can do this [74]. However, this negative potential will also oxidize

iron, and will even do this preferentially to oxidizing hydrogen (since $E_{oxidation(Fe)}$= +0.409V). In order to prevent this from happening, the output side of the sample can be coated with a metal that is noble enough (very negative $E_{oxidation}$) to withstand corrosion at the imposed anodic potential. Pd was used such a protective layer. It is permeable to hydrogen, its potential is quite high (-0.83V), its diffusivity for hydrogen is of the order of 3.2×10^{-7} cm^2/sec, and its hydrogen solubility is very much higher than iron (approx. 10^6 times higher). Pressouyre [74] gave the following limits for the anodic potential:

$$\text{anodic potential} > E_{anodic}(\text{ref:}H_2 \text{ electrode}) > -0.830V.$$

If the specimen to be measured is cathodically charged, very important is also the choice of the cathodic potential. In order for the reaction $2H_2O + 2e = H_2 + 2OH^-$ to occur, the cathodic potential had to be greater than 0.830V [74].

Deionizing the solution is a very important step, because all the reactions with an oxidation potential less than 0.830V could occur as a reduction reaction (ex: $Fe^{2-} + 2e = Fe$). This would have resulted in deposits on the input side of the specimen, which could have reduced its permeability to hydrogen. The solution must be deionized and then electrolyzed at a current of few mA.

Hydrogen that passes through the specimen and reaches the output side is immediately oxidized to hydrogen ions by the potentiostatic circuit that maintains a constant anodic potential. At this potential, any hydrogen reaching the output side is oxidized. In such conditions, the only anodic reaction that can take place is the oxidation of atomic hydrogen according to the $H = H^+ + e^-$ reaction [74]. The arrival of first traces of hydrogen on the output (anodic) side of the specimen is measured and registered as an increase in the current. This current continues to increase with time and eventually will reach a steady-state value. The potentiostat supplies the current necessary for hydrogen oxidation, and the potentiostatic current is a direct measure of the amount of hydrogen leaving the output side of the specimen. The current in the anodic potentiostatic circuit, which maintains zero coverage on one side of the specimen is by Faraday's law a direct measure of the instantaneous hydrogen permeation rate. It is thus possible to obtain

a continous record of the instantaneous hydrogen permeation rate with all the sensitivity associated with current measurement.

Immediate oxidation of all atomic hydrogen reaching the output side maintains the hydrogen content at (or near) the surface very close to zero, as required by the diffusion theory [64-65,74,76-78].

Diffusion data may be extracted from experimental permeation curves, which gives the hydrogen flux versus time. The flux of hydrogen through the specimen is measured in terms of current density, I, which, in turn, is used to express hydrogen permeation flux according to the following equation:

$$J_{\infty} = \frac{I_{\infty}}{zF}[molH.m^{-2}\sec^{-1}] \qquad [25]$$

The permeation rate is defined by:

$$J_{\infty}L = \frac{I_{\infty}L}{zF}[molH.m^{-1}\sec^{-1}] \qquad [26]$$

where:

I_{∞}- steady-state permeation current density.

J_{∞}- steady-state hydrogen flux.

z- number of electrons transferred.

F- Faraday's constant.

L- specimen thickness.

Several mathematical models were developed and proposed in order to explain the permeation behavior of hydrogen through iron and iron-base alloys. Some take trapping into consideration, some do not. However, concerning the input side concentration it is generally assumed to be imposed instantaneously whatever the charging method. In all models it is assumed that the hydrogen concentration at the output side is zero.

The Devanathan-Stachurski method is very versatile in that of the numerous possibilities of varying, experimentally, the boundary conditions at both the input and output sides of the specimen. The sensitivity of this method reveals details in the permeation not detectable by other monitoring techniques.

2.3.2. Barnacle Electrode Method

A modification of the Devanathan-Stachurski method is the technique which is used in the "barnacle-cell", so-called because of its attachment to the metal surfaces. In the barnacle electrode system only the extraction side of the Devanathan-Stachurski cell is used [24,79-82].

The idea is to attach the anodic (extraction) side of the permeation cell onto the steel structure to be measured and with the aid of a non-polarizing electrode (cathode) to oxidize the hydrogen atoms that are electrochemically induced out of the metal to the water, thus maintaining zero hydrogen concentration at the output side of the steel (anode). The major simplification of the barnacle electrode technique is the use of the non-polarizing electrode to replace the potentiostat. Initially, a Ag/Ag_2O electrode was used. Though the Ag/Ag_2O electrode exhibited better long term stability than the Ni/NiO electrode, the latter proved to have sufficient stability. It was therefore chosen since it is more readily obtainable [79].

The barnacle electrode consists of a steel specimen (anode), a Ni/NiO electrode (cathode), and a Teflon block that has a circular opening and a rubber gasket, which, when clamped to the specimen, defines an exact area. For uneven surfaces, such as welds, a neoprene rubber gasket can be used between the cell and the specimen. The cell is filled with NaOH solution, which maintains the steel in the passive condition so that oxidation of the iron did not contribute to the current measured. The system is activated when the NaOH solution is poured into the cell. The measurement of the oxidation current is made by using the voltage (IR) drop across a resistor or by using a current follower-circuit. The output is monitored with a strip chart recorder. Because the oxidation current is very high and continuously changing in a major manner at the start of the measurement, it is not

recorded for the first 10 minutes. It has been determined [80] that a 30 minute reading leads to better precision because the rate of change of the current is almost insignificant at this time.

A schematic of the barnacle electrode system employing a Ni/NiO electrode is depicted in Figure 6 and a more complex one, employing a potentiostat, that will be used for the present research program, in Figure 7.

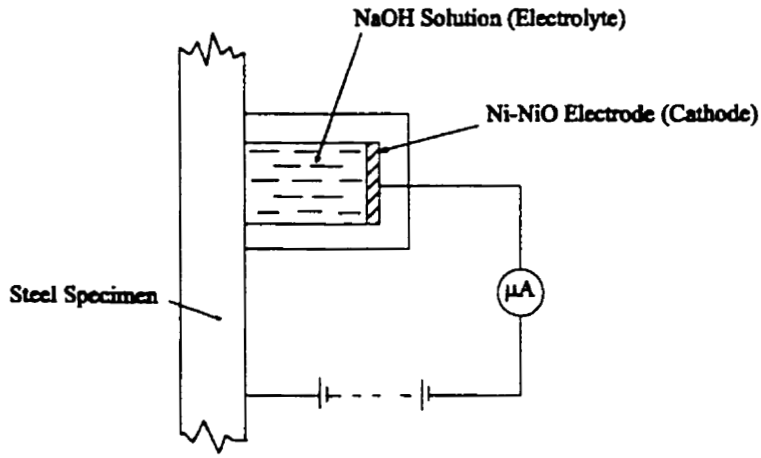

Fig.6: Schematic of the barnacle electrode employing a Ni/NiO electrode.
(after Lucas and Robinson,[81]).

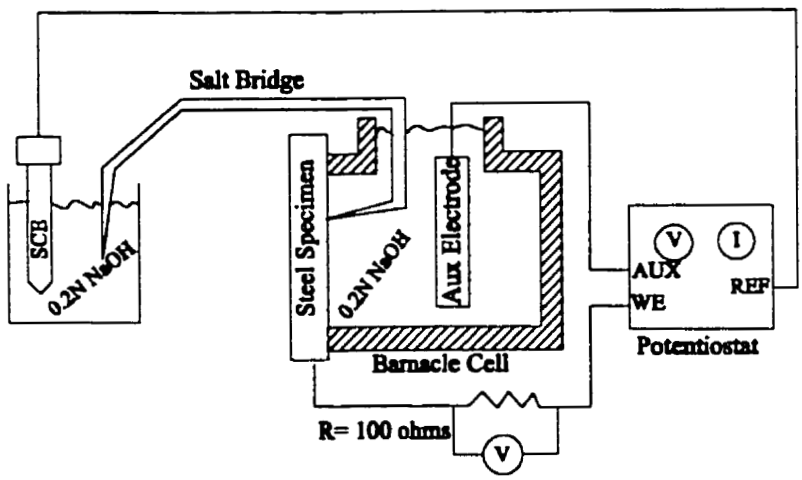

Fig.7: Schematic of a more complex barnacle electrode circuit employing a potentiostat.
(after Shaw,[87]).

Assuming a uniform initial distribution of hydrogen in the specimen, the hydrogen oxidation current is measured and related to the mobile hydrogen concentration by the solution to the diffusion equations. Barnacle electrode hydrogen extraction transients (current density versus time) obey the equations resulting from the solution of the diffusion equations so long as the specimen thickness is sufficient to ensure proper boundary conditions. This also means that no oxidation reactions other than that for hydrogen are significant [24]. The oxidation current can be related to the hydrogen concentration in the metal by the first term solution to the Fick's second law.

Figure 8 shows the boundary conditions for the barnacle electrode [24,79,82].

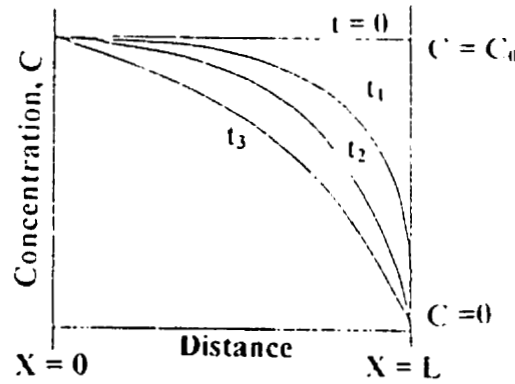

dC/dx = 0	x = 0	t ≥ 0
C = 0	x = L	t > 0
C = C_0	0 < x < L	t ≤ 0

Fig.8: Boundary conditions for barnacle electrode hydrogen extraction [24].

The diffusion (Fick's) equations to be solved are:

$$\frac{I}{zF} = -D\frac{dc}{dx} \qquad [27]$$

$$\frac{d^2c}{dx^2} - \frac{1}{D}\frac{dc}{dx} = 0 \qquad [28]$$

where:

z- number of electrons involved in the oxidation reaction (z=1).

I- permeation current density [$\mu A/cm^2$].

F- Faraday's constant.

D- hydrogen diffusion coefficient in the material [cm^2/sec].

c- hydrogen concentration in the material [mol/cm^3].

t- time [sec.]

x- distance into the specimen [cm].

For the barnacle electrode the equation of interest is Fick's second law, equation 28. The equation is to be solved with appropriate boundary conditions. Using a Laplace transform method and several simplifications the solution to equation 28 is [24,80-82]:

$$C_0 = \frac{I}{zF}\left(\pi \frac{t}{D}\right)^{1/2} \qquad [29]$$

It has been demonstrated that equation 29 holds true for the actual times for measurements, usually on the order of 30 minutes [24,80].

If the experimental extractive current density-time transient fits the theoretical curves plotted from equation 29, and if the hydrogen diffusion coefficient in the material is known, a measurement of I at any given extraction time will give the hydrogen content,C_0. If D is unknown, the value of $D^{1/2}C_0$ can be determined; that is, the current (or current density) at a given time is proportional to the hydrogen concentration [24].

The barnacle electrode has proved to be a fast, sensitive, and reliable monitoring technique for hydrogen permeation in metals. It has the ability to detect amounts of mobile hydrogen atoms less than 0.1 ppm [24,82]. The method is applicable to detect changes in hydrogen content in service, especially for high-strength low-alloy, HSLA, steels that have relatively high hydrogen diffusivities and low background currents.

The barnacle electrode system is applicable to a wide variety of situations:

- To determine threshold hydrogen values for indexing the degree of embrittlement.
- To study the delayed failure and hydrogen migration in plated steels.
- To determine the hydrogen loss in weldments as a function of time.
- To determine changes in hydrogen concentration after constant load testing.

It should be noted that a difference exists between the barnacle electrode and the Devanathan-Stachurski method since in the first one there is a time interval between charging and extracting. Also, by using the barnacle electrode method a measurement of the oxidation current at any time will yield the hydrogen concentration according to equation 29 derived from Fick's second law, while using the Devanathan-Stachurski technique the absorbed hydrogen concentration can be determined from the following equation, derived from Fick's first law:

$$C_0 = \frac{J_\infty L}{D} \qquad [30]$$

It must be noted that the degree of embrittlement is a function not only of the hydrogen concentration but also of the material, including its heat-treatment and its geometry, which determines the stress concentration at notches and sharp corners. It is therefore necessary to do mechanical testing and correlate failure data with the electrochemical measurements for the material of interest.

2.4. Hydrogen Vacuum Foil Technique

Originally patented in 1993, the Hydrogen Vacuum Foil (Beta Foil) technique provides a qualitative evolution of corrosion activity and hydrogen flux permeation. Through the ability of the Beta Foil to trap mobile hydrogen, this technique proved itself to be very well suited to the study and monitoring of HE problems in petrochemical facilities [13]. The Beta Foil measures the hydrogen flux indirectly, as a pressure increase inside the foil.

The hydrogen flux originates from the hydrogen atoms that are liberated at the cathode during the electrochemical process of corrosion. Graphically, this process for a pipeline is illustrated in Figure 9.

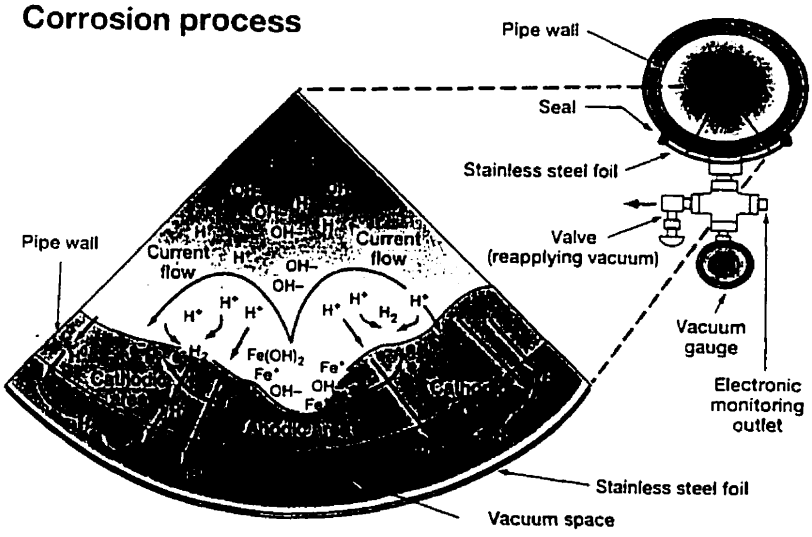

Fig.9: Schematic of corrosion process inside a pipeline and the Hydrogen Vacuum Foil (Beta Foil) assembly [13].

The atomic hydrogen flux generated as a result of corrosion on the inside pipe wall is captured under the Beta Foil as shown in Figure 10.

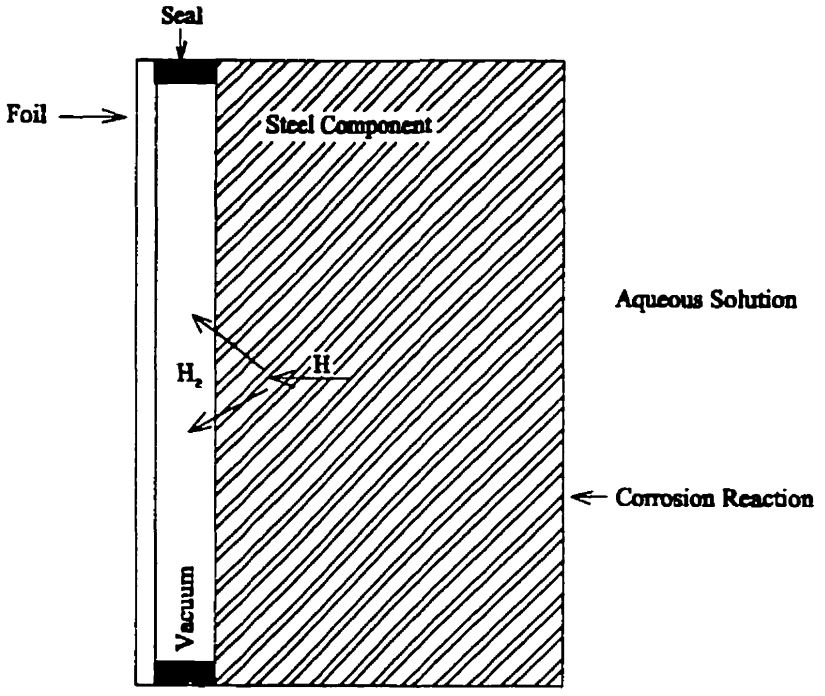

Fig. 10: Schematic of the Beta Foil principle (after Shaw and Matei,[85]).

Beta Foil consists of a thin (approx. 0.127 mm) 316 stainless steel foil, usually in 6 or 12-in. square configurations [11]. Other configurations can be produced to fit around nozzles or on elbows. The foil is attached to a length of capillary tube and the foil is applied directly onto the surface of the pipeline or vessel to be monitored by means of adhesive. This adhesive seal is only a perimeter seal and no adhesive is applied under the foil itself. At the other end of capillary tube, which can have a length of a few feet or a few hundred feet, a tree assembly is located. This tree assembly allows taking vacuum readings, establish the vacuum if corrosion decays it, and isolation of the vacuum after it is established. The tree assembly is located inside an instrument box for weather

protection, and to prevent tampering. The Beta Foil configuration is presented in Fig. 11.

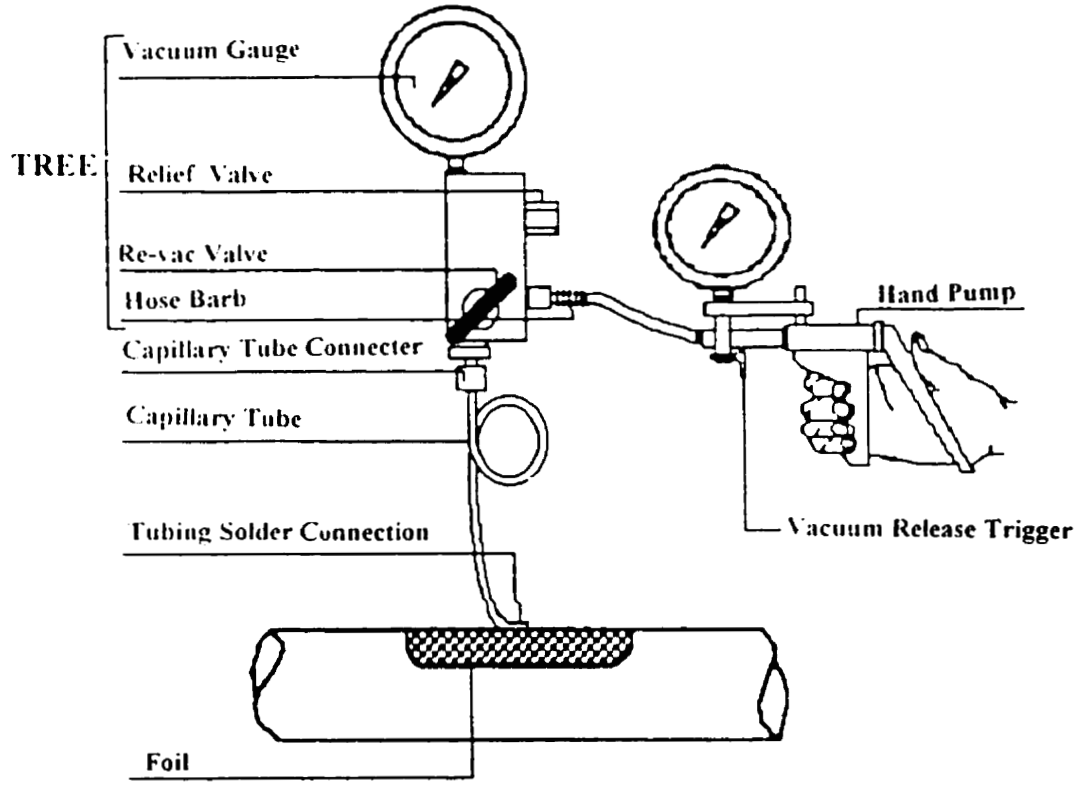

Fig.11: Beta Foil configuration,[84].

The thin stainless steel plate is designated to capture the molecular hydrogen as it is generated from the atomic hydrogen escaping to the outside surface of the pipeline and into the space between the pipe's outside and the foil's underside. Since the definable chamber of this hydrogen foil is under vacuum, the hydrogen atoms react almost instantly to form molecular hydrogen gas according to the following reaction

$$2H^* = H_2. \qquad [31]$$

Hydrogen molecules are many times larger than the single hydrogen atom, and are unable to escape from the vacuum chamber. As more atomic hydrogen escapes into the space between the pipeline and the foil and the molecular hydrogen, H_2, build-up, the

vacuum foil will decay in a ratio proportional to the intensity of the atomic hydrogen permeation taking place from the pipe's inside surface.

Because the Beta Foil works under vacuum, there is almost no air trapped beneath the foil. Also, because a vacuum or a partial vacuum is relatively immune to temperature changes the data gathered in a vacuum are even and are not subject to the wide temperature-induced swings [11-13,83-84].

Not all of the atomic hydrogen necessarily migrates into the steel of the pipe or vessel. Depending upon the process, and the corrosion environment, a certain percentage of these atoms can recombine on the inside surface of the pipe or vessel to form molecular hydrogen gas, H_2. This hydrogen gas ultimately goes into the product stream and is lost in the process flow.

Data (vacuum loss) can be retrieved using a manual vacuum gauge system, online (SCADA) system, an automated (datalogger) system, or by a Low Earth Orbit, LEO, satellite system [13].

The manual gauge system is utilized where the access to the site to be monitored is easy and where the pressure gauge can be frequently read. Depending on the severity of the corrosion or hydrogen permeation the readings can be take as frequently as one per hour or, on locations with little hydrogen activity, twice a month.

The online, SCADA, system is used in those locations with easy access to power sources and SCADA control panels.

The datalogger system seems to be the most accurate in retrieving data from the Beta Foil. Using the datalogger hooked to a pressure transducer one can store months of foil data if necessary. The pressure transducer converts the differential or gauge pressure signal into an electric signal for the datalogger. No external power is necessary as an internal battery lasting up to 5 years powers the device. The datalogger system provides the monitoring up to one per hour and records data more accurately than can be done manually by reading the standard pressure gauge. On top of that, as many as three different foils can be hooked to the same datalogger. The data that is stored in the datalogger can then be downloaded and processed into a computer. This system is recommended for sites where technicians would be visiting every 30-60 days.

The Beta Foil data can be also retrieved by using a state of the art network of 12 Low Earth Orbit, LEO, satellites that continuously circle the earth. The pressure reading is taken from satellite, then the information is transmitted to the nearest earth station, then to the Orbcomm (who operate the satellites) control center in Dulles, Virginia, and then to the customer via fax or Internet. The satellite retrieval gives the opportunity to put Beta Foil sensors in remote and/or difficult to access areas where data retrieval would have normally been cost prohibitive.

Beta Foil software completes the system. It is available in three versions [86]: manual entry into PC, use of the datalogger for downloading and uploading, and a full SCADA system.

The Beta Foil is a masterpiece of simplicity and exhibits several clear advantages over other existing corrosion and/or hydrogen flux monitoring:

- As there are no electronics involved and no access into any environment, there are no safety considerations to be worried about.
- The Beta Foil can be installed in buried locations, underwater, or on the surface.
- The Beta Foil can be installed on site without interrupting the process.
- The Beta Foil can be used virtually anywhere one might need to monitor internal corrosion (hydrogen flux): oil and gas production, petrochemicals, gas plants, pipelines, pressure vessels, pulp and paper, mining and smelting, waterfloods, steam systems, hot water systems, manufacturing processes etc.).
- There are no temperature limitations. The Beta Foil can be epoxied, soldered, brazed, or welded in place.
- The Beta Foil can be of virtually any desired shape and size.
- Except for periodic re-inducing the vacuum, the Beta Foil is maintenance-free and does not require a power source.
- The Beta Foil is non-intrusive.
- The Beta Foil is sensitive to the smallest amount of hydrogen flux.
- The Beta Foil monitors the actual corrosion of the pipe or vessel to which it is attached. In other words, Beta Foil effectively turns the pipe or vessel wall into a corrosion coupon.

- The Beta Foil is simple to operate and the software is user-friendly.

The competition to Beta Foil in monitoring hydrogen permeation is the Barnacle Electrode and the Devanathan-Stachurski cell. In those latter two techniques there are few main disadvantages: problems of leakage, limited applicable temperature range, readings susceptible to changes in temperature, electrolyte concentration, size of cell, material of the cell [69]. Also, both techniques need an external power source.

The development of the Beta Foil permeation technology for precision hydrogen-flux permeation monitoring has allowed the pipeline industry to be able to monitor accurately and rapidly almost all metal structures desired. The speed and control of hydrogen flux permeation had been found to exceed all expectations with changes in flux rates due to internal corrosion intensity being measured in minutes and hours rather than what the previous methods offered of days and weeks.

Although the flux rates vary due to many processes and system parameters, there are three fundamental principles that have evolved [11-14,83-84]:

1. Regardless of the percentage of internal atomic hydrogen that is emitted as a flux, it always represents 100% of the corrosion. Therefore, by reducing the hydrogen permeation rate (hydrogen flux) by 50%, the corrosion is reduced by 50%.
2. The versatility of non-intrusive monitoring allows for precise placement of the foils.
3. The sensor is the structure to be monitored and therefore no false readings are obtained.

It does not matter what caused the corrosion or the ratio of hydrogen atoms that are liberated. The principle of hydrogen flux to corrosion intensity is a reliable measurement of corrosion activity.

CHAPTER 3

EXPERIMENTAL TECHNIQUE AND PREPARATION

3.1. Test Material

The material investigated is AISI 1018 steel in hot-rolled condition. AISI 1018 steel was chosen because it is a representative material, 95% or more of the existing pipelines and pressure vessels exposed to corrosive environments being made from this type of low-carbon steel (0.18%C). Also, hot-rolled steel is much HE resistant than the cold-rolled one. All the specimens are 3.2 mm in thickness. Exposed areas of the various types of specimens are 15.2 x 15.2 cm for the vacuum foil specimen, and 2.54 cm diameter for the barnacle electrode specimen. Both sides of the specimens were hand ground to 600 grit in order to remove the scale from the surface. The specimens surface is consistent for all the tests. The specimen surface will affect the corrosion rate, hydrogen pick-up and permeation conditions.

3.2. Solutions Used

Three different solutions have been used in the testing cell. The first solution was NACE TM-0177-90, the second and the third ones being formulated by CANMET. NACE solution is representative in being one of the worst in evaluating materials in oil and gas industry. It is used extensively as a reference to material environment behavior. Since there are no standartized solutions that have evolved to date, a number of formulations as used by CANMET were selected. The CANMET solutions are set using some base of NaCl and various pH values being buffered. The solutions chemistry is as follows:

NACE solution (set pH = 2.44)		**CANMET#1 solution** (set pH = 5.9)		**CANMET#3 solution** (set pH = 1.1)	
$CH_3COONa.3H_2O$	5g	$CH_3COONa.3H_2O$	27.86g	Nacl	99.9g
NaCl	50g	HCl	2 ml	HCl	6.06g
H_2O	1L	NaCl	5 g	H_2O	946 ml
		NaOH	0.5g		
		H_2O	1L		

3.3. Test Equipment

3.3.1. The Hydrogen Vacuum Foil Cell

In order to achieve the objectives of this research program and to carry out comparative testing, a specialized cell was used. This unique cell was designed and made at The University of Calgary in 1997 [85]. The cell incorporates three ports such that a variety of parameters can be monitored and measured simultaneously. One port is used to measure the hydrogen permeation using a barnacle electrode. Another port consists of a larger sized specimen with the Beta Foil attached on the back side of the specimen and the pressure being monitored as a function of time. The special cell will allow direct comparisons between permeable hydrogen rates and changes in the vacuum. The cell is made out of AISI 1018 mild steel with the wall thickness of 0.31 cm, is 40 cm x 20 cm x 25 cm, and holds 18 litres of working solution.

A schematic of the cell (with the foil and barnacle electrode attached) is presented in Figure 12. Photos of the cell, front and back, without the foil and the barnacle electrode attached, are shown in Figures 13 and 14. A close-up of the cell with the vacuum foil attached is shown in Figure 15. A Plexiglass lid seals the top of the cell and allows passage of instrumentation as well as gas inlet and outlet ports.

The working solution is continually circulated through the cell with the assistance of an exterior plastic centrifugal pump with a flow rate of 15.89 L/min. This translates into a solution change within the cell of 1.13/min. This will ensure that the corrosion on the sample is maintained fairly consistant and that stagnation of corrosion products is not occurring throughout the cell.

The bottom of the cell is connected to a drain, which makes it possible to drain the solution after each experiment.

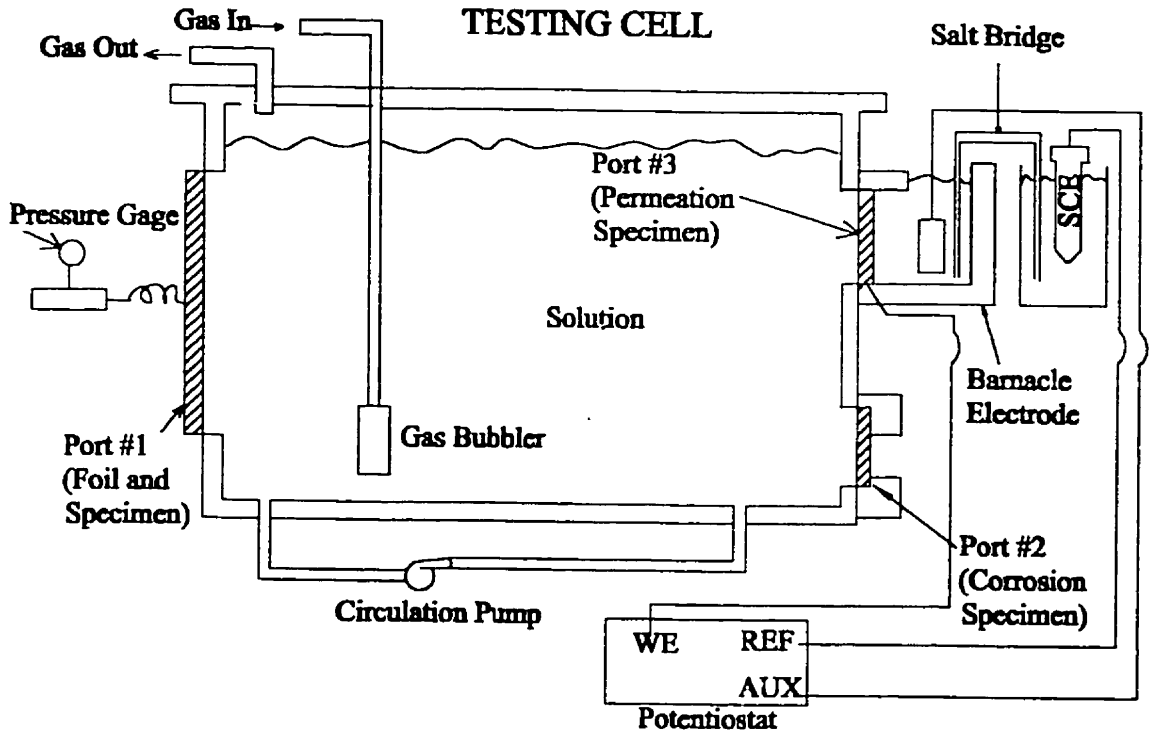

Fig.12: Schematic of the special testing cell [85].

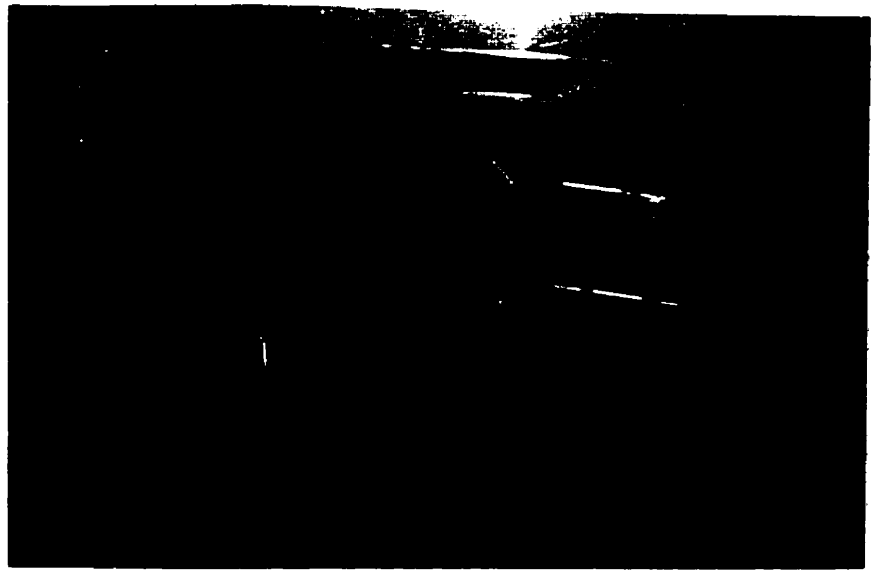

Fig.13: Close-up of front side of the cell.

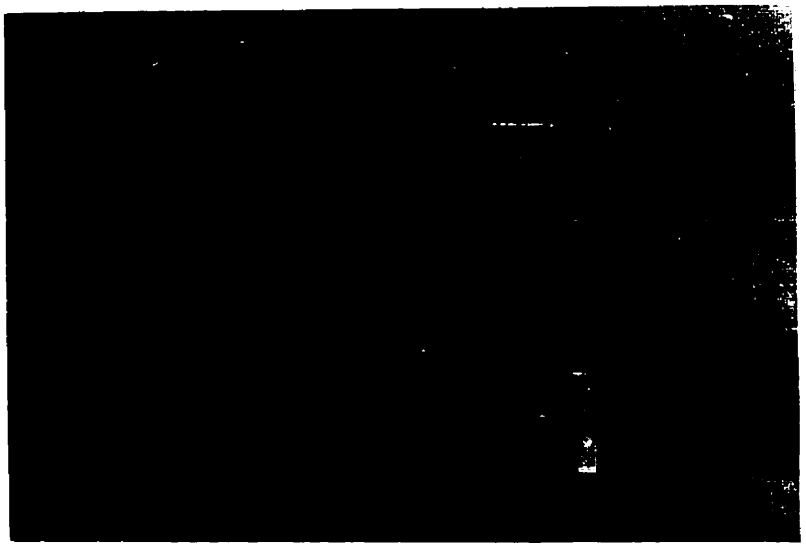

Fig. 14: Close-up of the back side of the cell.

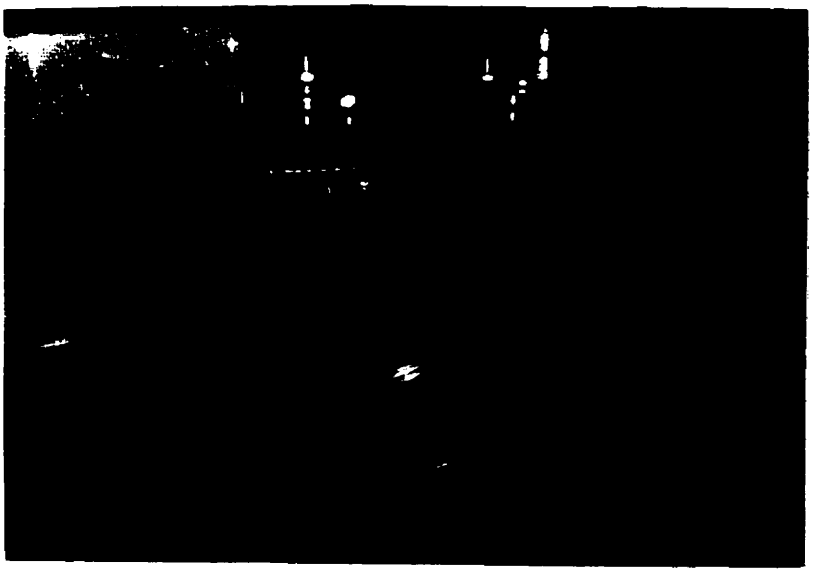

Fig. 15: Close-up of mounted vacuum specimen.

3.3.1.1. Coatings for Steel Fabricated Equipment

The cell is electrically isolated and corrosion protected, having been covered on the interior and on the exposed areas (around all ports) with a coating material. In this regard, a number of coatings were evaluated before use. First, two Teflon coating materials supplied by Whitford Corporation were applied and evaluated. The Teflon coatings were put on as an undercoating (XYLAN-P-92DF Primer-Sealer) and a top coat (XYLAN-1014DF870 Black) and were baked in oven at 200^0C in order to have them cured properly. The advantage of the Teflon coatings were that extremely thin coating thickness results. However, long term exposure to many of the extremely corrosive environments that were being used for this study resulted in general deterioration of the coating after a period of approximately a month, generally blistering took place indicating the presence of small pin holes. Thus, Teflon coatings can be used for various periods of time but eventually must be removed by sandblasting after each experiment and then re-coated.

Another coating material was also evaluated and used, that being a polyurethane with crumb rubber addition. This coating material is found to be extremely durable and is generally the material of preference for long term equipment exposure. However, the coating thickness is considerably thicker and therefore some of the intricate parts cannot be coated with this material. For these components Teflon coating must be used.

3.3.2. The Barnacle Electrode Cell

Electrochemical permeation of hydrogen was measured using a Teflon cell (barnacle electrode) with a 2.54 cm diameter specimen exposure, a liquid cell volume of 70 ml and a position of the auxiliary electrode at 53 mm from the specimen surface, attached to the back of one specimen [72]. Therefore, one side of the permeation specimen was exposed to the solution in the large cell and the other side was exposed to the barnacle electrode solution that is 0.2N NaOH.

A close-up of the hydrogen vacuum cell without and with the barnacle electrode attached on the front is presented in Figure 16 and 17.

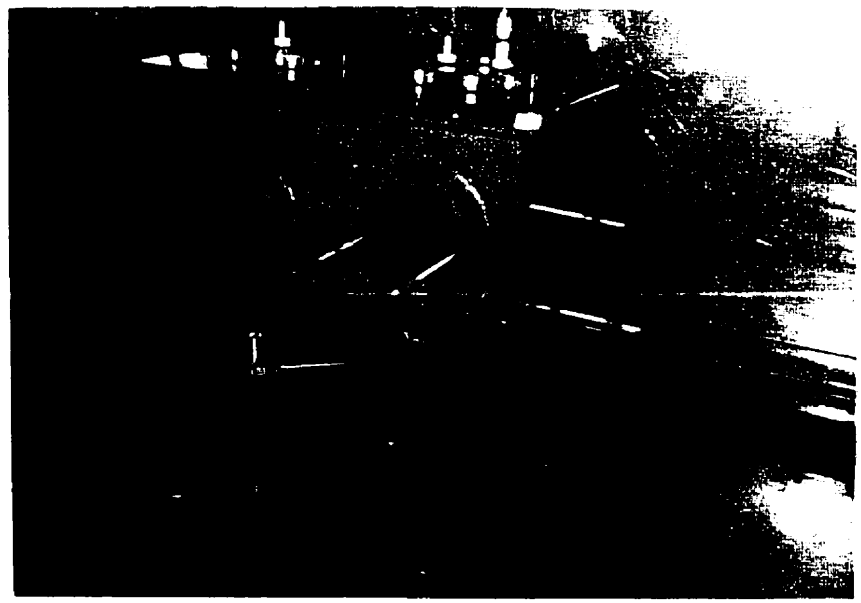

Fig.16: Close-up of the cell without barnacle electrode attached.

Fig.17: Close-up of the cell with the barnacle electrode, Luggin probe, and circulating pump attached.

3.3.3. Potentiostat

A potentiostat was used for all electrochemical testing for this project. The potential was able to hold a constant voltage on the steel specimen of -0.340V versus saturated calomel electrode, SCE, and to obtain a recording of current. The anodic potential was chosen to ensure oxidation of all hydrogen atoms coming out of the specimen and to avoid steel oxidation A front panel display provided readings of the current. The potentiostat was also connected to a computer capable to take and store the data (hydrogen oxidation current) every minute. The average values of the current density after each 5 minutes were recorded and printed out.

3.3.4. Reference Electrode

A saturated calomel electrode, SCE, was used outside the barnacle cell via a salt-bridge (Luggin-probe) to provide feedback to the potentiostat. The SCE was immersed in a beaker filled with 0.2N NaOH solution. The NaOH solution (also used in the barnacle electrode) maintains the specimen surface in a passive condition so that oxidation of steel does not contribute to the measured current.

3.3.5. Auxiliary Electrode

The auxiliary electrode was made of AISI 316 stainless steel, with a 2.54 cm in diameter and was placed inside the barnacle electrode. This electrode was also connected directly to the potentiostat. The auxiliary electrode is commonly used in polarization studies to pass current to or from a test electrode.

3.3.6. Salt-Bridge

A Luggin-probe salt-bridge (conducting path) connected the barnacle electrode to a beaker filled with 0.2N NaOH solution containing the reference electrode.

3.3.7. Hydrogen Vacuum Foil

The vacuum foil was attached on the back of the plate specimen with an active area being 15.2 cm x 15.2 cm. Between the specimen and the port an O-ring gasket was placed in order to prevent any leakage. The foil is made of AISI 316 stainless steel, 0.127 mm in thickness, and was attached by sealing with epoxy around it's edges.

The applied vacuum at the start of a test was 80 kPa below atmospheric pressure, or 604 torr, or 0.78 atm., or 0.8 bar, or 601.14 mmHg. The foil was evacuated and the vacuum re-induced every time it approached 20 kPa vacuum.

The capillary between the foil and the pressure transducer was 1.70 mm in internal diameter with a length of 3.10 m. In order to study the influence of capillary length on the vacuum decay response time capillaries with a length of 1.24 m and 18.60 m respectively, were also used.

3.3.8. Vacuum Data Recording Module

A Beta Pac^{TM} data recording module (datalogger model CP-XA) connected to a pressure transducer was used for storing the vacuum readings taken automatically every hour during the experiments. At the end of each experiment the collected data was downloaded into a computer (using the LS-4 Datalogger version 4.3X software by Lakewood Systems Ltd.) and then imported into Betaworks 32 software for graphing. From Betaworks 32 the graphs were imported again, into Excel.

The overall equipment set-up, including: the so-called Beta box (containing the datalogger, pressure transducer, pressure gauge, and the manual pump for re-inducing vacuum), the experimental cell with the barnacle electrode cell and the Luggin probe attached on the back of the large cell (the attached Beta Foil is not visible in this photograph), the centrifugal pump for circulating the working solution, the potentiostat, the computer used to record the oxidation current, bottles with various gases used (H_2S, H_2, Ar, O_2), and Tygon tubing connections are illustrated in Figure 18.

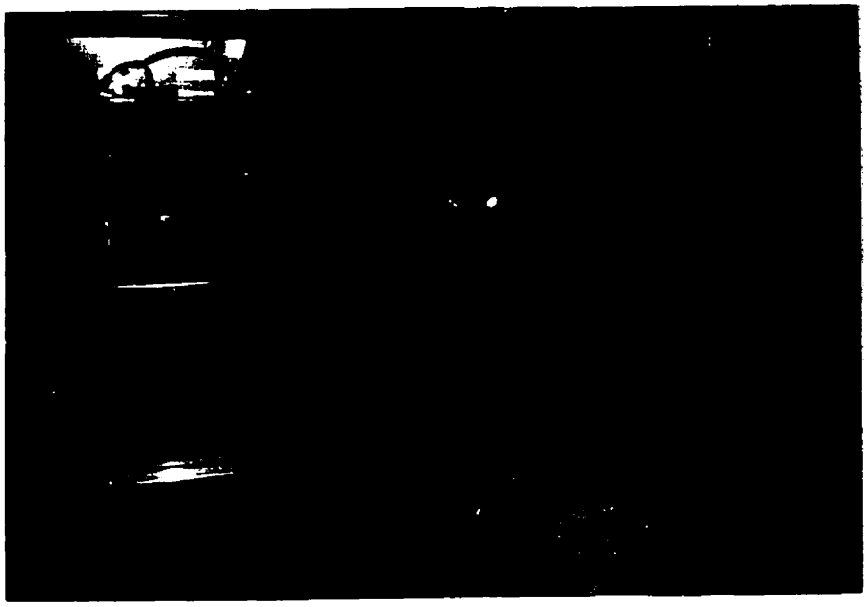

Fig.18: Overall equipment set-up.

Most individual tests were run 10 or 14 days in duration, some tests went on for periods from 4 to 6 weeks each. Thus, quite a varied duration in testing time took place. The testing time is dependent upon first obtaining steady-state conditions and second in accumulation of sufficient hydrogen for accurate measurements.

3.3.9. Discussion of Errors and Variability

The accuracy of the measurements is a very important aspect for this present research program. The accuracy of the datalogger pressure measurements is within ∓1kPa, while for the manual readings is ∓2kPa. The measured hydrogen oxidation current is accurate within ∓0.1-0.2μA, while the voltage supplied by the potentiostat is 1mV accurate. The time measurements as performed by the computer are accurate within 5 min/month.

From duplicate tests, under same experimental conditions, the voltage of the potentiostat varied between 0.339-0.342V, while the presure detected by the datalogger varied within ∓0.1kPa.

CHAPTER 4

EXPERIMENTAL RESULTS AND ANALYSIS

Table 1 presents the summary of all the 16 tests that were carried on for the present research program. The total duration of the tests was 5,520 hours, or 230 days. 38 sequences of various environments were analyzed. The last column in Table 1 indicates the scope of the each test.

Test no.	*Solution*	*Sequence of environments*	*Duration*	*Scope*
1	NACE	N_2 only	4,020 min. (67 hrs.)	check cell
2	NACE	N_2-H_2S-N_2	10,650 min. (178 hrs.)	effect of H_2S
3	NACE	N_2-H_2S-N_2	5,960 min. (100 hrs.)	effect of H_2S
4	CANMET#1	N_2-H_2S-N_2-H_2S-N_2	17,035 min. (284 hrs.)	effect of H_2S
5	CANMET#1	N_2-H_2S-N_2-H_2S-air-N_2	31,405 min. (524 hrs.)	effect of H_2S and air
6	NACE	N_2-air-N_2-H_2S-N_2	42,300 min. (705 hrs.)	effect of air and H_2S
7	NACE	N_2-air-N_2-H_2S	43,300 min. (721 hrs.)	effect of air and H_2S
8	NACE	N_2-H_2-Ar	53,020 min. (884 hrs)	effect of inert gases
9	NACE	N_2-H_2S-N_2-H_2S	50,080 min. (834 hrs)	effect of capillary length
10	NACE	N_2-H_2-N_2	8,890 min. (148 hrs.)	effect of extra H_2
11	CANMET#1	N_2-H_2-N_2	7,215 min. (120 hrs.)	effect of extra H_2
12	CANMET#3	N_2-H_2-N_2	10,110 min. (168 hrs.)	effect of extra H_2
13	CANMET#3	N_2-H_2-N_2	18,630 min. (310 hrs.)	effect of extra H_2
14	NACE	N_2 only	12,900 min. (215 hrs.)	effect of As
15	NACE	N_2 only	8,580 min. (143 hrs.)	effect of Se
16	NACE	N_2 only	7,125 min. (118 hrs.)	effect of Se

Table 1: Summary of tests performed.

4.1. Electrochemical Permeation Behavior

4.1.1. Transient Barnacle Electrode Behavior

A steady-state condition was obtained using the various environment combinations, starting the test off with nitrogen, N_2, gas. Once a steady-state condition had established itself then a change in gas was made which in turn resulted in a transient occuring. The results of these transient response times are given in Table 2, both for the barnacle electrode and the Beta Foil. Where "no change" is written in the table it means that there was no change in the electrochemical permeation behavior, or that change was so small (less than 1 μA/24 h) it was considered negligible. The same type of criteria was used for the Beta Foil, where the slope of the vacuum decay versus time remained the same.

It can be said that a fairly rapid response (13 minutes, average value) takes place especially when H_2S is introduced into the system, that is going from N_2 to H_2S. The response time when switching back, from H_2S to N_2, is much slower. This is due first to a time period required for the H_2S that is dissolved in the solution to dissipate and second due to the fact that N_2 does not promote hydrogen absorption on the steel surface to the same degree that H_2S does. The latter is a poison known to promote HE by permitting a large fraction of hydrogen atoms to enter the metal and further accelerate the iron dissolution reaction. Poisons are known to block the hydrogen-hydrogen, H-H, recombination reaction and thus favor entry of the adsorbed hydrogen into the metal or alloy. Two typical response behaviors for these two cases are illustrated in Figure 19 and Figure 20. Figure 19 presents the electrochemical response for the sequence going from N_2 to H_2S. Here a very sudden spiked response occurs. Later the steady state establishes itself at a lower level due to film formations on the steel surface. The film formed on the surface was observed at the end of the test. The other response going from H_2S to N_2 is depicted in Figure 20. In this case a long elapse time occurs then a peaking followed by a settling down to a higher hydrogen diffusion rate as the film formation is removed from the specimen's surface.

Another typical response is shown for an environment that does not form a corrosion film on the surface. Here a typical overshoot type of response takes place, Figure 21. This is familiar to those using the electrochemical permeation measurement technique. However, it is not very clear why this form of a response takes place.

Test/Solution	*Environmental sequence*	*Time elapsed from beginning of test [min.]*	*Beta Foil Response time [min.]*	*Barnacle Electrode Response time [min.]*
Test#5/CANMET#1	N_2-H_2S	2,680	30	15
	H_2S-N_2	12,000	150	405
	N_2-H_2S	18,970	30	35
	H_2S-air	21,865	15	30
	air-N_2	24,995	55	not determined
	N_2-air	30,095	65	not determined
Test#6/NACE	N_2-air	4,500	10	not determined
	air-N_2	12,720	not determined	not determined
	N_2-H_2S	32,970	30	10
	H_2S-N_2	37,320	10	30
Test#7/NACE	N_2-air	9,895	5	5
	air-N_2	24,205	55	15
	N_2-H_2S	30,010	25	5
Test#8/NACE	N_2-H_2	30,025	no change	no change
	H_2-Ar	37,720	no change	no change
Test#9/NACE	N_2-H_2S	21,480	120	30
	H_2S-N_2	25,800	55	10
	N_2-H_2S	39,875	20	10
	H_2S-N_2	42,945	25	no data
Test#10/NACE	N_2-H_2	6,065	no change	no change
	H_2-N_2	8,765	no change	no change
Test#11/CANMET#1	N_2-H_2	5,755	no change	no change
	H_2-N_2	7,185	no change	no change
Test#12/CANMET#3	N_2-H_2	5,605	no change	no change
	H_2-N_2	9,925	no change	no change
Test#13/CANMET#3	N_2-H_2	7,350	no change	no change
	H_2-N_2	8,745	no change	no change
Test#14/NACE	6 µg/l $NaHAsO_4$ added	5,795	no change	no change
	30 µg/l $NaHAsO_4$ added	10,090	no change	no change
	60 µg/l $NaHSO_4$ added	10,360	no change	no change
	600 µg/l $NaHSO_4$ added	11,560	< 60	10
Test#15/NACE	600 µg/l H_2SeO_3 added	5,590	< 60	5
	H_2S	7,020	5	5
Test#16/NACE	600 µg/l H_2SeO_3 added	5,490	< 60	5

Table 2: Transient response comparisons of hydrogen permeation.

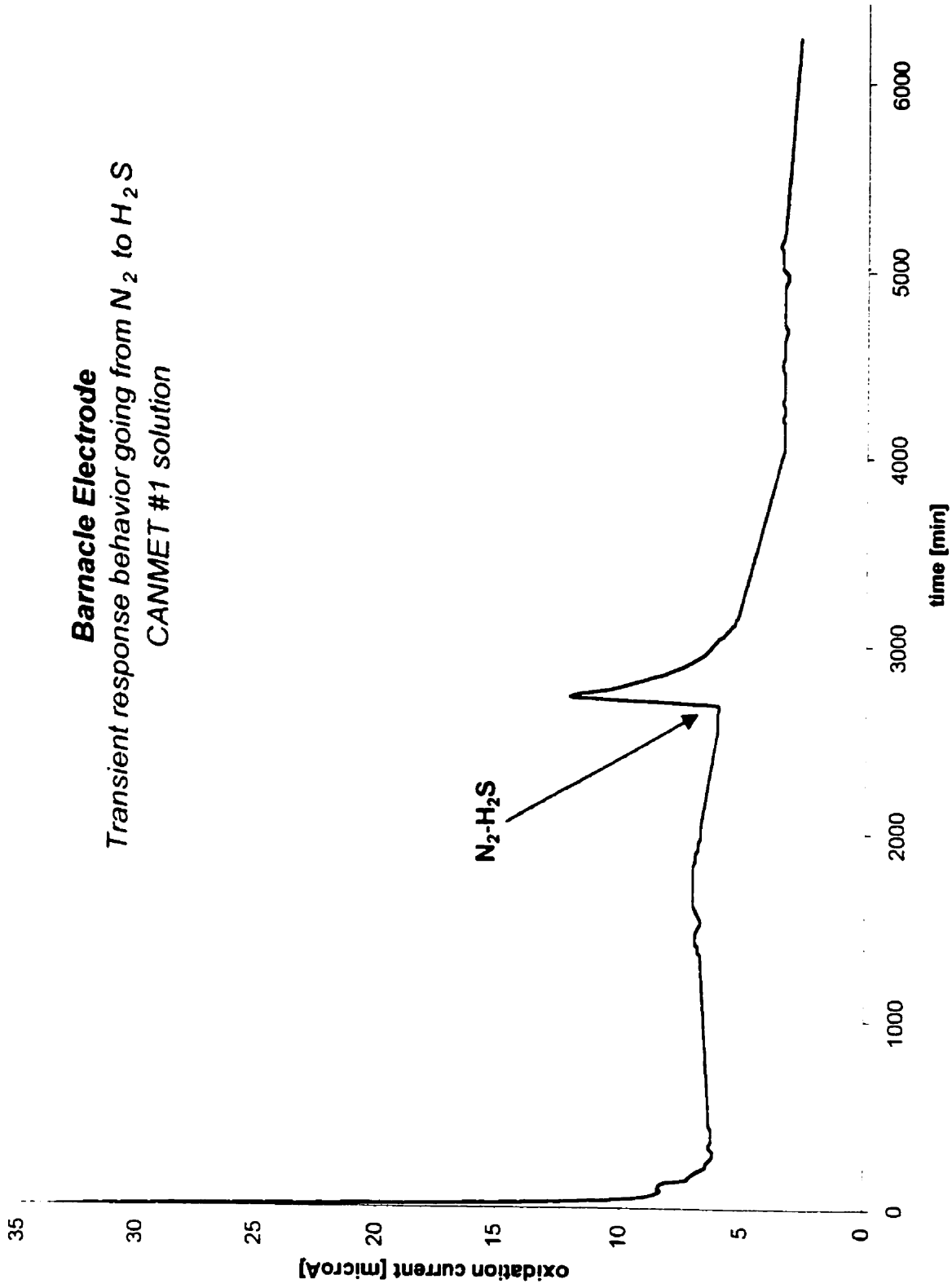

Fig.19: Barnacle electrode response behavior going from N_2 to H_2S (CANMET sol.).

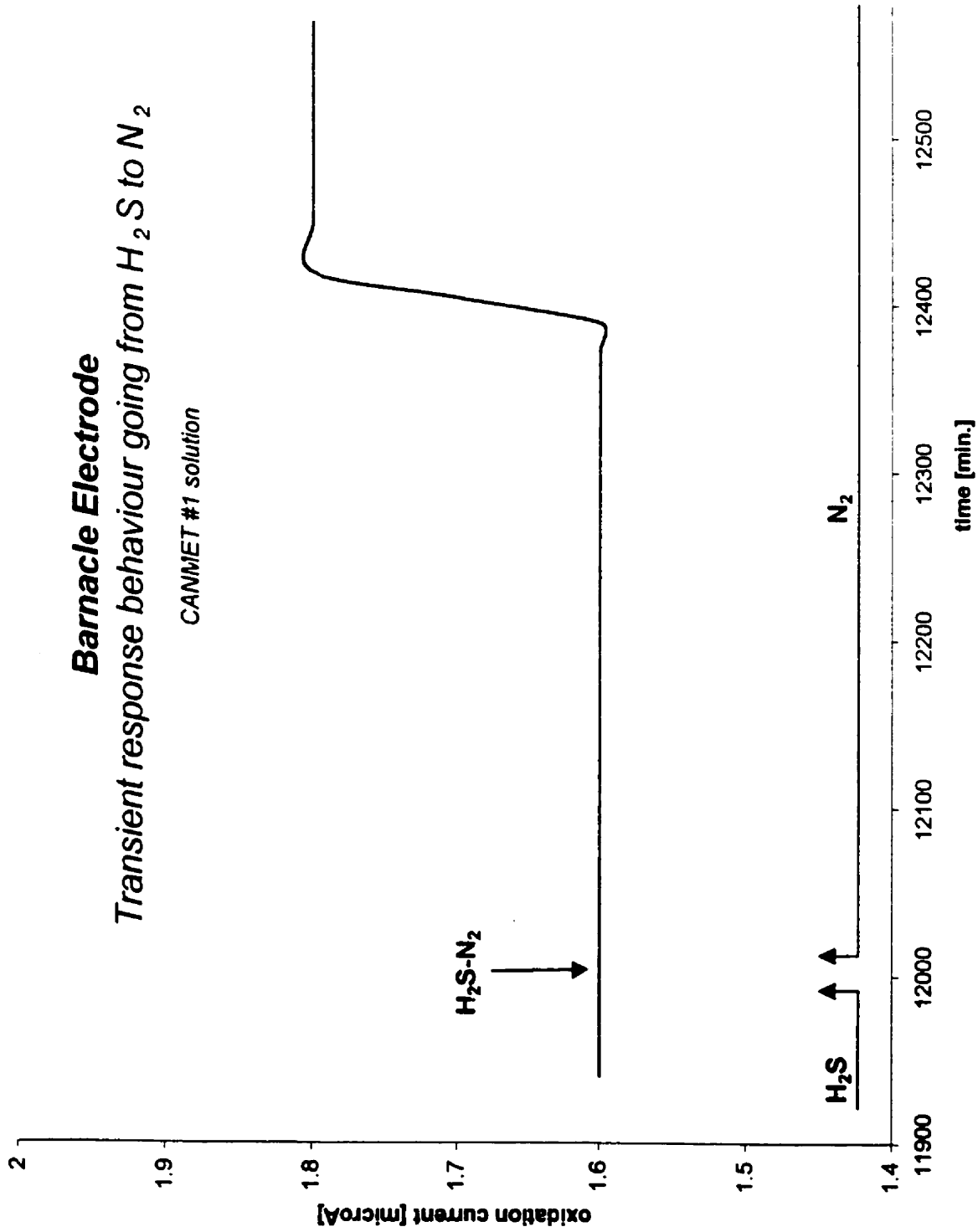

Fig.20: Barnacle electrode response behavior going from H_2S to N_2 (CANMET sol.).

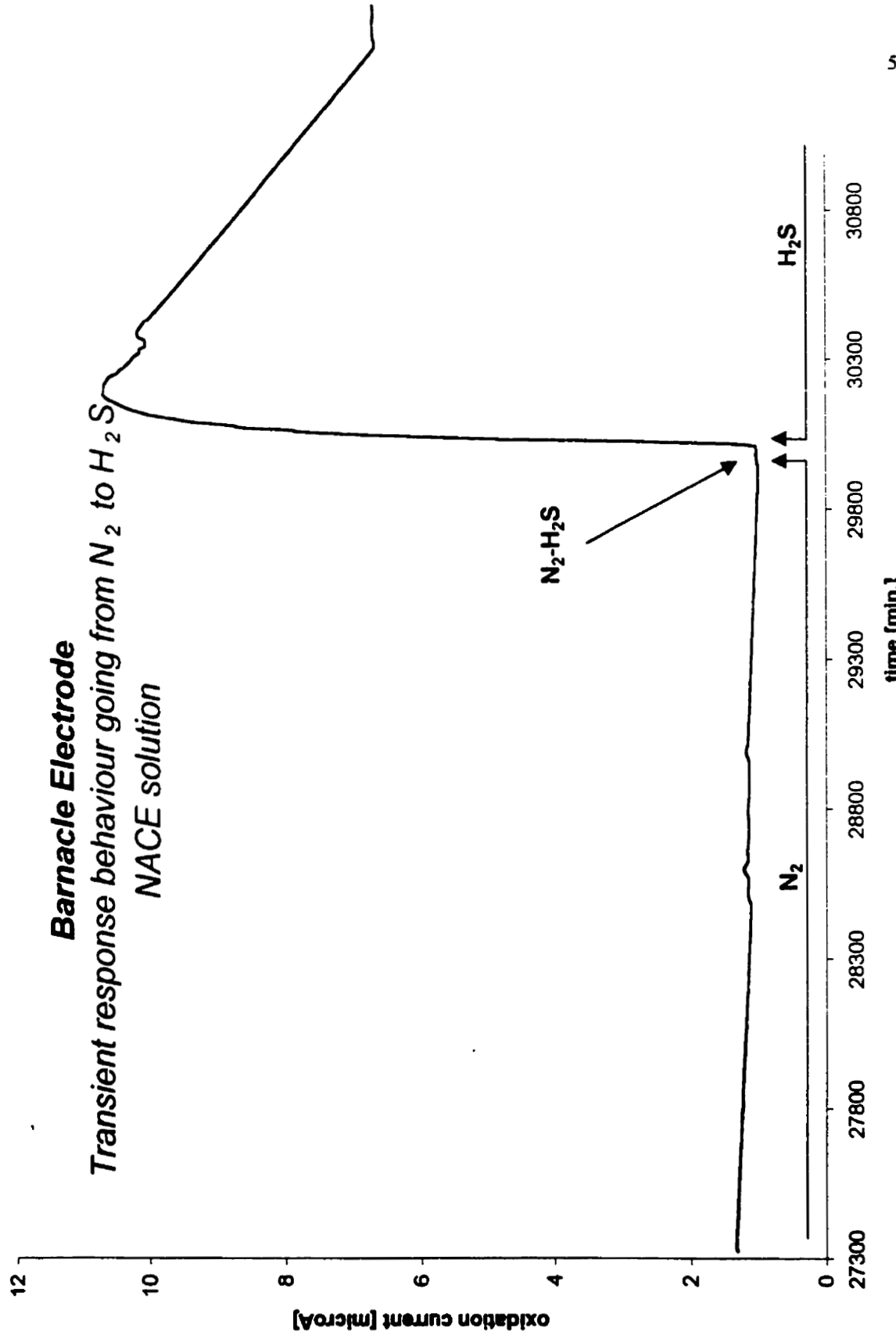

Fig.21: Barnacle electrode response behavior going from N_2 to H_2S (NACE sol.).

4.1.2. Steady-State Barnacle Electrode Behavior

As shown in Figures 19, 20, and 21, a steady-state condition requires a considerable period of time to establish itself. Theoretically a full steady-state condition is not attained, a small continuous decrease in the oxidation current was observed even after longer times of exposure (more than 10 days). However, a steady-state condition was defined as being when the decrease in the oxidation current is less than 1 μA/24 h. At the beginning of each test N_2 was purged into the cell. A steady-state condition is obtained after 5-8 days of continuous exposure.

The results of the steady-state relationships are given in Table 3. It can be seen at a glance that depending on the environment and its sequencing, the steady-state value of the hydrogen oxidation current can vary quite significantly.

Taking information from Table 3 using the NACE solution, an average value of steady-state hydrogen permeation current is 2.96 μA. In most tests the permeation of hydrogen was measured first under a N_2 environment, then the environment was changed to H_2S and then back to N_2. In the case where H_2S was purged into the cell, an average value of steady-state hydrogen permeation current is 5.5 μA. The flux difference between the H_2S condition and N_2 condition would indicate that in the case of NACE solution corrosion in the H_2S environment is higher than in the N_2 testing, as expected. The magnitude of the hydrogen oxidation current in the barnacle electrode is a direct indication of the extent of corrosion occurring in the large cell. When purging N_2 again, after H_2S exposure, the average value of steady-state hydrogen permeation current is now 1.63 μA. The difference in the steady-state permeation currents between the first exposure and the second exposure to N_2 is likely due to the formation of a film on the specimen during H_2S exposure that was not completely removed from the solution when switching back to the N_2 environment. This film is a barrier to active corrosion and hence generation of hydrogen. When purging H_2 gas through the large cell an average value for the steady-state current was then found to be 3.05 μA, a very close value to the one obtained when purging N_2. All the values discussed above are graphically presented in the bar chart from Figure 22.

Test/Solution	*Environment*	*Time to reach steady-condition measured from the last change in environment [min.]*	*Steady-State Current [μA]*
Test#2/NACE	H_2S N_2	4,380 6,210	3 83 2 64
Test#3/NACE	H_2S	4,500	6 8
Test#5/CANMET#1	N_2 H_2S N_2 H_2S	2,560 9,260 5,755 2,990	6 1 1 6 2 1 2 6
Test#6/NACE	N_2 air N_2 H_2S N_2	2,700 8,160 10,169 3,150 4,920	3 9 0 7 0 4 2 2 0 8
Test#7/NACE	N_2 air N_2 H_2S	4,075 14,310 5,770 10,505	3 7 1 38 1 05 4 14
Test#8/NACE	N_2 H_2 Ar	27,345 3,045 10,170	1.9 2.2 1 7
Test#9/NACE	N_2 H_2S N_2 H_2S N_2	14,155 4,320 10,215 3,050 6,985	2 10.7 2 5.4 1.4
Test#10/NACE	N_2 H_2	5,760 -	3.9 3 9
Test#11/CANMET#1	N_2 H_2 N_2	5,655 - -	1.9 1.9 1.9
Test#12/CANMET#3	N_2 H_2	5,530 -	4.4 3 8
Test#13/CANMET#3	N_2 H_2	7,065 no data	9.6 no data
Test#14/NACE	N_2 6 μg/l $NaHSO_4$ added 30 μg/l $NaHSO_4$ added 60 μg/l $NaHSO_4$ added 600 μg/l $NaHSO_4$ added	4,805 4,275 270 1,200 1,340	2.4 1.6 1.6 1.4 1.1
Test#15/NACE	N_2 600 μg/l H_2SeO_3 added	5,590 1,430	2.8 0.8
Test#16/NACE	N_2 600 mg/l H_2SeO_3 added	5,415 1,350	2.2 0.9

Table 3: Steady-state hydrogen permeation response from the barnacle electrode.

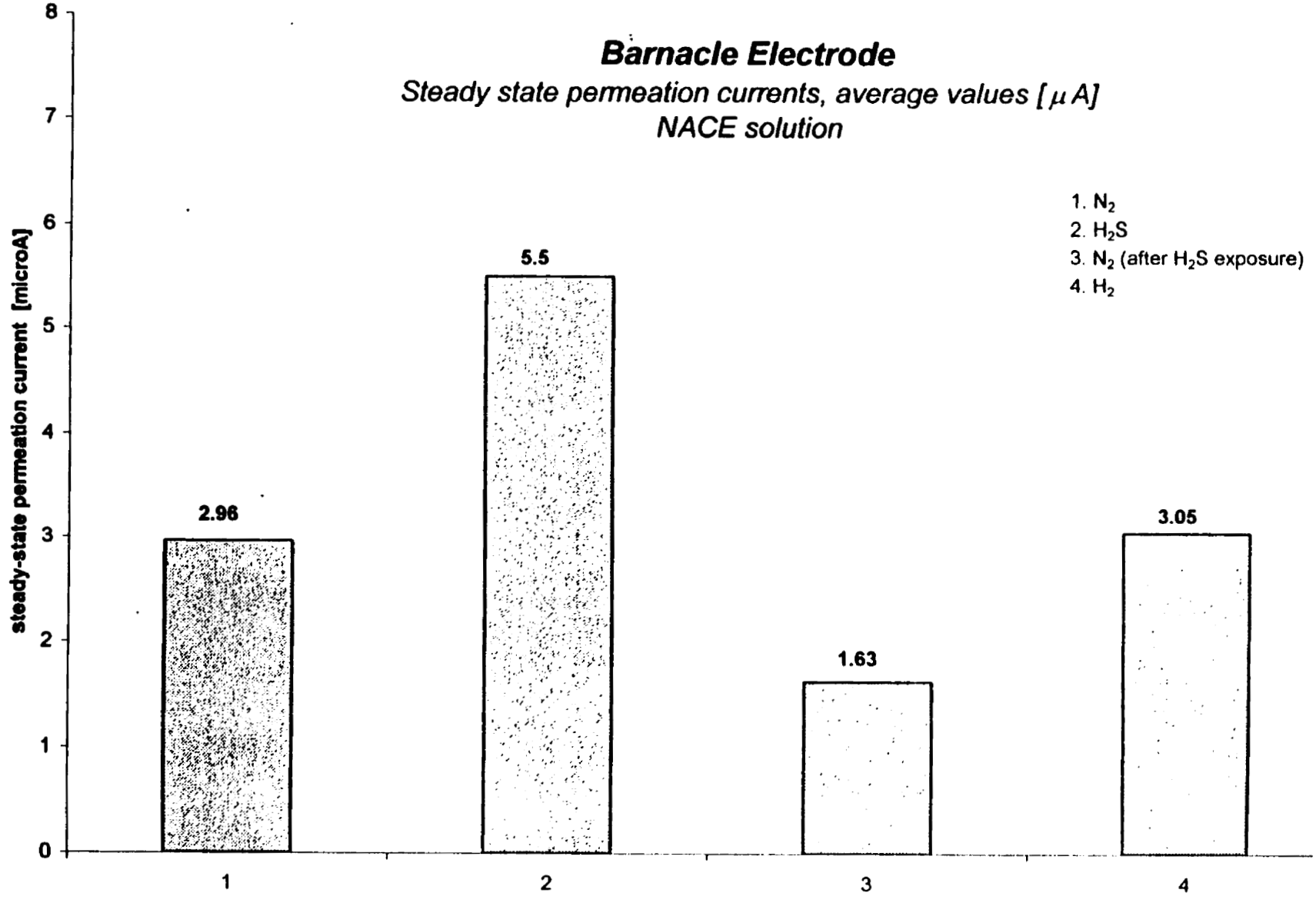

Fig.22: Barnacle electrode: steady-state permeation currents, average values.

The effect of extra hydrogen, H_2, on permeation curves will be presented in more detail in Section 4.5.

As shown in Figure19 and Figure 20, when CANMET#1 solution was employed, the steady-state hydrogen permeation current is higher in the N_2 condition than in the H_2S condition. This flux difference would indicate that for CANMET#1 solution, corrosion in the N_2 environment is higher that in the H_2S environment. That is, for the CANMET#1 solution the steel specimen has a tendency for film formation when the specimen is exposed to the H_2S environment. The overall electrochemical response for the N_2-H_2S-N_2 sequence of environments in the CANMET#1 solution is graphically presented in Figure 23. After a steady-state condition occurred the N_2 was switched off and H_2S was introduced into the system. The response time is almost instantaneous and the electrochemical permeation current rises. After the film started to form on the specimen's surface the current started to decrease; less hydrogen atoms can now permeate through the material. After the condition in the system was changed again, from the H_2S environment back to the N_2 environment, there is some delay time needed for the H_2S to be dissipated out from the solution. Under N_2 influence the film formed on the steel's surface starts to be removed, thus more hydrogen atoms are then generated and can now permeate the material. This effect is illustrated by an increase in the permeation current. Eventually, this current will reach a steady-state condition after the film on the specimen is completely removed.

An average value for the steady-state permeation current when purging N_2 or H_2S using the CANMET #1 solution and CANMET #3 solution cannot be accurately obtained since the continuous formation and then dissolution of the surface's film occurs over a long period of time.

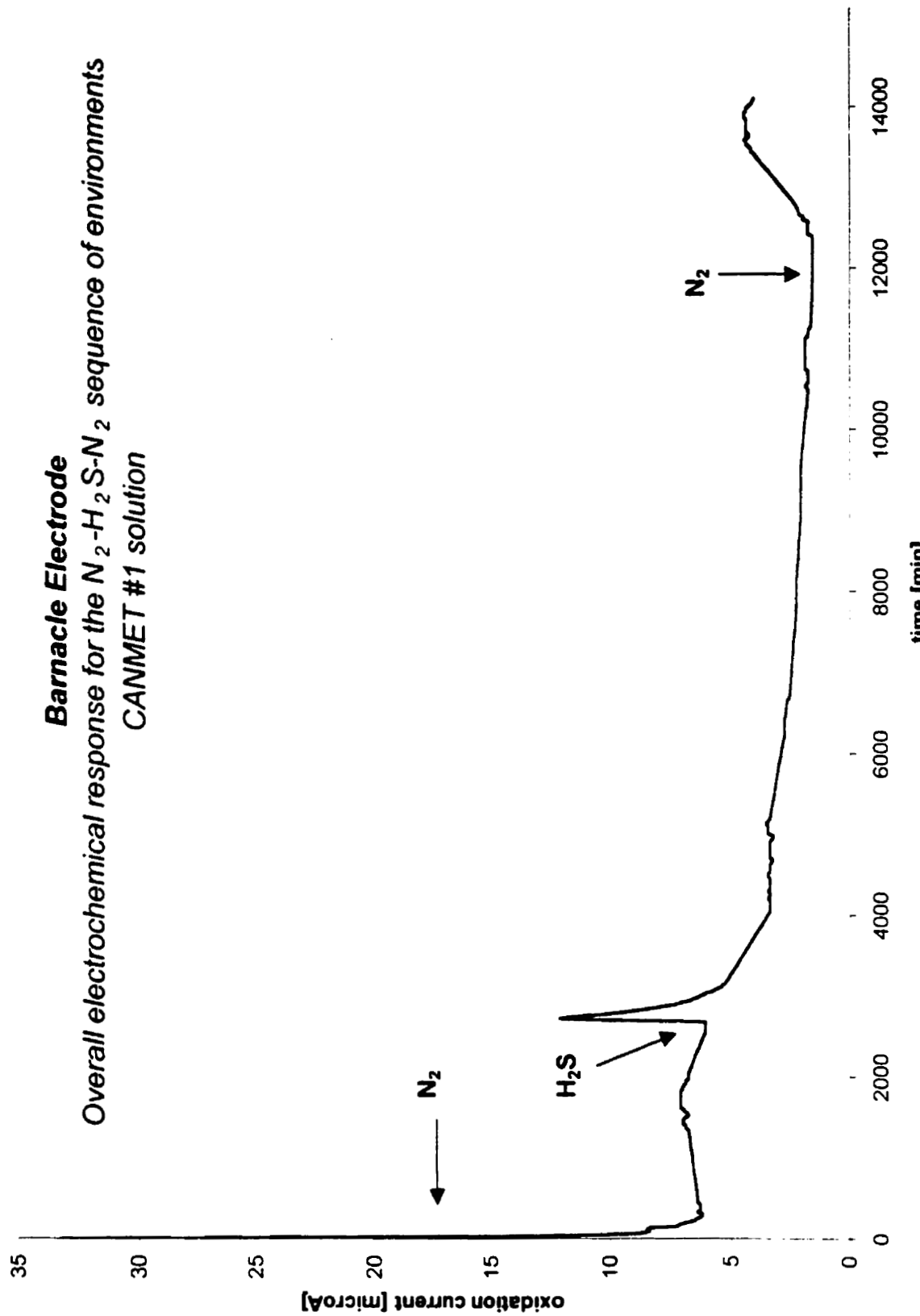

Fig.23: Barnacle electrode: overall electrochemical response for the N_2-H_2S-N_2 sequence of environments, CANMET sol.

4.2. Vacuum Foil Hydrogen Permeation Tests

Vacuum decay was explored under the same conditions as the electrochemical permeation parameters.

A typical vacuum response, in CANMET solution, is depicted in Figure 24 for the N_2 environment and the changing to H_2S environment. The response time is nearly instantaneous. This is in keeping with what was found in the barnacle electrode tests. A similar transient response, when going from N_2 to H_2S, was found for the NACE solution also, and it is graphically illustrated in Figure 25.

However, the response going the other way, from H_2S to N_2, is delayed significantly. This is also in keeping with what was found in the barnacle electrode tests, the delay being due to the fact that there is some time necessary for the H_2S to dissipate out from the solution. A typical vacuum decay, when going from H_2S to N_2, in the NACE solution, is depicted in Figure 26.

The fact that for the CANMET solution corrosion is higher in the N_2 environment than that in the H_2S environment is confirmed by the hydrogen vacuum foil experiments as well, Figure 27. The decay rate of vacuum pressure loss is a main parameter in the interpretation of hydrogen flux. The parameter is a pressure change with time or the slope of the vacuum pressure versus time curve and it is designated as dp/dt. It can be seen from Figure 27, that immediately after switching to the H_2S environment from the N_2 environment the corrosion rate (hydrogen flux) is higher. As soon as the film started to form on specimen's surface the hydrogen flux started to decrease. This behavior is illustrated by the modification of the slope of the vacuum decay versus time curve in Figure 27. After changing the environment back to N_2 again, as soon as the film from the specimen's surface is removed and the H_2S is dissipating out from the solution the hydrogen flux started to increase. This is evident by comparing the slopes from the graph depicted in Figure 27. This is in keeping with what was found in the barnacle electrode tests.

The loss of vacuum or vacuum pressure differential was found to depend upon environment and whether a poison for promoting hydrogen pick-up is present or not.

The effect of various poisons (such as arsenic and selenium) on the hydrogen permeation will be presented in detail in Section 4.6.

Table 4 presents the vacuum decay rate, measured in -kPa/hour, for various environmental conditions. The average values for vacuum decay rate in the N_2, H_2S, and H_2 environments, in NACE solution, are given in the bar chart, Figure 28.

Test/Solution	*Environment*	*Vacuum Decay Rate [-kPa/hr.]*
Test#5/CANMET#1	N_2 H_2S N_2 (after H_2S exposure) air (after H_2S exposure)	0.65 4.89 1.97 0.7
Test#6/NACE	air N_2 H_2S	0.92 0.65 7.53
Test#7/NACE	N_2 air H_2S	1.37 0.56 7.68
Test#8/NACE	N_2 H_2 Ar	0.98 0.94 0.91
Test#10/NACE	N_2 H_2	0.50 0.51
Test#12/CANMET#3	N_2 H_2	1.89 1.74
Test#13/CANMET#3	N_2 H_2	1.28 1.20
Test#14/NACE	N_2 6 µg/l $NaHAsO_4$ introduced 30 µg/l $NaHAsO_4$ introduced 60 µg/l $NaHAsO_4$ introduced 600 µg/l $NaHAsO_4$ introduced	0.23 0.21 0.19 0.19 0.04
Test#15/NACE	N_2 600 µg/l H_2SeO_3 introduced	no data no data
Test#16/NACE	N_2 600 µg/l H_2SeO_3 introduced	0.46 0.03

Table 4: Beta Foil: Vacuum Decay Rates.

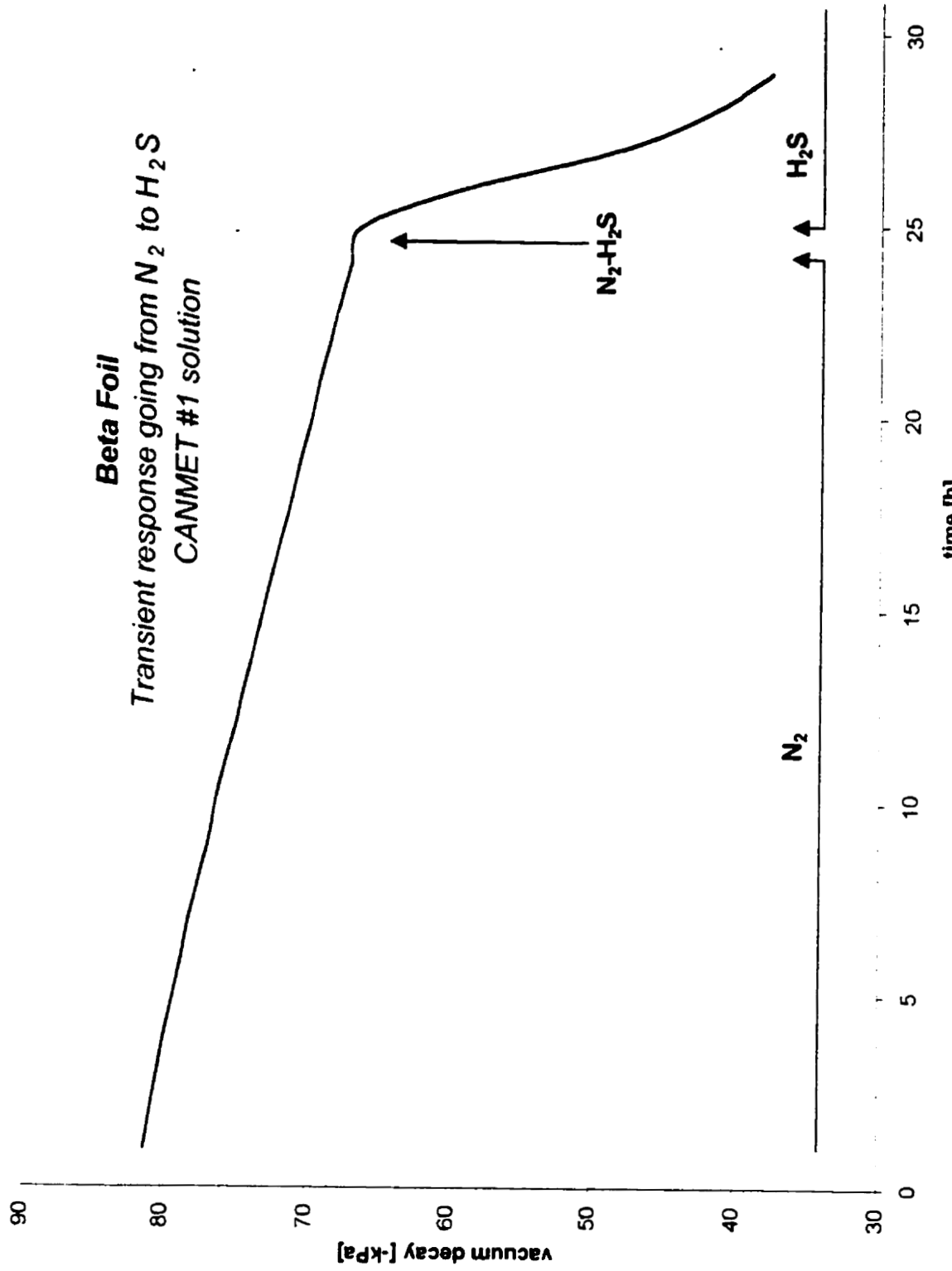

Fig.24: Beta Foil: Transient response behavior going from N_2 to H_2S, CANMET sol.

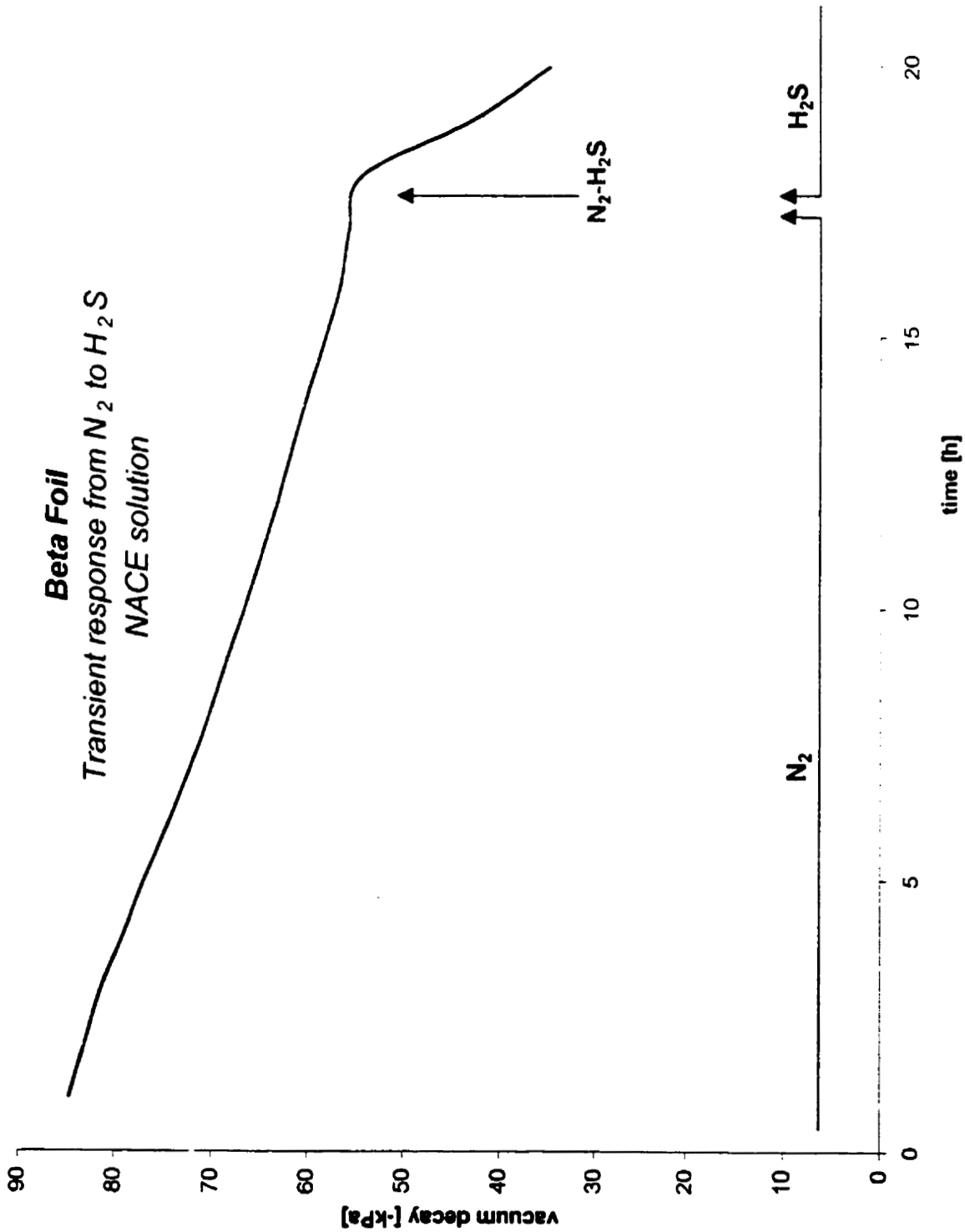

Fig.25: Beta Foil: transient response behavior going from N_2 to H_2S, NACE sol.

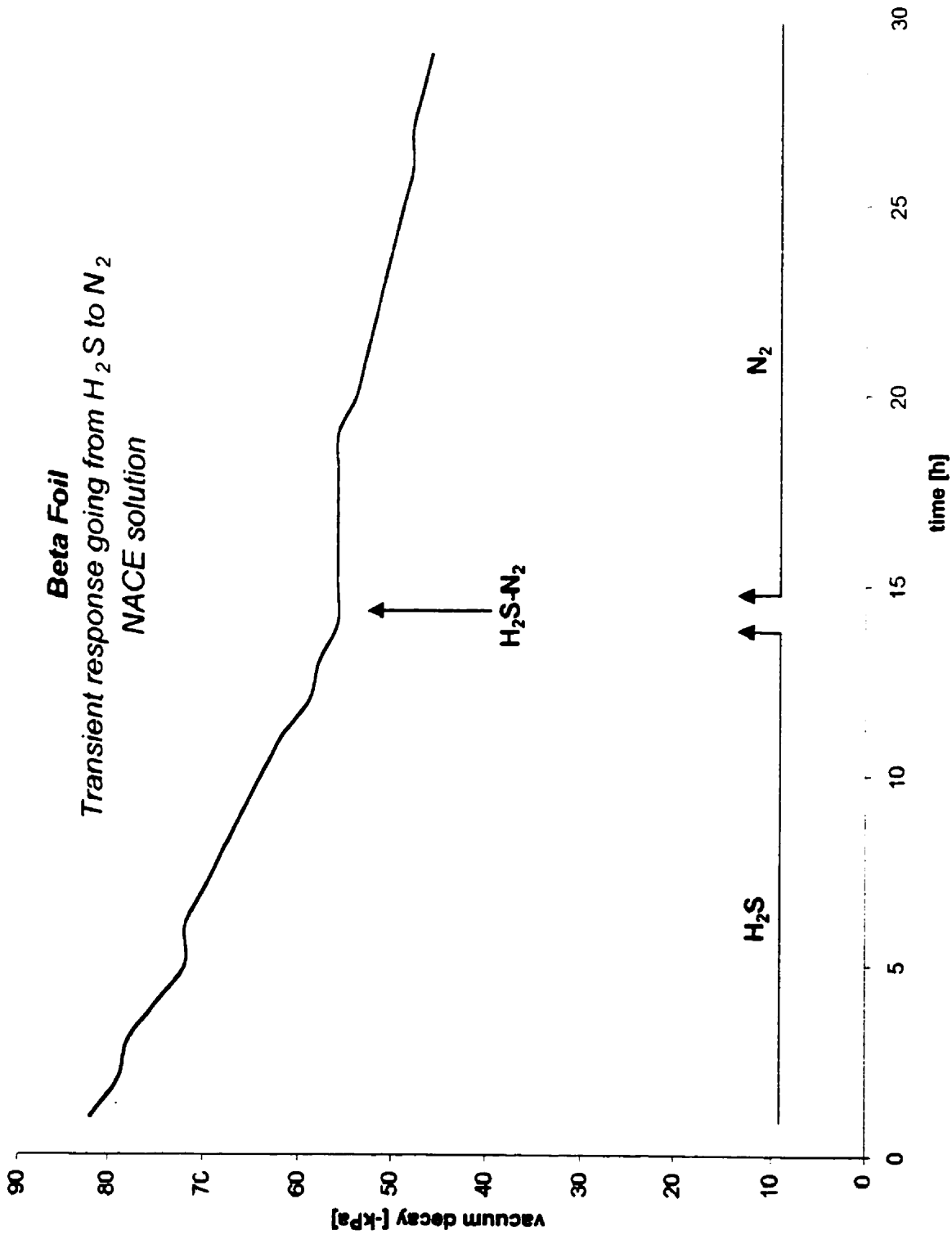

Fig.26: Beta Foil: transient response behavior going from H_2S to N_2, NACE sol.

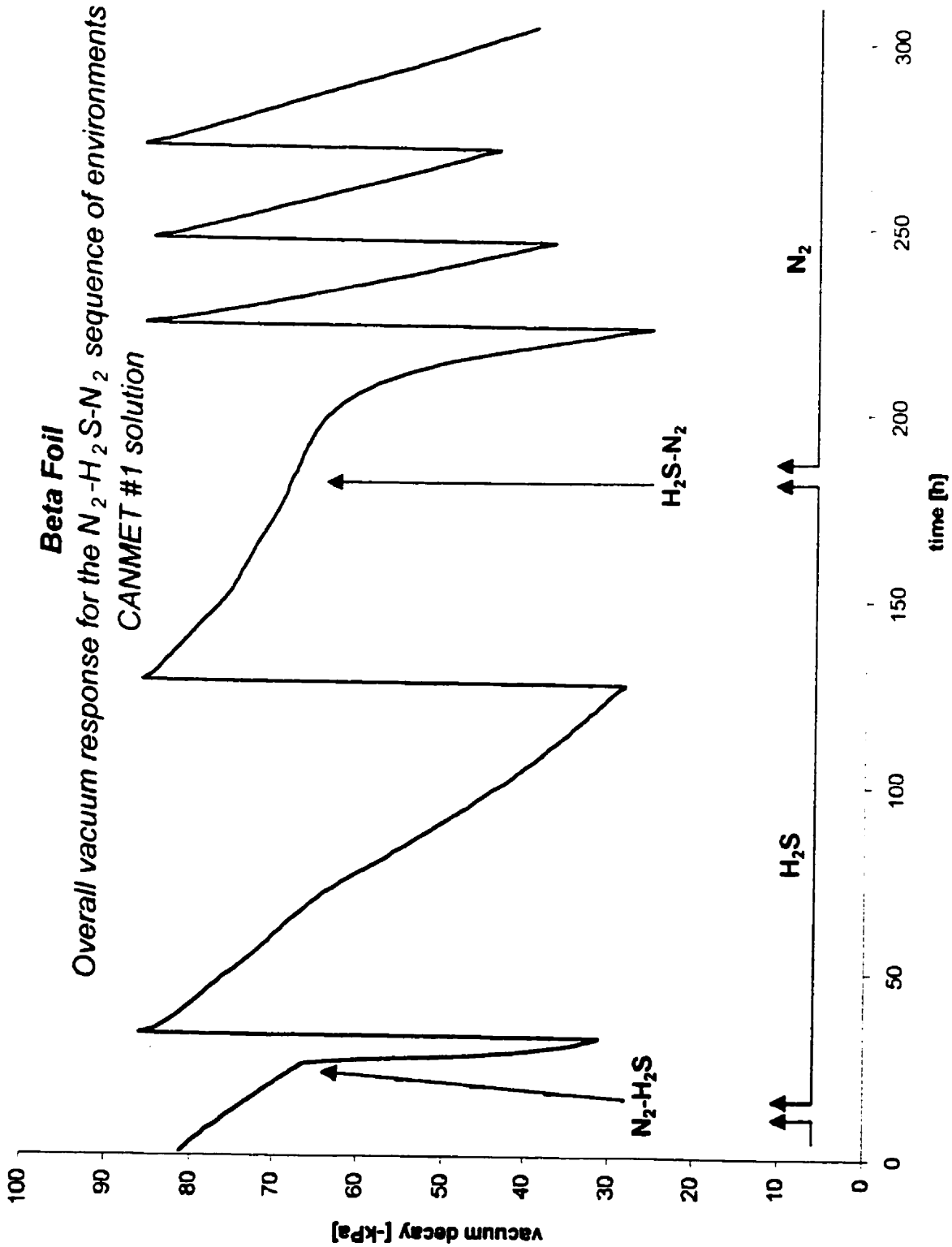

Fig.27: Beta Foil: overall vacuum response for the N_2-H_2S-N_2 sequence of environments, CANMET sol.

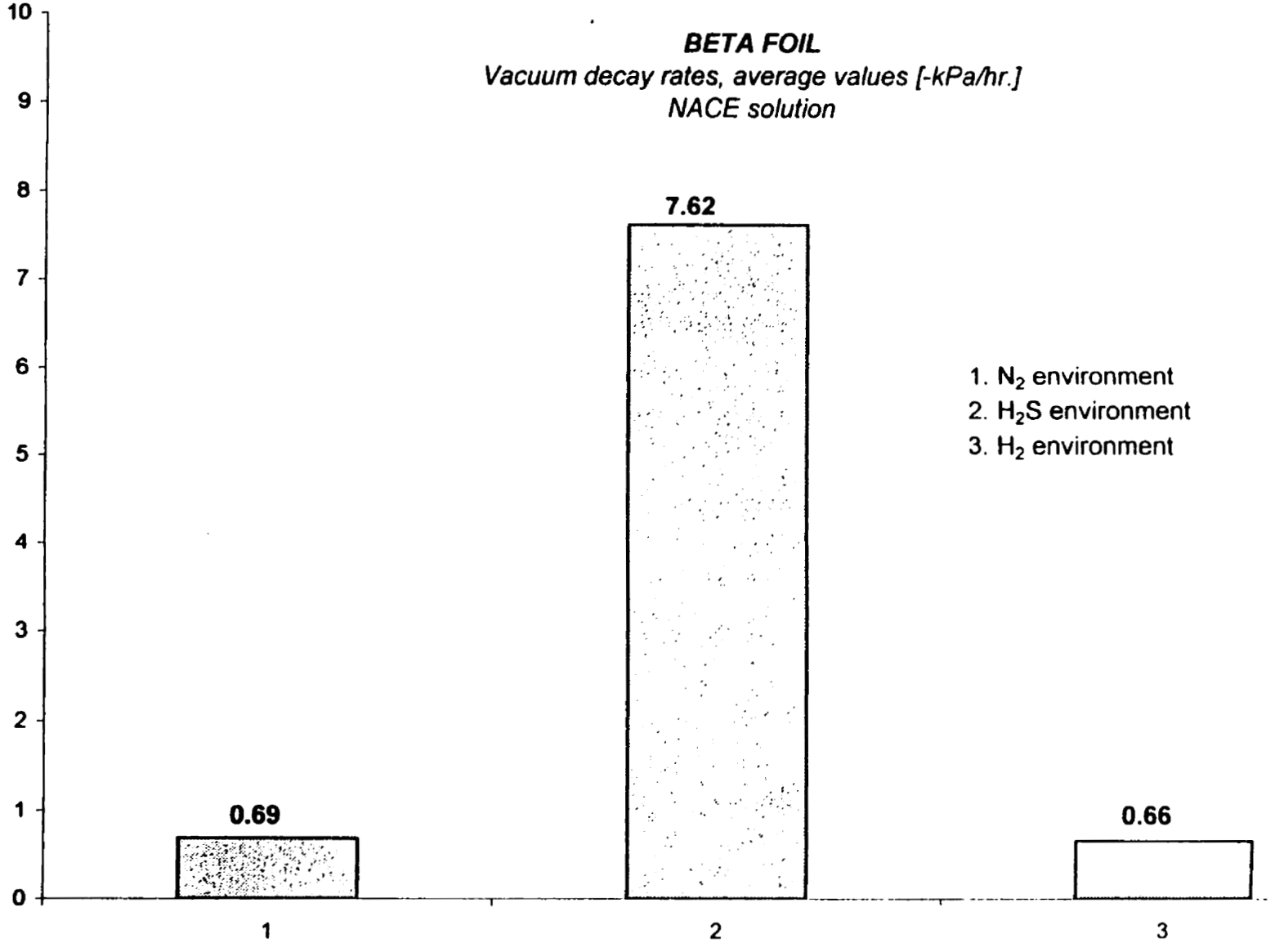

Fig.28: Beta Foil: vacuum decay rates, average values.

4.3. Film Formation

The alteration of the hydrogen flux and corrosion rate is very much dependent upon film formation on the exposed surface of the specimens investigated.

As mentioned in the previous sections, for CANMET solution the vacuum decay rate was found to change as time elapses. This is indicative of film formation on the exposed surface of the specimen and in its ability in providing a protective layer of some degree. This behavior is graphically illustrated in Figure 29. It can be seen at a glance that the vacuum decay rate, dp/dt, drops down with time for a H_2S gas environment. See also Figure 27. A similar response occurs for hydrogen oxidation current from the barnacle electrode cell, as previously shown in Figure 23. The vacuum decay rate for the N_2 gas in the CANMET solution shows a much reduced change in the decay rate. This indicates that in the N_2 environment a protective film is not forming at least to any significant degree as compared to the H_2S condition. This observation was also confirmed by the hydrogen oxidation behavior determined with the barnacle electrode method.

On the other hand, when NACE solution was used the hydrogen flux was higher in the H_2S environment than the N_2 environment. This is indicative that the NACE solution does not promote film formation on the exposed surface of the specimens.

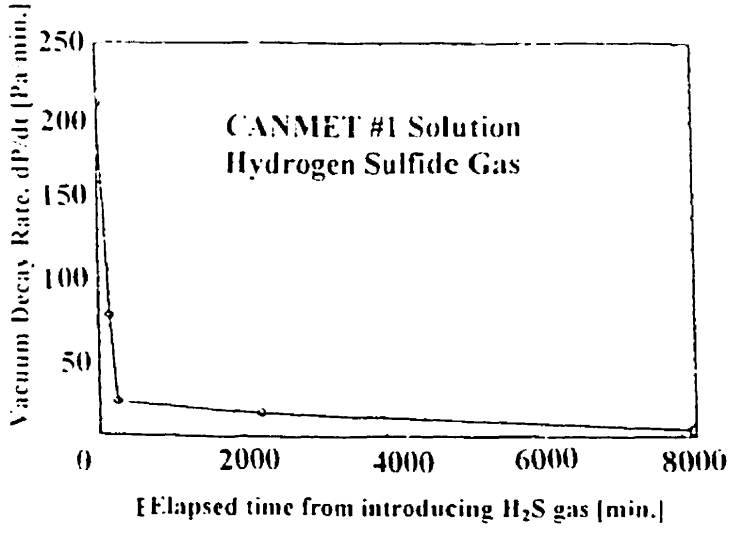

Fig.29: Vacuum decay rate vs. time for H_2S and CANMET solution [22,73,85,89-92].

4.4. Capillary Length Influence on Vacuum Decay Measurements

The influence of the capillary length on the vacuum decay was also investigated. Most experiments were carried on using a 10 foot (3.10 meters) long tube. In order to study the capillary length influence on the vacuum decay measurements a 4 foot (1.24 meters) long and a 60 foot (18.60 meters) long tube were connected in parallel on the same line that connects the vacuum chamber under the Beta Foil and the pressure detector. Initially, the 60 foot long line was open and the vacuum decay recorded. Long after the steady-state condition had established itself (3 days), the 60 foot line was closed and the 4 foot long one was open. As in all the experiments performed the measurements were done simultaneously with the barnacle electrode measurements. The latter clearly indicates that after some time (5 days or longer) a steady-state condition establishes itself in the NACE solution under N_2 environment. As already mentioned in Section 4.1.1., a steady-state condition was defined when the change in the electrochemical permeation behavior was 1 μA/24 h or less. Because all the currents measured are extremely small this assumption seems to hold. The steady-state condition is clearly indicated in Figure 30 by the hydrogen oxidation current behavior that exhibits no increase or decrease as time elapses.

On the other hand, the overall vacuum decay rate behavior for this experiment is totally different. Under the same conditions the vacuum decay rate looks to be higher when the 4 feet long tubing was employed (1 kPa/h) than when the 60 foot one was used (<0.50 kPa/h). This is clearly indicated by the differences in the slopes of the vacuum decay vs. time, as illustrated in Figure 30. It is obvious that the amount of hydrogen permeating through the steel specimen is not a function of capillary length, but a function of the material and the environmental conditions.

A similar behavior was observed to occur also in H_2S environment.

It is clear now that in order to obtain comparable and accurate measurements in the laboratory or in the field using the Beta Foil technique, the equipment needs to be calibrated.

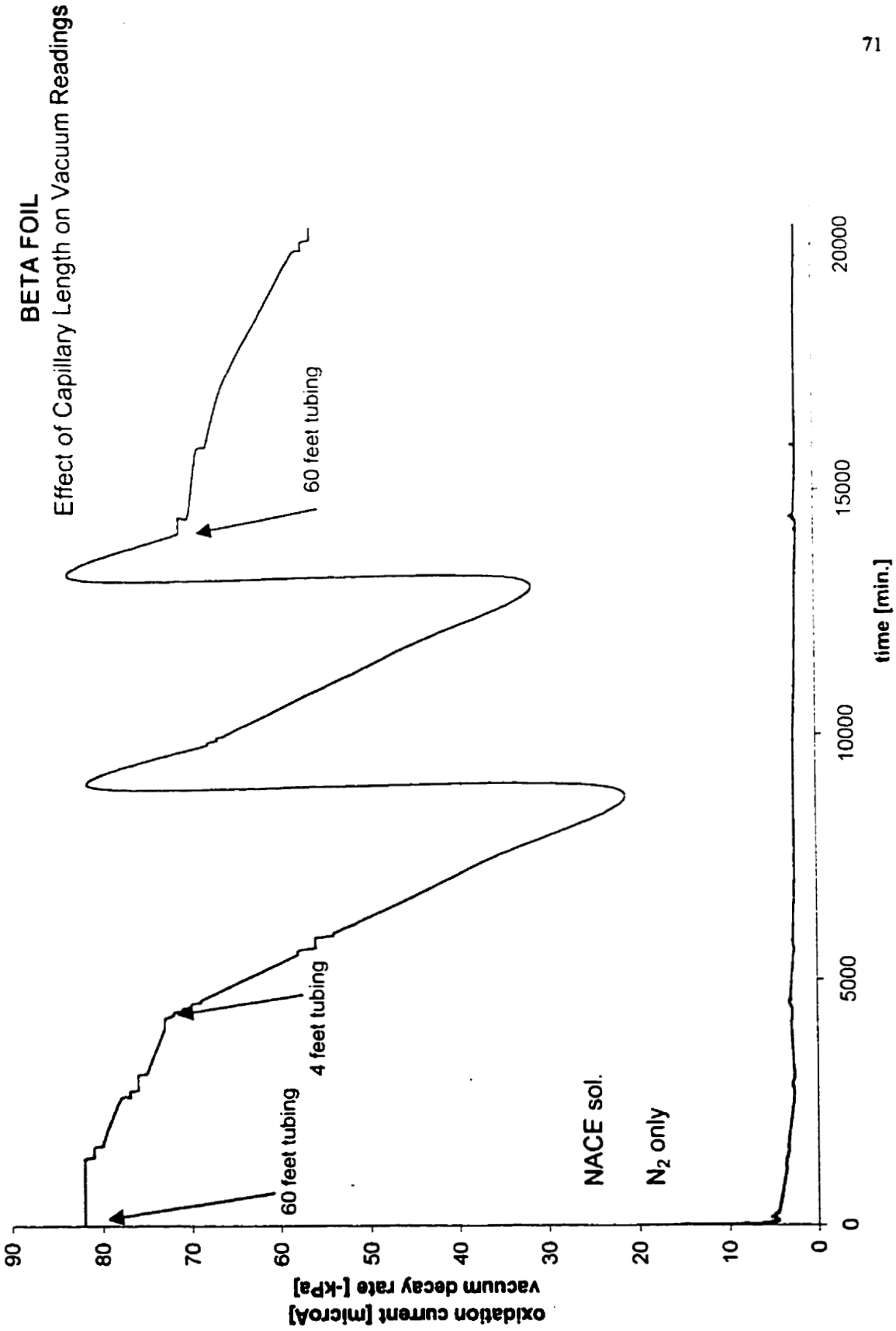

Fig.30: Effect of capillary length on vacuum readings.

4.5. Effect of Surplus Hydrogen on Vacuum Decay

Hydrogen flux permeation usually originates from the hydrogen atoms that are liberated at the cathode during the electrochemical process of corrosion. It is also possible that the atomic hydrogen may exist due to a chemical reaction inside the pipe unrelated to the corrosion processes [87].

Not all the hydrogen atoms generated by a corrosion reaction will migrate into the pipe steel. Depending on the process and the corrosion environment a percentage of these atoms can recombine in pairs on the pipe's inner surface to form molecular hydrogen gas, H_2. This hydrogen gas goes ultimately into the product stream and it is lost in the process flow as it is carried down the pipe.

The experiments described in this Section were carried on in order to see if the presence of extra hydrogen gas inside the large cell has any effect on the hydrogen permeation behavior. Tests were carried on for both NACE and CANMET #3 solutions.

After a steady-state condition had established itself, the N_2 was switched off and the H_2 was turned on. Same procedure was applied for both solutions, NACE and CANMET #3. The vacuum decay behavior in NACE solution is graphically illustrated in Figure 31 and for the CANMET solution in Figure 32. As it can be seen from both graphs there is no change in the vacuum decay behavior when switching from N_2 gas to H_2 gas. This observation is confirmed by calculating the vacuum decay rate, dp/dt, for both cases. When NACE solution was used the vacuum decay rate under N_2 environment was found to be -0.50 kPa/h, while under H_2 environment was found to be -0.51 kPa/h. Similarly, when CANMET #3 solution was used, the vacuum decay rate under N_2 environment was -1.28 kPa/h, while under H_2 environment was -1.20 kPa/h. These experiments confirmed also that corrosion activity is higher in CANMET solution under N_2 environment.

The fact that extra hydrogen gas, H_2, has no effect at all on hydrogen permeation behavior through steel specimens has also been confirmed by barnacle electrode results. When NACE solution was used, the hydrogen permeation current under N_2 environment was found to be 2.96 μA, very close to the value of the hydrogen oxidation current

measured under H_2 environment, which was determined to be 3.05 μA. Similar results were obtained for both CANMET solutions as well. A very important observation made was that the currents measured are extremely small and the potentiostatic circuit is so sensitive it sometime measures a decrease (0.1-0.2 μA) when the beaker and/or the barnacle electrode are refilled with distilled water. This is done in order to maintain a constant level of NaOH solution in both the barnacle electrode cell and the salt-bridge system, to prevent loss of solution due to evaporation.

In conclusion, it can be said that the presence of extra gaseous hydrogen, H_2, in the system, other than that involved in the local corrosion reaction beneath the foil, has virtually no effect on the vacuum decay behavior.

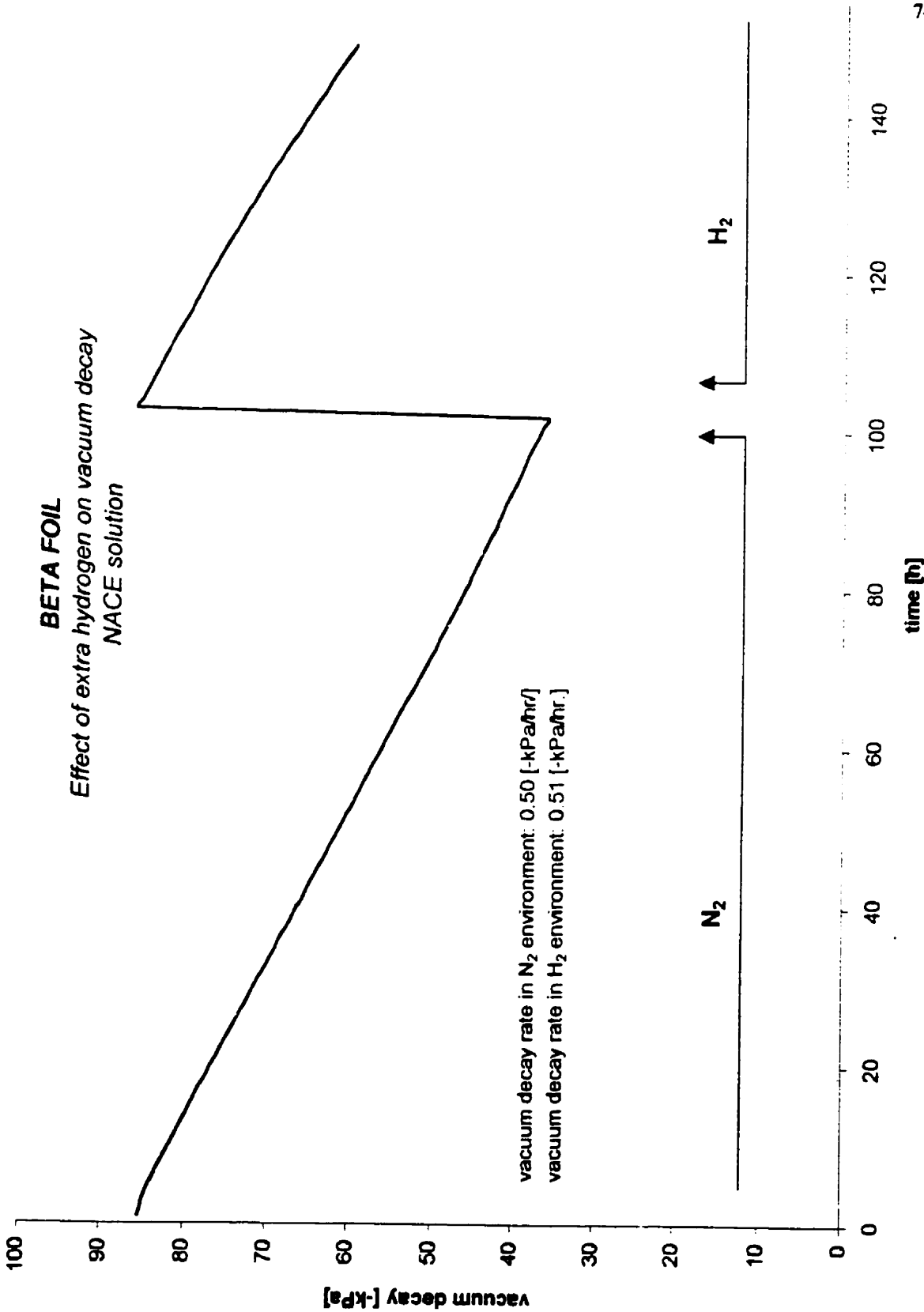

Fig.31: Beta Foil: Effect of extra hydrogen on vacuum decay, NACE solution.

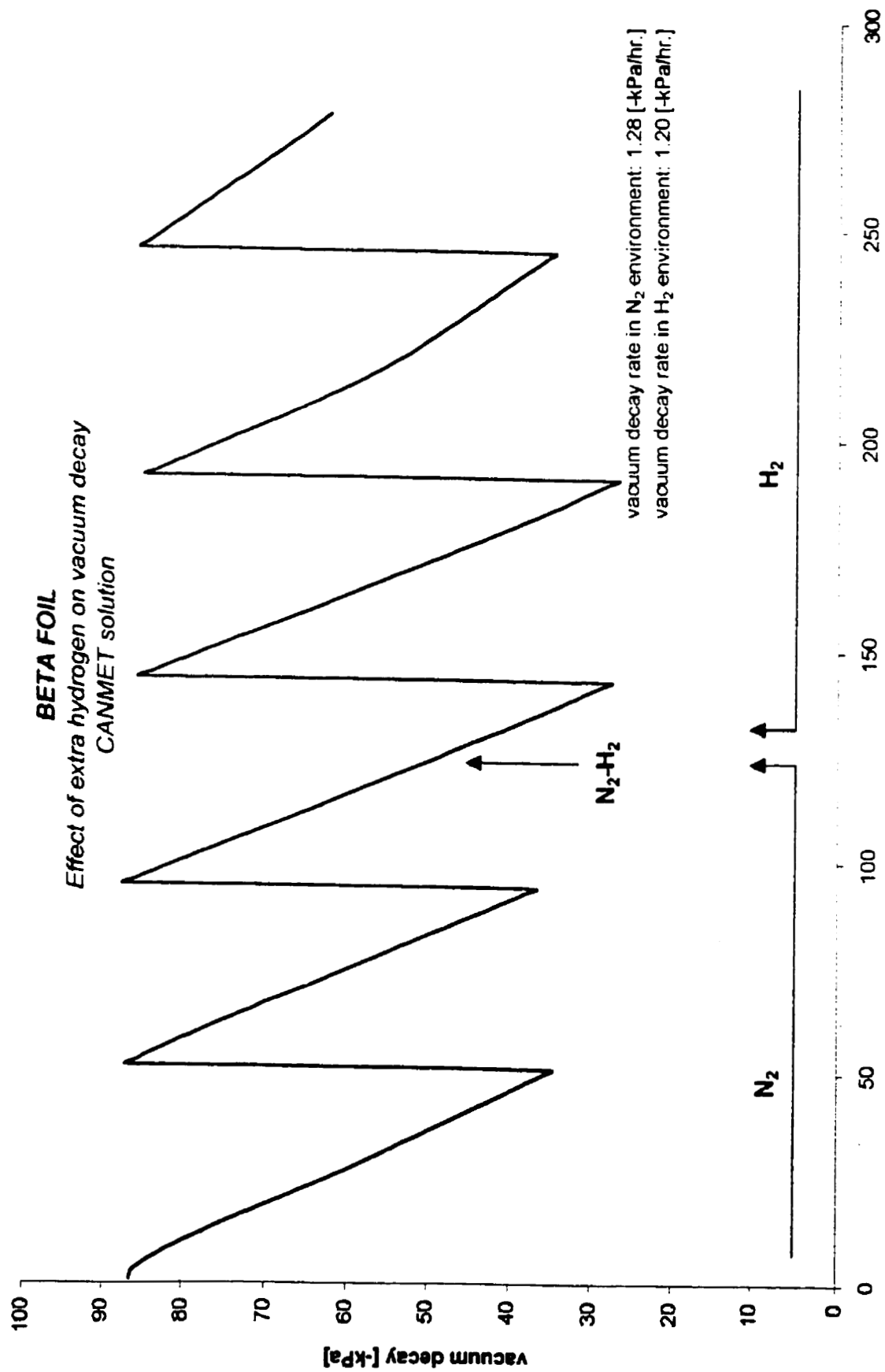

Fig.32: Beta Foil: effect of extra hydrogen on vacuum decay, CANMET #3 solution.

4.6. Effect of Poisons on Vacuum Decay

It has been established that the rate of hydrogen entry in a metal is affected by the nature of the electrolyte, presence of surface films, temperature, and/or presence of impurities.

Generally speaking, if the environment in the system contains poisons, more of the atomic hydrogen being generated at the cathode will be driven through the thickness of the specimen. Those poisons, when present in the system, have a marked effect in increasing hydrogen entry into metals and alloys. They block the hydrogen-hydrogen, H-H, recombination reaction and thus favor entry of the adsorbed hydrogen into the metal or alloy.

In the present research program the effect of poisons, such as H_2S, As, and Se, on the hydrogen permeation behavior was studied.

As already presented in Section 4.1. and Section 4.2. a fairly rapid increase in the hydrogen permeation occurs when H_2S is introduced into the system, that is going from N_2 to H_2S. In the NACE solution, as expected, a larger amount of hydrogen is permeating through the steel specimen when H_2S is present in the system, compared with the situation when N_2 is present in the system. On the contrary, in the experiments in which CANMET #1 solution was used the hydrogen permeation rate is higher under N_2 environment than under H_2S environment. This somewhat strange behavior is due to the formation and presence of a protective film on the exposed surface of the specimen. It can be said that H_2S is an effective promoter of hydrogen entry into the steel in the NACE solution. Its effectiveness as a promoter of hydrogen entry into the steel is very much reduced when CANMET #1 solution is used. Under an H_2S environment the average vacuum decay rate in the NACE solution was found to be -7.08 kPa/h, while in the CANMET #1 solution was found to be -4.89 kPa/h. Those findings are also confirmed by the barnacle electrode results, the hydrogen oxidation current in the NACE solution being 5.5 μA, while in the CANMET #1 solution is 1.6 μA, in H_2S environment.

The effect of arsenic, As, on the vacuum decay behavior in the NACE solution was studied using sodium arsenite, $NaHAsO_4.7H_2O$. After a steady-state condition had

established itself in the system, a concentration of 6 μg/L of sodium arsenite was added into the system. As it can be seen in Figure 33 the addition of 6 μg/L sodium arsenite has no effect on the hydrogen permeation behavior. The hydrogen permeation behavior was monitored further and after 180 hours the concentration of the poison was adjusted to 30 μg/l. Again, no effect was observed on the vacuum decay behavior, the vacuum decay rate being measured as -0.19 kPa/h. Similarly, no effect occurred when sodium arsenite concentration was raised to 60 μg/L. These findings were confirmed by the barnacle electrode measurements, during those changes in the system the electrochemical permeation current remaining constant, with no decrease or increase observed or recorded. This means that up to a concentration of 60 μg/L in the system the sodium arsenite has virtually no effect on the hydrogen permeation rate, thus on the hydrogen entry into the steel specimen. Again, it must be underlined that this observation is valid only for the NACE solution. When the sodium arsenite concentration was raised to 600 μg/L a totally unexpected response took place. In the barnacle electrode system a sudden decrease in the electrochemical permeation current occurred, the response time being 5 minutes. The vacuum decay rate also decreased within 60 minutes up to a point where it was virtually almost zero. Both the vacuum decay and the electrochemical permeation behavior clearly indicate that the presence of a concentration of 600 μg/L sodium arsenite in NACE solution into the system (or less, but higher than 60 μg/L) will lead to the formation of a protective film on the exposed steel surfaces. This film acts as an effective barrier to the hydrogen entry into the material as long as it is not chemically or mechanically disturbed. At the end of this experiment the exposed steel specimen surfaces were examined. It was observed that a relatively thick, uniform greenish film was formed on the surfaces exposed to the solution in the large cell. Unfortunately, neither the thickness nor the chemical composition of this film could be determined. The effect of sodium arsenite added to the NACE solution on the hydrogen permeation behavior is in total contradiction with what is known from the literature that arsenic is one of the most effective promoters of hydrogen entry into the steel.

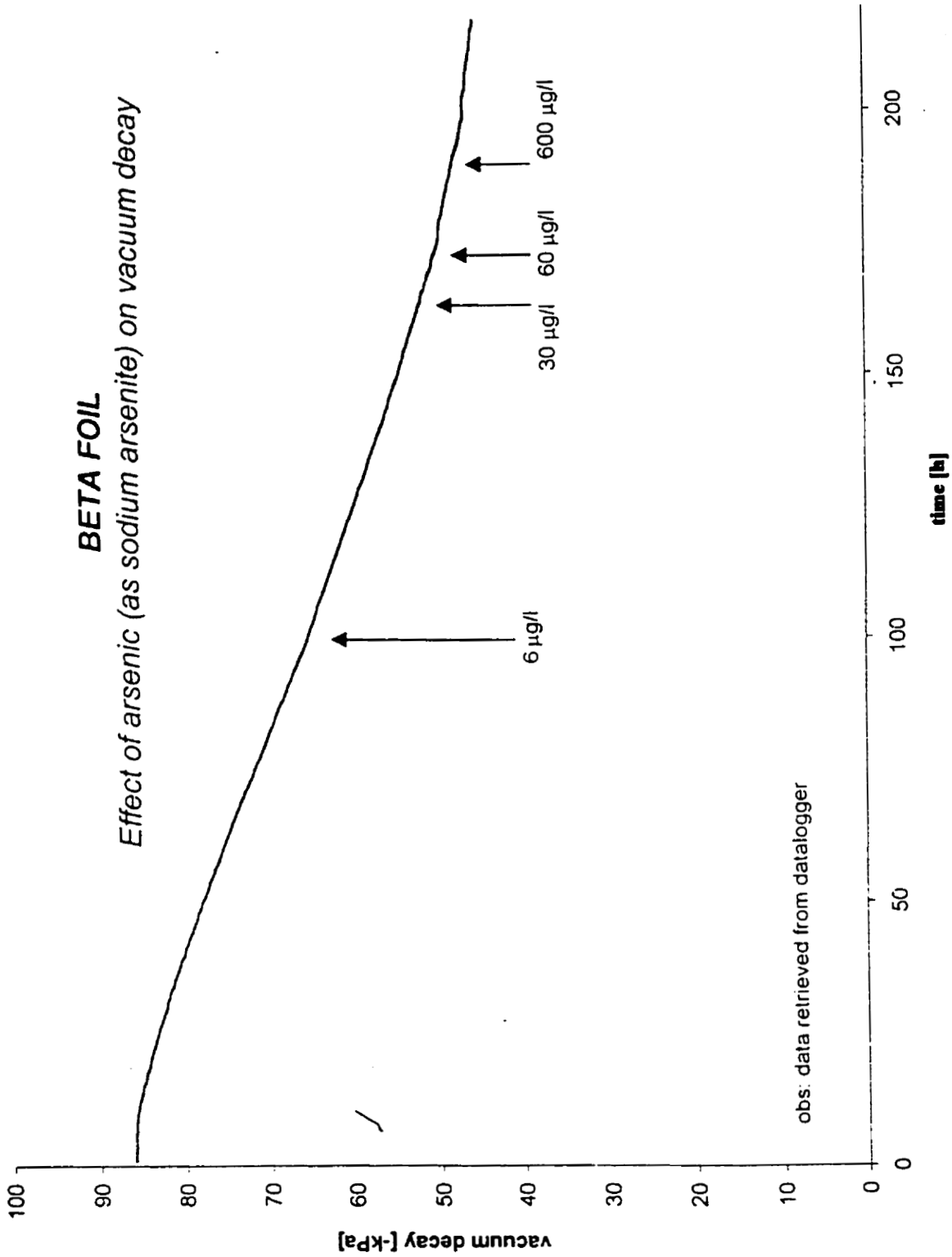

Fig.33: Beta Foil: Effect of arsenic on the vacuum decay.

Presumably, a chemical reaction occurs between the sodium arsenite and the NACE solution, the products of that reaction forming an extremely effective barrier to the corrosion of the steel specimen.

A third poison for which effects on the vacuum foil readings were analyzed is selenium, Se, in the form of selenious acid, H_2SeO_3. Again, the analysis was conducted using the NACE solution and the N_2 environment. After a steady-state condition had established itself a concentration of 600 μg/L selenious acid was added into the system. It was observed that the response time was quick for both the barnacle electrode and the hydrogen vacuum foil. For the barnacle electrode the response time was 5 minutes, while for the hydrogen vacuum foil it was observed to be within 60 minutes. A sudden decrease in the oxidation current occured, from 2.2 μA to 0.9 μA, as well as a sudden decrease of the vacuum decay rate, from -0.46 kPa/h to virtually almost 0 kPa/h. Again, this is indicative of a very effective film formed on the steel surfaces exposed to the solution. This film formed probably due to a chemical reaction between the selenious acid and the NACE solution has a reddish appearance, it is relatively thick and uniform. Unfortunately neither its thickness nor the chemical composition could be determined due to inaccessibility of equipment. It is known that these surface films are effective barriers to corrosion of the steel as long as they are not chemically or mechanically disturbed. The film formed cannot be mechanically disturbed during the experiments because the large cell is closed. In order to check film response, N_2 was switched off and H_2S was then introduced into the system. A sudden response took place in both the barnacle electrode (10 minutes) and the hydrogen vacuum foil (less than 60 minutes). An increase in the oxidation current was observed, as well as an increase of the vacuum decay rate, thus indicating the degradation of the protective film previously formed and an enhanced hydrogen entry rate into the steel specimen. This behavior is graphically presented in Figure 34.

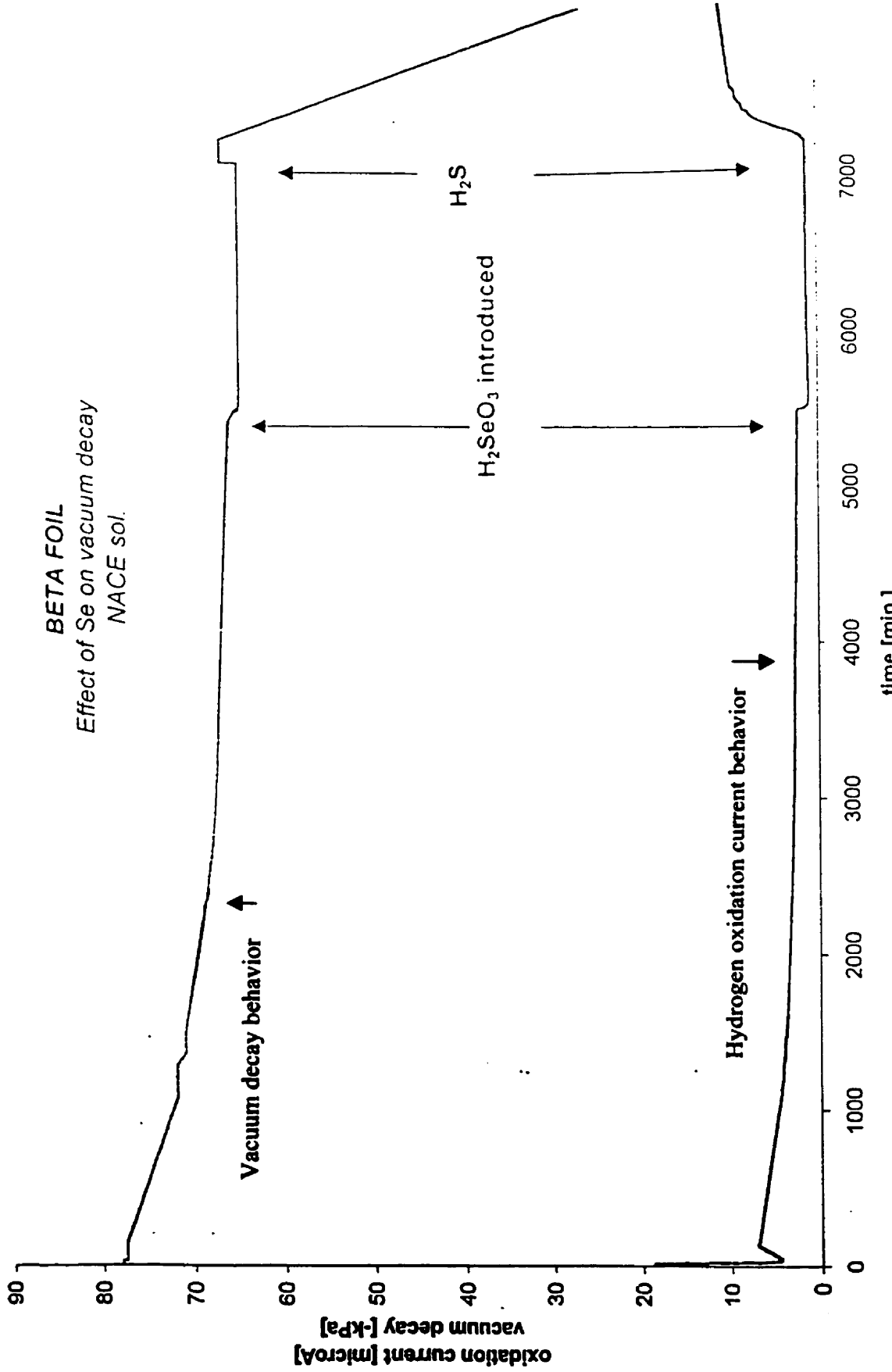

Fig.34: Beta Foil: Effect of selenium on the vacuum decay.

4.7 Deaerated Conditions vs. Aerated Conditions

A very important aspect that needed to be clarified was to find out if the Beta Foil technique is also suitable for monitoring hydrogen permeation under aerated conditions, that is where oxygen is present. For this purpose, after a steady-state condition had established itself, air was introduced into the large cell. One experiment was conducted using the CANMET #1 solution with H_2S being first introduced into the large cell followed by air. A second test was conducted using the NACE solution with N_2 being first introduced into the system followed by air after the steady-state condition was reached.

In both experiments it was observed that the rate of vacuum decay decreased to a very low level immediately after the air was introduced into the system. The fact that the measured hydrogen permeation rate under aerated condition is much lower than under deaerated conditions was confirmed by the simultaneously performed barnacle electrode measurements. As seen in Figure 35, for the CANMET #1 solution, when changing from H_2S to air the hydrogen permeation current drops significantly to a very low level. This would indicate a significantly lower corrosion rate in the presence of oxygen as compared to a higher corrosion rate in the H_2S environment. However, this is not the case as found from direct corrosion rate measurements [88-89, 90-92]. It indicates that under aerated conditions, where oxygen is present, the hydrogen reduction reaction is no longer the dominate reaction and the measurement of mobile hydrogen through the material is no longer reflective of the corrosion rate. The presence of oxygen changes the reduction reaction such that only minimal hydrogen permeates through the steel specimen. In aerated conditions the oxygen reduction would be the dominate reaction, not the hydrogen reduction reaction. Similarly, for the NACE solution, Figure 36, when switching from N_2 to air the electrochemical permeation current drops significantly, indicating again that the measurement of hydrogen under aerated conditions is not a sensitive or a good test for indication of corrosion rates.

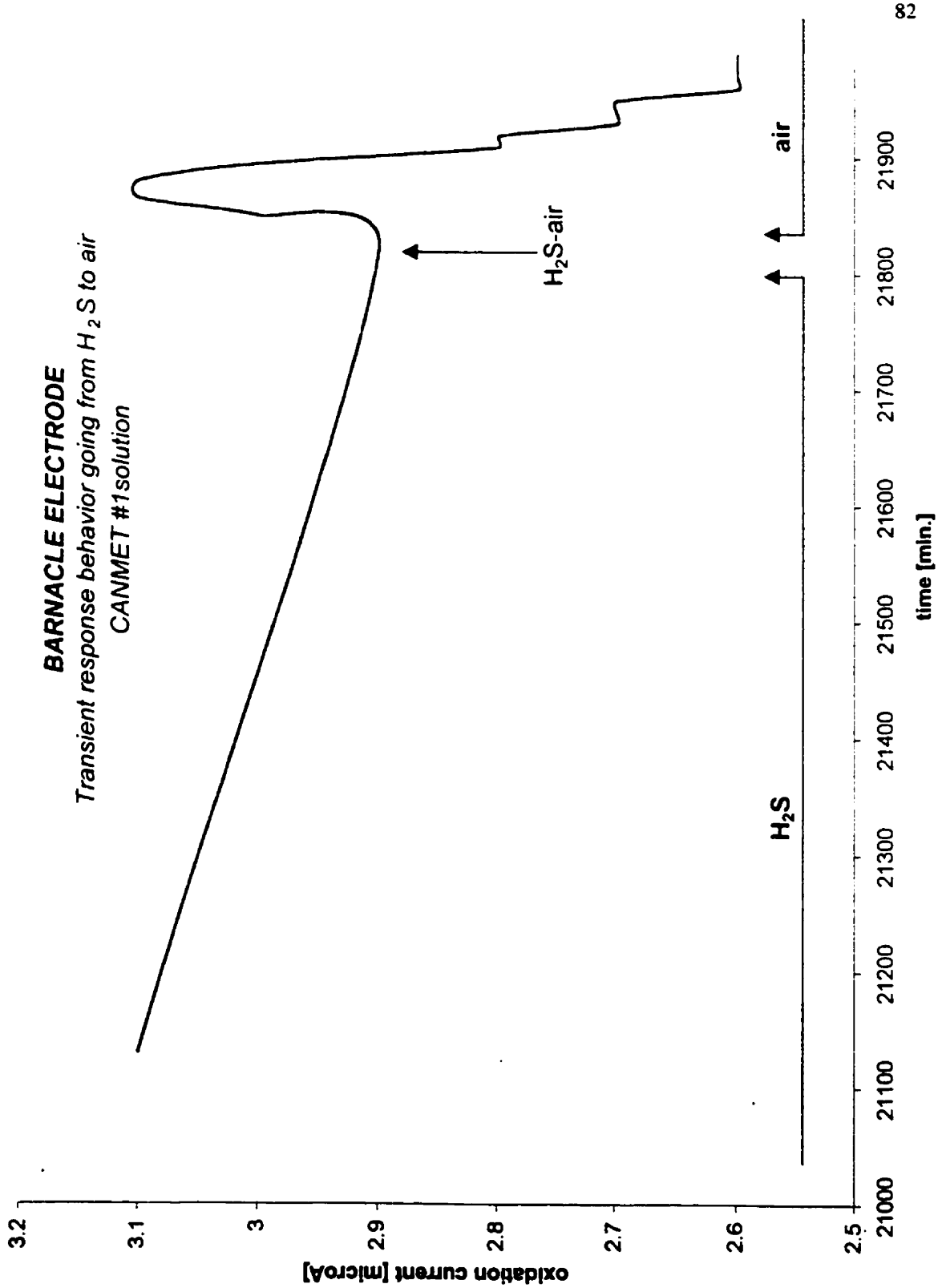

Fig.35: Barnacle electrode: transient response behavior going from H_2S to air. (CANMET #1 solution)

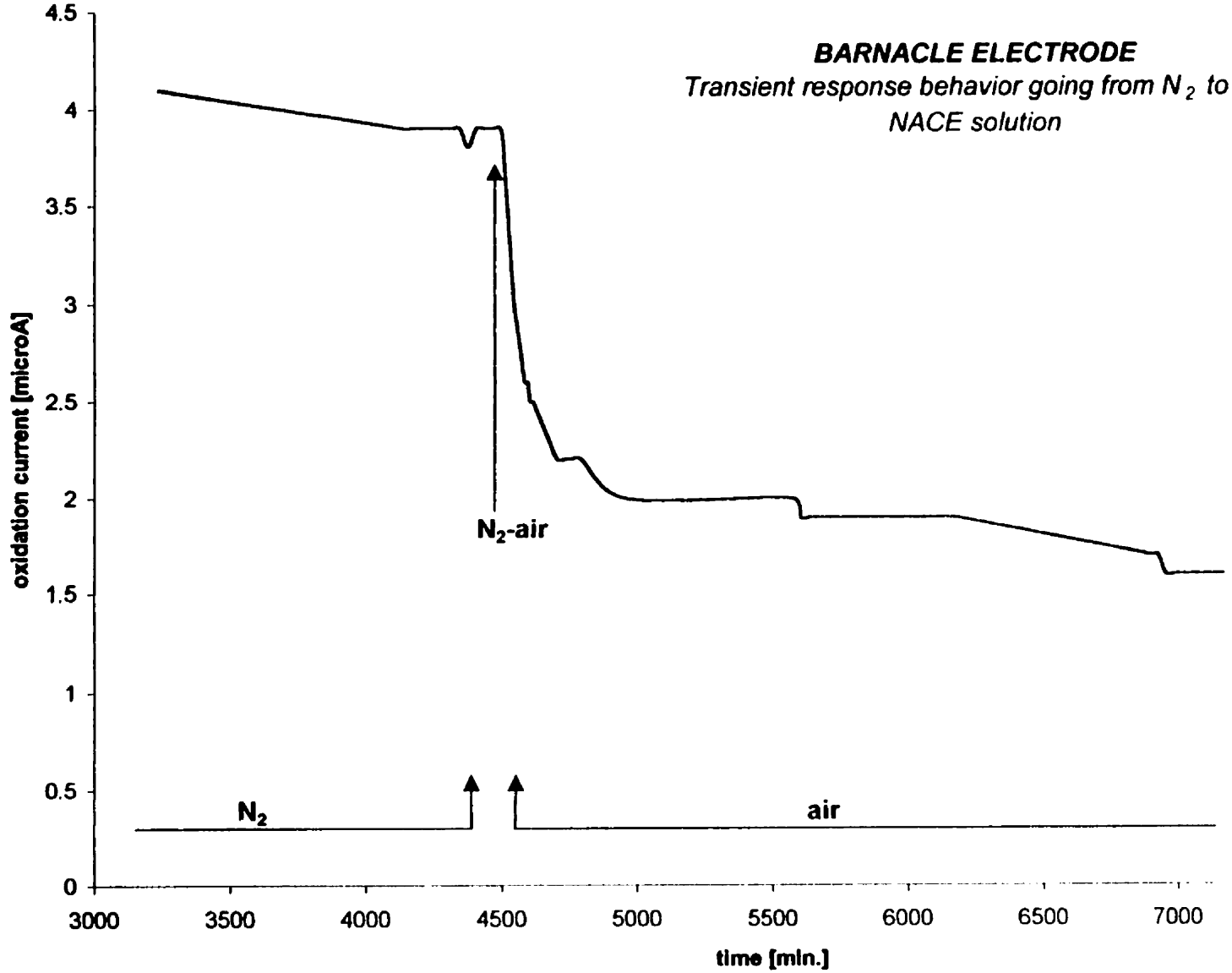

Fig.36: Barnacle electrode: transient response behavior going from N_2 to air. (NACE solution).

In conclusion, it can be said that the hydrogen permeation as a measure of corrosion rate should not be used under aerated conditions. This confirms reduction reaction conditions as would be predicted from corrosion theory, where only under deaerated conditions is the hydrogen reduction reaction dominant.

4.8. Effect of Inert Gases on Vacuum Decay

The main characteristic of inert gases is that they have an especially small tendency to form stable compounds. Because of their inertness, such elements should have no influence on the hydrogen permeation through the steel, hence on the Beta Foil measurements. In order to study the effect of inert gases on the hydrogen vacuum decay a sequence of N_2-H_2-Ar environments was employed in the large cell that was filled with the NACE solution. Hydrogen, H_2, shares some similarities with inert gases and nitrogen, N_2, it is often used as an inert gas due to its unreactive nature with many materials. Both hydrogen and nitrogen are inert with respect to the corrosion reactions taking place on the exposed steel surface in the aggressive environment.

For this test the vacuum decay was explored first under N_2 environment and once a steady-state condition had established itself then a change in gas was made, from N_2 to H_2. After a steady-state condition occurred under the H_2, the environment was changed again, from H_2 to Ar. As seen in Fig. 37 there was no change in the hydrogen vacuum decay behavior, dp/dt, under these three different environments. However, as indicated in Figure 38, due to variability in the corrosion reaction the hydrogen flux is not constant. This variation is extremely small ($\mp$0.09kPa for H_2 gas)it can ne neglected. Calculation of vacuum decay rate indicates an average value of -0.98 kPa/h under N_2 environment, -0.94 kPa/h under H_2 environment, and -0.91 kPa/h under Ar environment, respectively. The fact that those three values are almost identical is a clear indication that, as expected, inert gases have virtually no influence on the vacuum decay measurements. This observation was again confirmed by simultaneous permeation measurements by the barnacle electrode method. For this particular test the steady-state oxidation current under

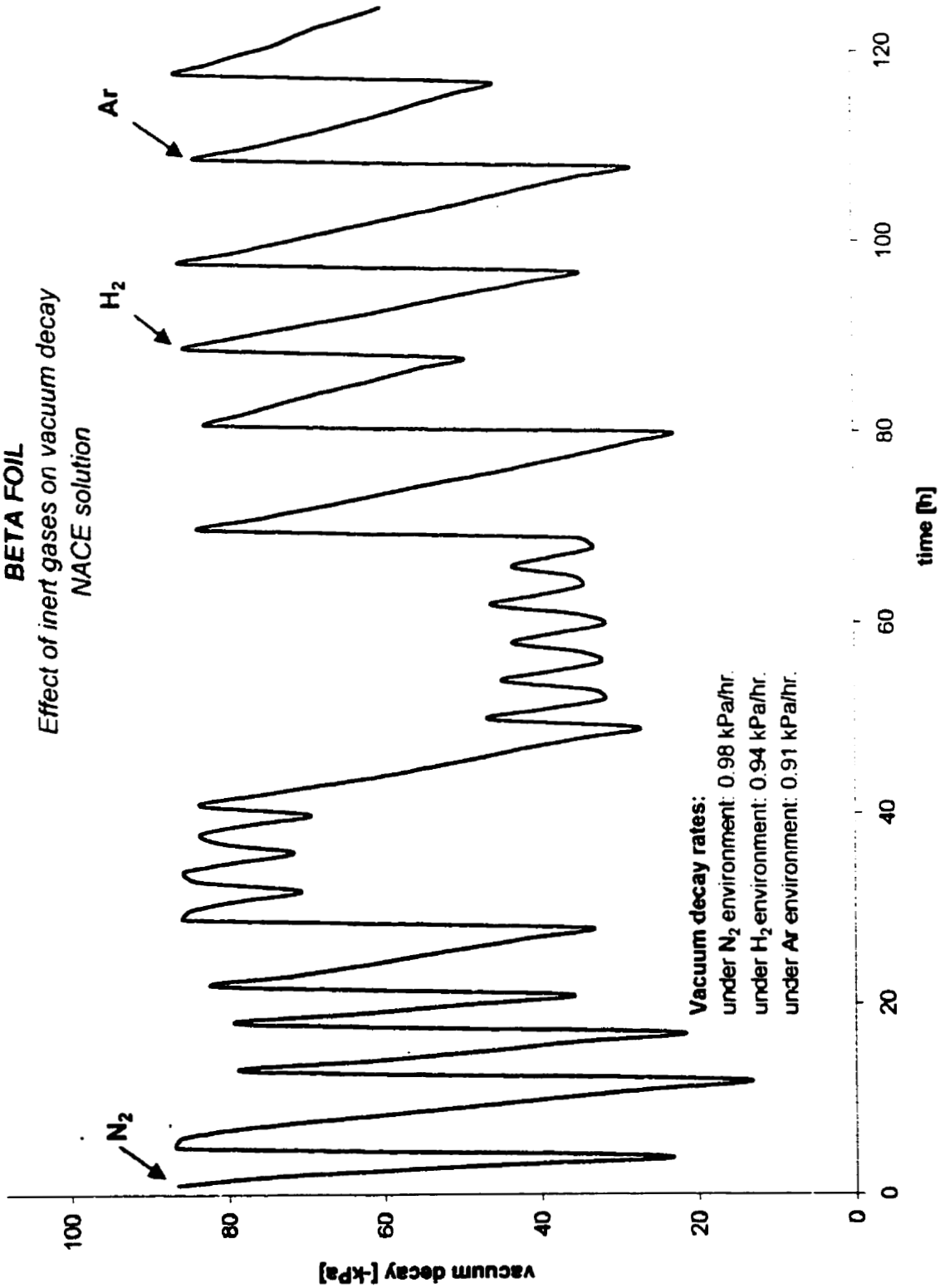

Fig.37: Effect of inert gases on vacuum decay, NACE solution.

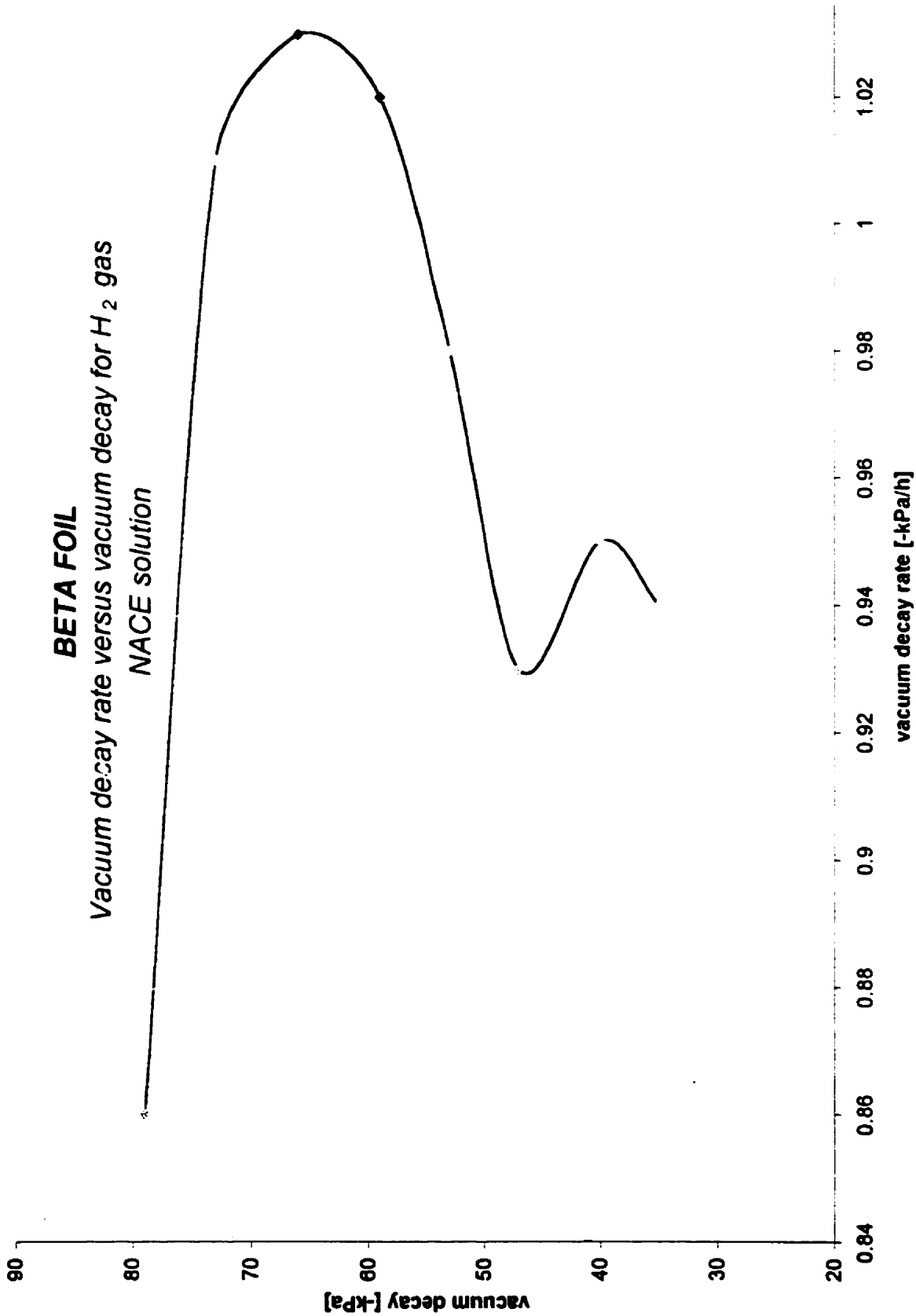

Fig.38: Vacuum decay rate versus vacuum decay for H_2 gas, NACE solution.

N_2 environment was measured 1.9 μA, under H_2 environment 2.2 μA, and under Ar environment 1.7 μA. It must be mentioned that extremely small currents are measured and every time a change in the system is made it is immediately reflected in the readings. This is an indication of how sensitive the barnacle electrode method is. However, after a few hours the current again reached approximately its previous value.

In conclusion, it can be said that the presence of inert gases has no influence on the hydrogen vacuum permeation behavior, hence on the Beta Foil measurements.

4.9. Effect of Barometric Pressure on Hydrogen Permeation

The barometric pressure was monitored every hour during various barnacle electrode tests as well as hydrogen vacuum foil tests until a fairly substantial amount of information was available for comparison. Correlations could not be found for either the barnacle electrode measurements or the hydrogen vacuum foil measurements as a function of barometric pressure change. Therefore, this parameter is not one that needs to be monitored or corrected for.

4.10. Hydrogen Quantity Measurements

The general gas law states that the absolute pressure of an ideal gas is directly proportional to the temperature and the number of moles of the gas and it is inversely proportional to the volume of the gas [93]. The atomic hydrogen flux generated as a result of corrosion on the inside of the steel specimen is captured under the Beta Foil. Under vacuum these hydrogen atoms recombine in pairs to form molecular hydrogen, H_2. Molecular hydrogen is unable to escape from the vacuum induced between the specimen's outside and the foil's inside, thus the vacuum will decay in a ratio proportional to the hydrogen permeation flux (related to the severity of the internal corrosion). Combining the principle of the Beta Foil and the general gas law one may calculate the hydrogen quantity that is permeating through the steel specimen.

In order to achieve this goal the volume under the foil, the volume of the capillary tube, and the volume of the tree, transducer, and the pressure gage must be known.

As it can be seen from Figure 39 the volume under the Beta Foil is extremely small (practically it can be considered negligible) up to a vacuum of -19.4 kPa (average value) versus the atmospheric pressure. This is in keeping with the recommendations from the manufacturer [84] which suggests that the foil should be evacuated and the vacuum re-induced any time it approaches -20 kPa.

BETA FOIL
changes of movement under foil observed @ ...-kPa.
area where measurements were made is indicated by arrow.

Foil no.1 (previously tested): *15; 15; 16; 16; 16.*
Foil no.2: (not tested) : *21; 20; 20; 20; 20.*
Foil no.3: (not tested) : *17; 21; 22; 20; 24.* Total average: 19.4 kPa.
Foil no.4: (not tested) : *26; 28; 25; 25; 26.*
Foil no.5: (previously tested): *15; 15; 14; 14; 14.*

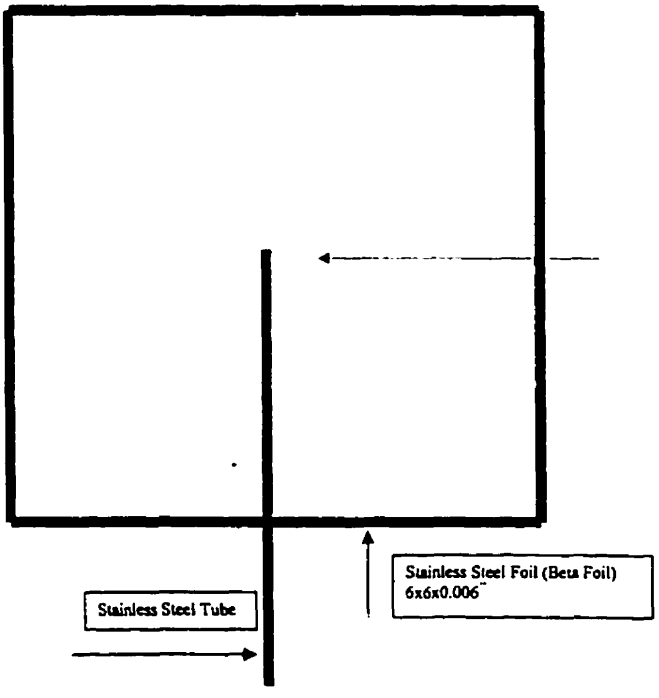

Fig.39: Determination of the movement under the Beta Foil.

A series of inducing-releasing vacuum under the foil using the vacuum pump was done in order to obtain the vacuum values at which the volume under the foil starts to change from negligible. When the vacuum is induced under the foil, at the beginning of each test, the volume of the vacuum chamber is considered negligible. A vacuum of -82 kPa was induced and then air was admitted into the system. The first change in the foil's volume was detected using a stationary dial gage and the corresponding vacuum was recorded. Five different measurements were made for five different foils and the average value of the 25 measurements was taken into consideration. The difference between the vacuum values obtained for "not tested" and "previously tested" foils is due to the larger stresses present in the "not tested" foils. "Not tested" foils are the foils as-received and affixed on the steel specimen, while the "previously tested" ones are the foils that were used in experiments and the vacuum was re-induced several times beneath them.

The capillary tube diameter was 1.70 mm, and the length of the tube used for this test were 4 foot (1.24 m), 10 foot (3.10 m), and 60 foot (18.60 m) respectively. The corresponding volume of the tube for those three cases was 2.77 cm^3, 6.92 cm^3, and 226.1 cm^3 respectively. The manufacturer's drawings of the tree, transducer, and pressure gage were used in order to calculate their respective volumes. Also, a more precise method was employed as well. Vacuum was first induced by a high-displacement electrical vacuum pump, then air was allowed to enter into the system from a marked syringe with a known volume. After the equilibrium was reached the total volume of the three components (tree, transducer, pressure gage) was read directly on the syringe. It was found to be 5.58 cm^3. In conclusion, the total volume of the system (tube, tree, transducer, pressure gage) for the 4 foot long tube is 8.35 cm^3, for the 10 foot long one 12.50 cm^3, and for the 60 foot long one 231.68 cm^3.

The general gas law was used to calculate the amount of hydrogen that is permeating through the steel specimen. The temperature during the measurements was constant, being 21^{0}C (294K). For vacuum values between -86 kPa and -20 kPa the volume under the Beta Foil was considered negligible, as demonstrated. In all calculations the real pressure (the difference between the atmospheric pressure and the pressure beneath the foil) was used. A detailed algorithm of these calculations is given

below. The amount of hydrogen permeating the steel specimen was calculated according to the following equation:

$$m = \frac{pVx10^{-3}}{R_{H2}T} \qquad [31]$$

where:

p- real pressure beneath the Beta Foil.

V- total volume of the system (tube, tree, transducer, pressure gage).

T- absolute temperature.

R_{H2}- hydrogen gas constant.

For hydrogen [94]:

$$R_{H2} = 766.53\frac{ft\,lb_f}{lb_m\,^0R} \qquad [32]$$

Using the following conversion factors [95-99]:

1 lb_f = 1.356 Nm.

1 lb_m = 453.59 g.

1 ft = 0.304 m.

$^0R = 1.8\ ^0K$.

$$\frac{ft\,lb_f}{lb_m\,^0R}\,x\,\frac{1.356Nm}{453.59x\left(\frac{1}{1.0079}\right)molex\left(\frac{1}{1.8}\right)^0K} = 5.424x10^{-3}$$

equation [32] can now be written in the following form:

$$R_{H2} = 766.53 \text{ x } 5.424 \text{ x } 10^{-3} \text{ J/gmol}^0\text{K}. \qquad [34]$$

$$R_{H2} = 4.1573 \text{ J/gmol}^0\text{K}. \qquad [35]$$

At a temperature of 21^0C (294K) the amount of hydrogen permeating through the steel can be calculated now using the following formula:

$$m = \frac{PVx10^{-3}}{4.1573x294} = pVx8.18x10^{-7}[mol] \qquad [36]$$

The total area of the Beta Foil is 232.25 cm^2. Therefore, one may calculate the amount of hydrogen that is permeating through the steel specimen per unit area. The total amount of hydrogen permeating through the steel specimen versus the vacuum decay is presented in Table 5 and graphically illustrated in Figure 40 (for 4 foot tube), Figure 41 (for 10 foot tube), and Figure 42 (for 60 foot tube) respectively.

Vacuum [-kPa]	*4 foot tube*	*10 foot tube*	*60 foot tube*
86	–	–	–
80	$0.0176x10^{-5}$	$0.0264x10^{-5}$	$0.48x10^{-5}$
70	$0.047x10^{-5}$	$0.0704x10^{-5}$	$0.93x10^{-5}$
60	$0.076x10^{-5}$	$0.1144x10^{-5}$	$2.12x10^{-5}$
50	$0.105x10^{-5}$	$0.1584x10^{-5}$	$2.93x10^{-5}$
40	$0.135x10^{-5}$	$0.2025x10^{-5}$	$3.75x10^{-5}$
30	$0.164x10^{-5}$	$0.2465x10^{-5}$	$4.56x10^{-5}$
20	$0.194x10^{-5}$	$0.2905x10^{-5}$	$5.38x10^{-5}$

Table 5: Amount of hydrogen permeating the steel specimen per unit area.

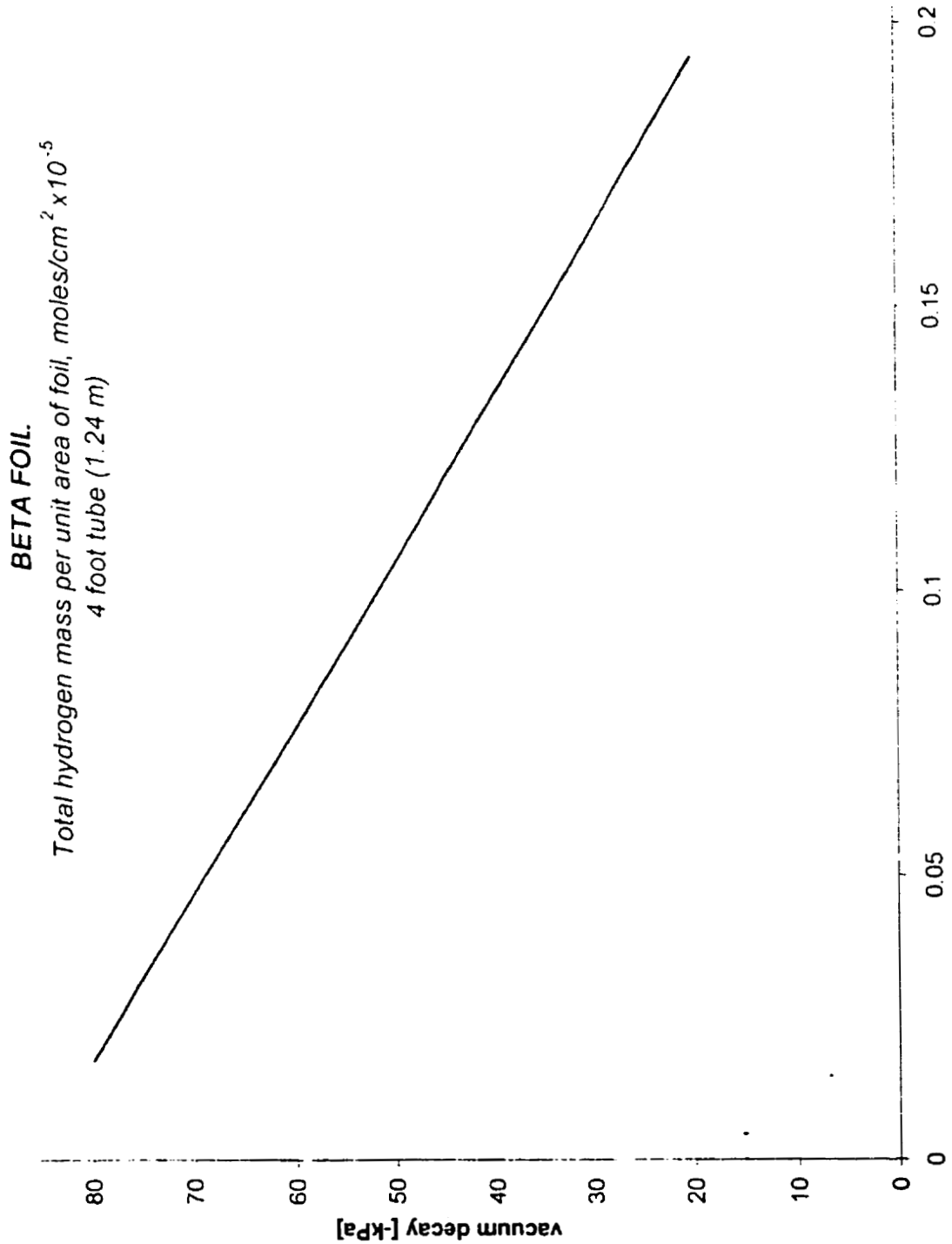

Fig.40: Total hydrogen mass per unit area of foil (4 foot tube).

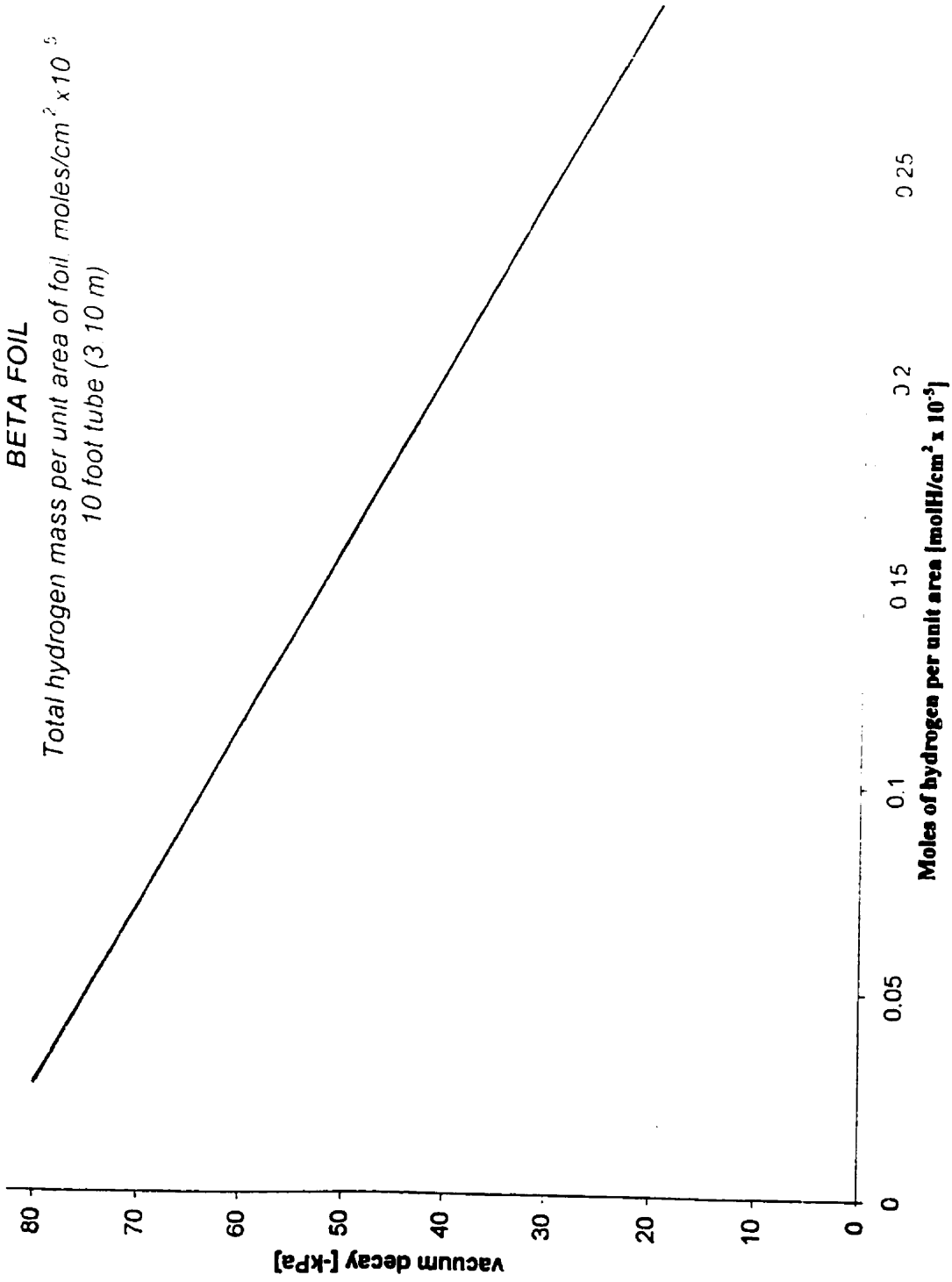

Fig.41: Total hydrogen mass per unit area of foil (10 foot tube).

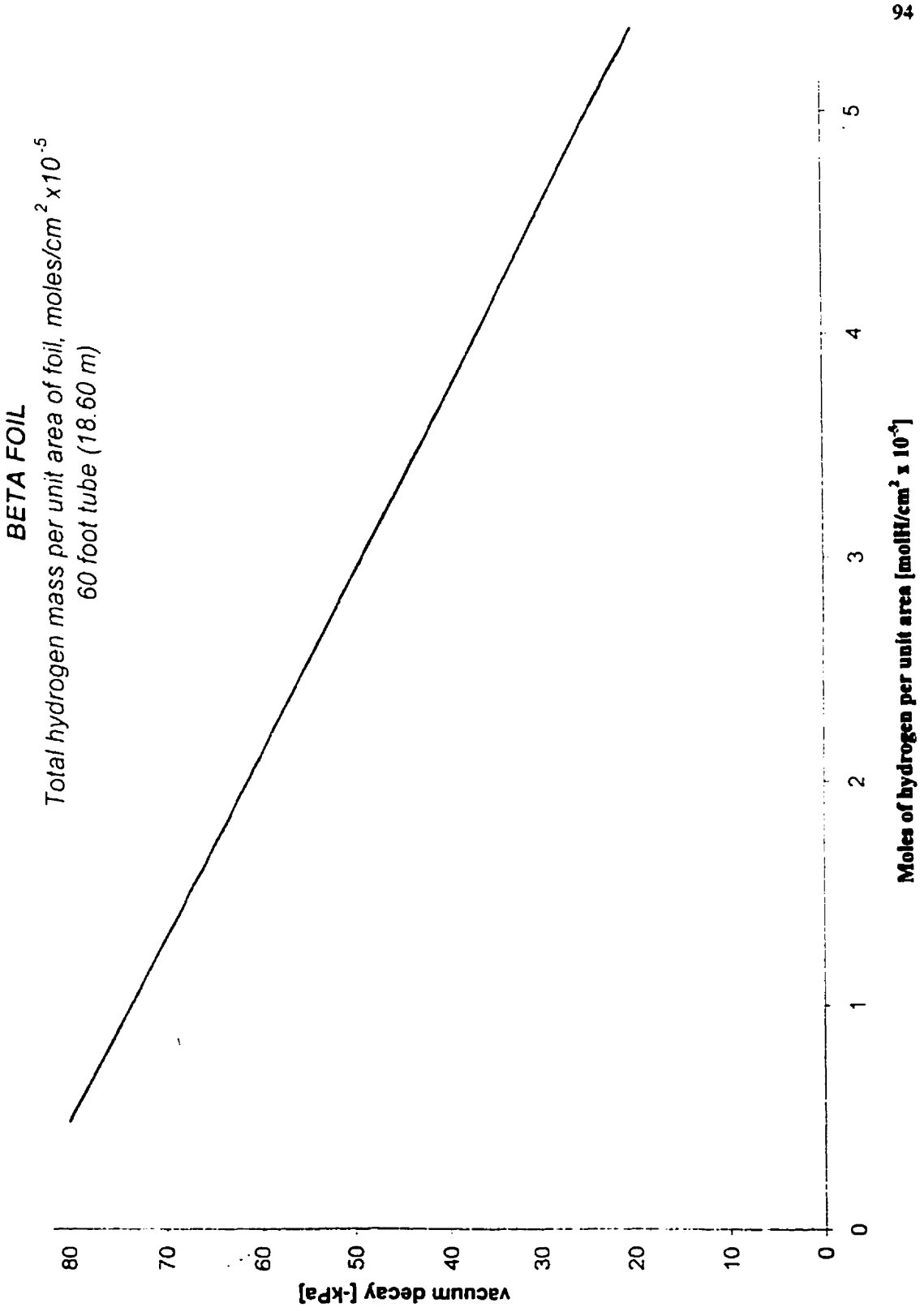

Fig.42: Total hydrogen mass per unit area of foil (60 foot tube).

CHAPTER 5

DISCUSSION

Hydrogen vacuum foil, Beta Foil, proved to be a powerful device for determining whether corrosion exists, the relative magnitude, the changes that occur in the system, and for determining the quantitative amount of hydrogen that is permeating the steel when exposed to a corrosive environment. A comparison between the Beta Foil technique and a conventional electrochemical permeation technique (barnacle electrode) for measuring hydrogen permeation through metals has been made by laboratory experiments on pipeline steel specimens (AISI 1018 steel, in hot rolled condition). Comparison of the results obtained from the two different techniques showed that both give the same transient response, thus a comparison between results obtained is possible. There is a directly comparable response of hydrogen flux measurement between the two techniques. Each technique applies a specific but different gradient in inducing the hydrogen to exit the steel specimen.

Except for this work and some preliminary results presented at various conferences and posted on the Internet [22,85,89-92], also obtained at The University of Calgary, only one another paper on the Beta Foil , by Yepez et. al. [100] has been made available. However, many conclusions drawn by its authors are in contradiction with what has been found from the present work and it is therefore concluded that Yepez at. al. findings are false. It was considered that the length of capillary tube and the thickness of the steel specimen have no significant influence on the response time of the Beta Foil. This is obviously not true and the contrary was demonstrated in the present work. Also, Yepez et. al. observed pressure fluctuations mainly at the end of their experiments. They related these fluctuations to changes in the ambient temperature. In all experiments performed for this present work there were no indications of pressure fluctuations either at the beginning or at the end of the tests. Those fluctuations reported by Yepez et. al. are caused by the fact that the authors induced only a -2 kPa vacuum versus near atmospheric vacuum under the foil. This is in total contradiction with what the manufacturer suggests,

that the vacuum should be re-induced every time it approaches -20 kPa, also demonstrated in this work. Despite the fact that Yepez et. al. found similarities between the vacuum decay vs. time and the hydrogen oxidation current vs. time curves, they found a time delay of about 60 hrs. in the data obtained from the vacuum foil compared to those obtained from the electrochemical permeation technique. This large delay is caused by the fact that for a vacuum "less" than -20 kPa the Beta Foil is fairly insensitive to any changes in the hydrogen flux. This is because the volume under the foil is no longer negligible and the foil is no longer rigid and tight on the steel specimen to be monitored. When switching the environment to a very aggressive (corrosive) one, the results obtained in the present work showed the response time for the two techniques is reasonable comparable and in the order of 13-26 minutes. Finally, Yepez et. al. concluded that it is easy to detect a change in the hydrogen permeation flux using the electrochemical permeation technique, which is not so clear with the vacuum foil. This again is a false conclusion since both methods clearly indicate any changes that occur in the corroding system, both systems being extremely comparable. Again, this false conclusion is drawn due to the fact that only a small vacuum was induced.

Despite being a masterpiece of simplicity as a hydrogen permeation monitoring technique the interpretation of the results obtained using the Beta Foil is extremely complex. There are many factors that have a strong influence on the measurements and all should be taken into consideration. This work was intended to relate the hydrogen vacuum foil measurements and the electrochemical permeation measurements. It establishes a base upon which to build further in understanding of this measurement and monitoring approach. The environmental conditions employed for this work were N_2, H_2S, air, H_2, and Ar gases and as charging solutions NACE, CANMET #1, and CANMET #3 solutions were used. The effect of various poisons on the hydrogen permeation, such as H_2S, As and Se, were also analyzed. A special and complex testing cell was made in order to carry on simultaneous hydrogen permeation measurements using the electrochemical technique (barnacle electrode) and the Beta Foil.

Direct correlations between the vacuum decay and the corrosion rate are difficult to be made. A number of corrosion parameters greatly affect the diffusible hydrogen, as was initially suspected. Those conclusions are not a direct result of this present work but from some corrosion experiments performed in parallel with the hydrogen permeation ones [85,89-91]. The effect of film formation on the steel specimen has a major effect, as does the presence of a poison, such as hydrogen sulfide, H_2S. In addition, the presence of oxygen changes the reduction reaction such that only minimal hydrogen permeates through the material. Thus, direct correlations between the vacuum decay and the corrosion rate can only be made providing the overall mechanism remain constant, which is not necessarily always occuring. However, changes in the corrosion rate are easily identified using the Beta Foil technique even when the corrosion mechanism changes. Thus, the hydrogen vacuum foil technique is very sensitive for comparative changes, but needs specific testing and correlation for establishing quantitative values of corrosion rates. This in turn is only directly applicable for conditions where the corrosion mechanism remains unchanged. This means for absolute corrosion correlations a data base will be needed to be built-up as different material/environment combinations result in different corrosion rates and hydrogen permeation amounts that are not necessarily directly comparable.

One lesson learned from the experiments is that the vacuum foil technique should not be used where oxygen is present in the corroding system. Under aerated environments, where oxygen is present, the hydrogen reduction reaction is no longer the dominant reaction and the measurement of hydrogen permeating through the steel specimen is no longer reflective of the corrosion rate. In aerated conditions the oxygen reduction reaction would be the dominant reaction, not the hydrogen reduction reaction. It is clear that the measurement of hydrogen under aerated conditions is not a sensitive or a good test for indication of corrosion rates or system changes.

It has been clearly shown that a qualitative agreement exists between the transients obtained from the Beta Foil and the barnacle electrode. That is, every time an upset condition occurred in the system, change in the hydrogen evolution was detected in a reasonable amount of time by both techniques. An increase in the hydrogen oxidation

current occurred in the barnacle electrode and an increase in the loss of vacuum (or vacuum pressure differential) occurred in the Beta Foil. The response time for both techniques is dependent upon the environment. When switching from N_2 gas to H_2S gas the response time for the barnacle electrode was found to be 13 minutes (average value), while for the Beta Foil was 23 minutes (average value). This finding is in contradiction to the manufacturer of the Beta Foil, which suggested that the response time is very fast, taking place in seconds. It is obvious that there is a time needed for the hydrogen to permeate through the steel specimen and then to be detected by the pressure transducer. This time, also called breakthrough time, is clearly specimen thickness dependent. It is widely known that the thicker the specimen the greater the breakthrough time. The increasing values of the breakthrough time with increasing the specimen thickness is long known from the literature [10,15,63-66] and this phenomenon has been demonstrated using electrochemical permeation techniques. It is likely that the Beta Foil response time is also specimen thickness dependent. Future investigations will clarify the effect of the specimen thickness on the Beta Foil response time. Another intriguing question is whether this dependence is linear or non-linear. Apparently, considering the same corroding conditions and that no changes occur in the system, that dependence should be fairly linear. However, only future investigations will clearly find an answer to this aspect. This conclusion doesn't mean at all that the Beta Foil technique is less useful than the barnacle electrode. Both techniques are capable of detecting changes in the system in a reasonable amount of time. It must be noted, however, that a true steady-state hydrogen flux is never attained. The hydrogen flux through the steel specimen is not constant, it varies due to the variability in the corrosion reaction and due to the variability in the material. This is indicated by the continuous drop in the hydrogen oxidation current even after long periods of time (>10 days). However, a steady-state condition had been defined when the drop in the oxidation current is equal or less than 1 μA/24 h. The measured currents are extremely small and the barnacle electrode is very sensitive to external factors. For example, every time distilled water was added to the Luggin probe salt bridge system a drop in the current occurred. On the other hand, as shown in Figure 31 (pag.74), and Figure 32 (pag.75), a fairly steady-state condition is detected using the Beta Foil

monitoring technique. After reasonable time since the last change in the system (usually in the order of 3-5 days, depending on the environment) the slope of the vacuum decay versus time curve is relatively constant. Extremely small variations occur sometime because, as mentioned earlier, the variability in the corrosion reaction and in the material. However, these small changes can be neglected when considering a steady-state condition. For example, the vacuum decay rate under N_2 environment in the NACE solution, for the graph illustrated in Figure 31, is 0.48kPa/h after 9 hours from the beginning of the test, 0.53 kPa/h after 22 hours, 0.52 kPa/h after 48 hours, 0.48 kPa/h after 72 hours, and 0.49 kPa/h after 96 hours. This gives an average vacuum decay rate of 0.50 kPa/h, as indicated in Table 4 (pag.62) for test #10. The vacuum decay rate under N_2 environment in the CANMET #3 solution is 1.28 kPa/h after 72 hours from beginning of the test, 1.25 kPa/h after 96 hours, and 1.31 kPa/h after 120 hours. This would give an average vacuum decay rate of 1.28 kPa/h, as indicated in Table 4 for test #13. The vacuum decay rate under H_2S environment in the NACE solution is 7.69 kPa/h after 72 hours from the last change in the environment, 8.04 kPa/h after 156 hours, and 7.32 kPa/h after 180 hours. This would give an average vacuum decay rate of 7.68 kPa/h, as indicated in Table 4 for test #7. Those small variations in the vacuum decay rate shows that a steady-state condition is achieved in the Beta Foil system. When switching back, from H_2S to N_2 the response time is much slower and difficult to be determined for both techniques. This is because there is some time needed for the H_2S to be dissipated out from the solution. However, both techniques will clearly indicate after longer times that a modification in the system occurred.

It must be noted that the datalogger was programmed by the manufacturer to take and store vacuum readings every hour. If this would have been programmed to take readings every minute, more accurate response times for the Beta Foil could have been determined. The response times indicated in Table 2 (page 53) were determined by visual readings of the pressure gage every 5 minutes. Those are not as accurate as pressure transducer (datalogger) values.

The presence of inert gases, such as Ar, N_2, and H_2, have virtually no effect on the hydrogen permeation as detected using the Beta Foil and the barnacle electrode.

No changes in the vacuum loss, or the oxidation current, were detected by the two monitoring techniques when the various gas combinations were introduced into the system. The presence of inert gases, such as Ar and N_2, was expected to have no effect on the hydrogen permeation. Uncertainties existed regarding the presence of extra hydrogen gas into the system. It is possible that atomic hydrogen may exist due to a chemical reaction inside the pipe unrelated to the corrosion process. It was desirable to find out if this so-called extra hydrogen has an effect on the Beta Foil measurements. Experiments clearly demonstrated that the presence of extra gaseous hydrogen in the system, other than that involved in the local corrosion reaction, has no effect on the vacuum decay behavior. This means that the Beta Foil technique measures actual corrosion that is occurring and the measurements are not at all affected by the presence of extra hydrogen gas from other sources.

The Beta Foil measurements are directly affected by the film formation on the exposed side of the steel specimens. When using the NACE solution measurements indicated a higher hydrogen flux in the H_2S environment than in the N_2 environment, as expected. On the contrary, when CANMET #1 solution was used, hydrogen flux was found to be higher in the N_2 environment than in the H_2S environment. This observation was confirmed by the barnacle electrode measurements as well and that is a clear indication that the steel in the CANMET #1 solution has a tendency for film formation, which in turn reduces the hydrogen flux through the specimen. These films are effective barriers to corrosion of the steel, thus reducing hydrogen generation and permeation.

The presence of poisons in the system has a marked effect on the hydrogen entry into the steel specimen. A fairly rapid increase in the hydrogen permeation occurs when H_2S is introduced into the system, that is going from N_2 to H_2S in the NACE solution, as expected. In the CANMET solution, under H_2S environment, a film had formed on the exposed steel specimen, thus leading to a lower hydrogen permeation as compared to the N_2 environment for the same solution. Similar behavior was observed to occur also when As (as sodium arsenite) and Se (as selenious acid) were introduced into the testing cell. For a poison concentration of 600 μg/l a very rapid response occurred (5 minutes for the barnacle electrode and less than 60 minutes for the Beta Foil). Contrary to what was

expected, the presence of As and Se into the system, in NACE solution, led to a drastical reduction of hydrogen permeation. This is likely due to the formation of a film on the exposed steel specimens. Why these films reduce the hydrogen flux through the steel specimen was explained earlier. Once these films are removed (mechanically or chemically) a sudden increase in the hydrogen permeation takes place. The films formed on the steel surface in the NACE solution when As and Se are present are fairly uniform and thick. These findings, confirmed by simultaneous barnacle electrode measurements are in total contradiction with what is known from the available literature that As and Se are effective promoters of hydrogen entry into the steel. In the NACE solution they proved to be very effective inhibitors.

It was found that the barometric pressure is not a parameter that should be monitored or corrected for. It was experimentally demonstrated that the foil is rigid and tight to the steel specimen to be monitored and that there is practically no volume under the foil up to a vacuum of -20 kPa. The steel structure to be monitored (pipeline, pressure vessel) is also rigid, as well as the capillary tube. Practically, variations of barometric pressure have no influence on the hydrogen vacuum foil measurements.

One other parameter that needs to be accounted for is the temperature. The temperature is expected to have a marked effect on the hydrogen measurements. Despite the fact that, theoretically, the total amount of hydrogen permeating through the steel specimen could be calculated at virtually any temperature (by knowing the volume of the whole system and by using the general gas law) the corrosion rate (hydrogen generation) and the hydrogen permeation are very much influenced by the temperature. Future investigations will also clarify this important aspect.

As mentioned earlier, the specimen thickness appears to have an influence on the Beta Foil response time. This is an important parameter that needs to be investigated as well. The effect of the temperature and specimen thickness on the hydrogen permeation was not analyzed in the present work.

In order to obtain accurate measurements the vacuum under the Beta Foil should be maintained "above" -20 kPa. For "lower" vacuum the Beta Foil is fairly insensitive to the changes that occur in the system. The volume under the foil is now detectable and this

would clearly lead to inaccuracies in the measurements. Also, the general gas law cannot readily be applied anymore since the volume of the system is no longer constant.

It was found that the length of the capillary tube has a significant influence on the Beta Foil measurements. Different lengths employed lead to different slopes of the vacuum decay vs. time, both in N_2 and H_2S environments. However, it is obvious that the amount of hydrogen permeating through the steel specimen is a function of the material and the environmental conditions and not a function of the capillary tube length. For obtaining comparable and accurate measurements using the Beta Foil technique is it necessary for the equipment to be calibrated with respect to the total volume being present. This is necessary if quantitative values of hydrogen amount are required to be calculated. The sensitivity of the Beta Foil measurements is strongly affected by the capillary tube length. The shorter the tube, the more precise the measurements. The ideal case would be that in which the pressure transducer is affixed directly onto the foil without any capillary tube involved.

By knowing the volume of the system (tree, transducer, capillary tube) and by using the general gas law the total amount of hydrogen that is permeating through the steel specimen can be easily and accurately obtained. It was demonstrated that the volume under the foil is negligible up to a vacuum of -20 kPa. However, for obtaining comparable results the equipment needs to be calibrated.

The hydrogen vacuum foil technique can be also used in sweet service (i.e., no H_2S present). Contrary to the general belief, a measurable hydrogen flux is generated in sweet service.

Comparing to the electrochemical permeation techniques, the hydrogen vacuum foil technique exhibits two major advantages: it is extremely easy to be applied and to be operated both in the filed and in the laboratory, and the vacuum decay can be directly correlated with the amount of hydrogen that is permeating through the steel specimen. Another advantage is that the vacuum foil technique monitors a larger area of the structure than the barnacle electrode, thus is more representative for monitoring changes that occur in the corroding system A correlation is not seen to occur at this present time between the vacuum decay rate and the electrochemical hydrogen oxidation current. This

is mainly due to the fact the hydrogen oxidation current measured with the barnacle electrode method is not constant over long period of time. On the other hand, as mentioned earlier, after reasonable time after a change in the system the vacuum decay rate attains a steady-state condition. The vacuum decay was found to depend upon environment, corrosion mechanism, and the presence of poisons, as expected. Measurements indicate a somewhat slower response time for the Beta Foil as compared to the barnacle electrode, although both are reasonably comparable.

The Beta Foil technique is an excellent qualitative tool in determining changes that occur in a corroding system. This work proved that it can be also used as a quantitative device to determine the amount of hydrogen resulting from the corrosion reactions.

A major drawback of the Beta Foil technique is the limitation of its use in aerated conditions. Also, the foil is very sensitive to the quality of the peripheral sealing. Even small leaks, hard to be detected when the foil is applied in the field, can modify significantly the shape of the vacuum decay versus time curve, thus leading to erroneous interpretation of the corrosion severity. The presence of even small leaks will clearly lead also to errors in the calculation of the total amount of hydrogen that permeates the specimen. The response times could not be determined very accurately since the datalogger is limited to take readings only every hour, and not at smaller intervals of times. Another area where improvement is needed is in making the datalogger software (LS-4 Datalogger version 4.3X) and the graphing software (Betaworks 32) more user friendly. The data recovered from the datalogger can be plotted utilizing a 0-100 kPa on the vertical axis and the time on the horizontal axis of the graph. This way the trending shows a slope. The line will be perfectly horizontal when corrosion is zero (no hydrogen flux exists). However, in some systems a certain amount of hydrogen flux can represent a perfectly acceptable corrosion rate.

This work examined the effect of various parameters on the operation of the hydrogen vacuum foil technique. Based upon these results, the hydrogen vacuum foil technique of monitoring corrosion conditions is extremely sensitive. It has relatively short response times to changing corrosion conditions. An important work has been laid down

laid down with respect to sorting and correlating the interaction of operating and system parameters for this technique.

Hydrogen Vacuum Foil technique proved to be a powerful device for determining whether corrosion exists and the relative magnitude. The concept of using this technique is applied generally both in the field and in the laboratory except in deaerated conditions, as previously discussed. The data itself generated in this work cannot be used directly. First, because real life situations cannot be exactly reproduced by any means in the laboratory. Any other material-environment combinations will clearly led to different values of the vacuum decay than the ones presented in this work that are not necessarily comparable. Also, as it is generally known, mass transport and fluid velocity affects the corrosion rate, hence the hydrogen flux. In real situations the fluid velocity is obviously different than the one provided by the circulating pump in the testing cell in the present research program (15.89L/min). Corrosion rates (hydrogen fluxes) will be different even the same material and same environmental conditions are employed. However, a general correlation between the vacuum decay, kPa/h, and the corrosion rate in mills per year, mpy, is given in the Table 6. It is important to note that this chart is a general guideline only. System experience will ultimately provide the greatest interpretation accuracy.

Vacuum loss [kPa/h]	***Relative corrosion***	***Aprroximate mpy***
0.0013-0.013	very slight	0 to 5
0.013-0.27	moderate	5 to 30
0.27-1.38	high	30 to 100

Table 6: General correlation between the vacuum decay rate and the corrosion rate

CHAPTER 6

CONCLUSIONS AND FUTURE INVESTIGATIONS

6.1. Conclusions

Based on the results obtained and presented in this work, the hydrogen vacuum foil technique for monitoring corrosion conditions is one of the most sensitive technique available today. It has relatively short response times to changing corrosion conditions and it is sensitive in detecting even small changes in the corroding system. The vacuum decay is a responsive parameter that directly relates the hydrogen flux, which in turn is in a complex manner related to the changes in the corroding system. Ground work has been laid down with respect to sorting and correlating the interaction of operating and system parameters for this technique.

Several important conclusions can be drawn based on the experiments and results obtained from this present work:

- Beta Foil technique is very sensitive to any changes that occur in a corroding system.
- Beta Foil technique doesn't measure the corrosion rates, but relative changes in the corrosion rates.
- Except for periodic re-inducing vacuum, Beta Foil is maintenance free and extremely simple to operate.
- Beta Foil technique offers an excellent qualitative evolution of corrosion activity and hydrogen flux permeation.
- Beta Foil technique also offers a quantitative evaluation of the total amount of hydrogen permeating through the material investigated.
- Vacuum decay rate is a parameter that directly relates to the hydrogen flux.
- There are comparable responses of hydrogen flux measured by the Beta Foil and the barnacle electrode. Despite this, at this point there is no correlation between the vacuum decay rate and the hydrogen oxidation current.

- Because the corrosion mechanism is not constant a correlation between the vacuum decay and the actual corrosion rate is very difficult to be obtained.
- The Beta Foil measurements are directly affected by the film formation on the exposed steel specimens and by the presence of poisons.
- Inert gases appear to have virtually no influence on the Beta Foil measurements.
- The hydrogen pick-up rate and permeation are a function of the solution inside the testing cell and the material to be investigated.
- The hydrogen flux detected by the Beta Foil is not constant, it varies due to the variability in the corrosion reaction and due to the variability in the specimen.
- The hydrogen vacuum technique should not be used where oxygen is present in the corroding system.
- In order to obtain accurate measurements the vacuum under the Beta Foil should be maintained "above" -20 kPa.
- The Beta Foil measurements are not affected by variations in the barometric pressure.
- When determining the total amount of hydrogen that is permeating through the material a factor that needs to be controlled or compensated for is the tube capillary length and/or instrumentation volume.
- The Beta Foil technique is very sensitive for comparative changes but needs specific testing, correlation, and calibration for establishing of absolute corrosion rates.
- For absolute corrosion correlation a database is needed to be constructed as different material/environment combinations result in different corrosion rates and hydrogen permeation amounts that are not necessary directly comparable.

Without being directly related to the investigation on the Beta Foil technique two other major conclusions are drawn from this present work:

- A polyurethane base coating with recycled rubber additions proved to exhibit excellent resistance to the aggressive action of the very corrosive environments that were employed, compared to a Teflon coating.

- Contrary to the general belief, As (as sodium arsenite) and Se (as selenious acid) proved to be excellent inhibitors to the hydrogen entry into the steel in the NACE solution.

6.2. Future Investigations

Efforts were made in order to find out and sort out the effect of many initial parameters that have or might have an influence on the hydrogen vacuum foil technique. However, there are still some that were not investigated or sorted out. The extent of the exploratory nature of this study suggests the following additional work:

- Analysis of the temperature effects on the Beta Foil measurements.
- Analysis of the specimen thickness influence on the response time.
- Calibration of the equipment, namely the capillary tube length.
- To find a correlation between the vacuum decay rate and the hydrogen oxidation current.
- To find a correlation between the corrosion rate and the vacuum decay.
- To carry on experiments in order to find out if the Beta Foil technique is suitable also for stainless steel, aluminum, and aluminum-base alloys.
- To build-up a database with corrosion rates and hydrogen permeation amounts for different material/environment combinations. However, those tasks would require several years of continuing testing.

REFERENCES

1. Raymond, K., "The Many Faces of Hydrogen Embrittlement", ASTM Standartization News, pp.40-43, October (1996).
2. Timmins, P.F., Solutions to Hydrogen Attack in Steels, ASM International, Materials Park, Ohio, USA (1997).
3. Yao, J., Cahoon, J.R., "Theoretical Modeling of Grain Boundary Diffusion of Hydrogen and Its Effects on Permeation Curves", Acta Metallurgica et Materialia, Vol.39, No.1, pp.111-118 (1991).
4. Nelson, H.G. (1983), "Hydrogen Embrittlement", Treatise on Materials Science and Technology: Hydrogen Embrittlement, C.L. Briant, S.K. Banerji eds., Academic Press, New-York, USA, Vol.25, pp.275-361 (1983).
5. Wipf, H., "Diffusion of Hydrogen in Metals", Topics in Applied Physiscs: Hydrogen in Metals III, Springer Verlag, Berlin-Heidelberg, Germany, Vol.73 (1997).
6. Peist, H., "Lattice Strains due to Hydrogen in Metals", Topics in Applied Physics: Hydrogen in Metals I, Springer Verlag Berlin-Heidelberg-New-York, Vol.28 (1978).
7. Tuyen, D.L., "Effects of Hydrogen on Micro-Twinning in a Fe-Ti-C Alloy", Acta Metallurgica et Materialia, Vol.41, No.12, pp.3363-3379 (1993).
8. DeLuccia, J.J., "Electrochemical Aspects of Hydrogen in Metals", Hydrogen Embrittlement: Prevention and Control, L. Raymond ed., ASTM, Philadelphia, USA, pp.17-34 (1988).
9. "Henri Cailletet", http://www.144.26.13.41./physists/cailletl.html.
10. Kiuchi, K., McLellan, R.B., "Solubility and Diffusivity of Hydrogen in Well-Annealed and Deformed Iron", Acta Metallurgica et Materialia, Vol.31, p.961 (1983).
11. Brown, G.K., Freeman, B., "Pipeline Internal Corrosion Monitoring Using Beta Foil Hydrogen Permeation Probes", Proceedings Prevention of Pipeline Corrosion Conference, Houston, USA, pp.1-6, October (1994).
12. "Beta Foil", http://www.dbs2.com/beta/foil.html.
13 "The Beta Foil as Hydrogen Flux Monitor Hydrogen in Steel", http://www.dvr.corp.com/dc_frame.html.

14. Kane, R.D., "Corrosion Monitoring for Industrial and Process Applications", http://www.clihouston.com/cormont8.html.

15. Milion, A, Milion, C., Hidrogenul in oteluri si in imbinari sudate, Editura Academiei, Bucuresti, Romania (1968).

16. Kumnick, A.J., Johnson, H.H., "Hydrogen Transport Through Annealed and Deformed Armco Iron", Metallurgical Transactions, Vol.5, pp.1199-1206 (1974).

17. Volkl, J., Alefeld, G., Diffusion in Solids, A.S. Nowick, J.J. Burton eds., Academic Press, New-York, USA, Chapter 5 (1975).

18. Matei, D.G., Shaw, W.J.D., Hydrogen Diffusivity in Materials, special report, The University of Calgary, Calgary, Canada, November (1998).

19. Matei, D.G., Shaw, W.J.D., Hydrogen Permeation and Equivalency Factors, special report, The University of Calgary, Calgary, Canada, May (1997).

20. Matei, D.G., Shaw, W.J.D., "Hydrogen Permeation and Equivalency Factors", to be published (1999).

21. Matei, D.G., Aspects of Hydrogen Embrittlement in Steels, special report, The University of Calgary, Calgary, Canada, August (1998).

22. Matei, D.G., Shaw, W.J.D., unpublished work (1999).

23. Astaf'ev, A.A., "Some Regular Features of Hydrogen Embrittlement of Structural Alloys", Metal Science and Heat-Treatment, Vol.39, No.1-2, pp.49-52 (1997).

24. DeLuccia, J.J., Berman, D.A., "An Electrochemical Technique to Measure Diffusible Hydrogen in Metals (Barnacle Electrode)", Electrochemical Corrosion Testing, F. Mansfeld, U. Bertocci eds., ASTM, Philadelphia, USA, pp.256-273 (1981).

25. Pasco, R.W., Ficalora, P.J., "Entry of Hydrogen from the Gas Phase", Hydrogen Degradation of Ferrous Alloys, R.A. Oriani, J.P. Hirth, M. Smialowski eds., Noyes Publications, Park Ridge, USA, pp.199-215 (1985).

26. Wedler, G., "Kinetics of Adsorption of Hydrogen onto Iron Alloys from the Gas Phase", Hydrogen Degradation of Ferrous Alloys, R.A. Oriani, J.P. Hirth, M. Smialowski eds., Noyes Publications, Park Ridge, USA, pp.180-197 (1985).

27. Shanabarger, M.R. et. al., "Influence of Hydrogen Chemisorption Kinetics on the Interpretation of Hydrogen Transport Through Iron Membranes", Scripta Metallurgica, Vol.15, pp.929-933 (1981).

28. Marcus, P., Oudar, J., "Gas-Iron Surface Equilibria", Hydrogen Degradation of Ferrous Alloys, R.A. Oriani, J.P. Hirth, M. Smialowski eds., Noyes Publications, Park Ridge, USA, pp.36-71 (1985).

29. Tromans, D., "On Surface Energy and the Hydrogen Embrittlement of Iron and Steels", Acta Metallurgica et. Materialia, Vol.42, No.6, pp.2043-2049 (1994).

30. Jerkiewicz, G., Zolfaghary, A., "Comparison of Hydrogen Electroadsorption from the Electrolyte with Hydrogen Adsorption from the Gas Phase", Journal of Electrochemical Society, Vol.143, No.4, pp.1240-1249 (1996).

31. Zachroczymski, T., "Entry of Hydrogen into Iron Alloys from the Liquid Phase", Hydrogen Degradation of Ferrous Alloys, R.A. Oriani, J.P. Hirth, M. Smialowski eds., Noyes Publications, Park Ridge, USA, pp.215-247 (1985).

32. Gao, L., Conway, B.E., "Absorption and Adsorption of Hydrogen into the Hydrogen Evolution Reaction and the Effects of Co-Adsorbed Poisons", Electrochimica Acta, Vol.39, No.11/12, pp.1681-1693 (1994).

33. Wilde, B.E., Kim, C.D., "Hydrogen Adsorption on Steels Undergoing Corrosion with Hydrogen Evolution", Corrosion, Vol.42, No.4, pp.243-244 (1986).

34. Kaesche, H., Metallic Corrosion, NACE, Houston, USA (1985).

35. Macdonald, D.D., "The Electrolyte-Iron Interface", Hydrogen Degradation of Ferrous Alloys, R.A. Oriani, J.P. Hirth, M. Smialowski eds., Noyes Publications, Park Ridge, USA, pp.78-110 (1985).

36. Huang, H., Shaw, W.J.D., "Cold Work Effects on SCC of Pipeline Steel Exposed to Sour Environments", Corrosion Science, Vol.34, No.1, pp.61-78 (1993).

37. Smialowski, M., Hydrogen in Steel, Pergamon Press, Oxford, UK (1962).

38. Kane, R.S., "Effects of H_2S on the Behavior of Engineering Alloys: A Review of Literature and Experience", http://www.intercorr.com/htopics.html.

39. Berkowitz, B.J., Heubaum, F.H., "The Role of Hydrogen in Stress Corrosion Cracking in Low Alloy Steels", Corrosion, Vol.40, No.5, pp.537-545 (1989).

40. Asahi, H. et.al., "Prediction of Stress Corrosion Cracking in High-Strength Tubulars", Corrosion, Vol.50, No.7, pp.537-545 (1994).

41. Eckert, W., "Electrochemical Identification of the H_2S System Using A pH_2S (glass/Ag^0,Ag_2S) Electrode", Journal of Electrochemical Society, Vol.145, No.1, pp.77-79 (1998).

42. Shanabarger, M.R., "A Comparison of Adsorption Kinetics of iron in H_2 and H_2S, Hydrogen Effects in Metals, I.M. Bernstein, A.W. Thompson eds., Metallurgical Society of AIME, Warrendale, USA, pp.135-142 (1983).

43. Wu, Y.M., "Applying Process Modeling to Screen Refinement Equipment for Wet H_2S Service", Corrosion, Vol.54, No.2, pp.169-173 (1998).

44. Wilhelm, S.M., Abayarathma, D., "Inhibition of Hydrogen Absorption by Steels in Wet H_2S Refinery Environments", Corrosion, Vol.50, No.2, pp.152-159 (1994).

45. Radhakrishnan, T.P., Shreir, L.L., "Permeation of Hydrogen Through Steel by Electrochemical Transfer. I-Influence of Catalytic Poisons", Electrochimica Acta, Vol.11, pp.1007-1021 (1966).

46. Zachroczymski, T. et.al., "Evolution and Entry of Hydrogen into Iron During Cathodic Charging in Alkaline Solutions with Ethylenediaminetetraacetic Acid", Journal of Electrochemical Society, Vol.145, No.4, pp.1142-1148 (1998).

47. Martin, R.L., "Inhibition of Hydrogen Permeation in Steels Corroding in Sour Fields", Corrosion, Vol.49, No.8, pp.694-704 (1993).

48. Nathan, C.C., Corrosion Inhibitors, 5^{th} ed., NACE, Houston, USA (1981).

49. Duarte, H.A. et.al., "The Effects of Organic Compounds on Inhibition of Hydrogen Permeation Through a Mild Steel Membrane", Journal of Electrochemical Society, Vol.144, No.7, pp.2313-2317 (1997).

50. Popov, B.N. et.al., "Surface Treatment for Inhibition of Corrosion and Hydrogen Penetration of Type 718 Alloy", Corrosion, Vol.50, No.8, pp.613-618 (1994).

51. Coleman, D.H. et.al., "The Effects of Multiple Elecrodeposited Zinc Layers on the Inhibition of Hydrogen Permeation Through an Iron Membrane", Journal of Electrochemical Society, Vol.143, No.6, pp.1871-1874 (1996).

52. Jones, D.A., Principles and Prevention of Corrosion, 2nd ed., Prentice-Hall, Upper Saddle River, USA (1996).

53. Stone, J.M., "Deuterium Permeation and Surface Effects", Environmental Degradation of Engineering Materials in Hydrogen, Virginia Polytechnic Institute, Blacksburg, USA, pp.83-100 (1981).

54. Kuhn, D.C., Shanabarger, M.R., "The Modelling of Gas Phase Permeation Through Iron and and Nickel Membranes", Hydrogen Effects on Materials Behavior, N.R. Moody, A.W. Thompson eds., TMS, Warrendale, USA, pp.33-42 (1989).

55. Bruzzoni, P., Garavaglia, R., "Anodic Iron Oxide Films and Their Effect on Hydrogen Permeation Through Steel", Corrosion Science, No.11, pp.1797-1807 (1992).

56. Marichev, V.A., Molokanov, V.V., "Effect of Formation of Surface Hydroxide on Hydrogen Permeability of Iron Membranes and Hydrogen Embrittlement of High-Strength Steels", translated from Fiziko-Khimicheskaya Mekhanita Materialov, No.3, pp.31-37 (1992).

57. Heubaum, F.H., Berkowitz, B.J., "The Effect of Surface Oxides on the Hydrogen Permeation Through Steels", Scripta Metallurgica, Vol.16, pp.659-662 (1982).

58. Townsend, H.E., "Effects of Zinc Coatings on the Stress Corrosion Cracking and Hydrogen Embrittlement of Low-Alloy Steel", Hydrogen in Metals, I.M. Bernstein, A.W. Thompson eds., ASM, Warrendale, USA, pp.223-233 (1974).

59. Chen, C.L. et.al., "The Use of Zinc and Tin Coatings and Chemical Additives for Preventing Hydrogen Embrittlement in Steel", Corrosion: Prevention and Control, pp.71-74, June (1993).

60. Murray, G.T. et.al., "Retardation of Hydrogen Embrittlement of 17-4 PH Stainless Steel by Nonmetallic Surface Layers", Metallurgical Transactions, Vol.18A, pp.162-164 (1987).

61. "AlumiPlate: Plating with Aluminum", http://www.alumiplate.com/html/body_embrittlement.com.

62. McNabb, A., Foster, P.K., "A New Analysis of the Diffusion of Hydrogen in Iron and Ferritic Steels", Transactions Meatllurgical Society of AIME, Vol.227, pp.618-627 (1963).

63. Hutchings, R.B. et.al., "Ratio of Specimen Thickness to Charging Area for Reliable Hydrogen Permeation Measurements", British Corrosion Journal, Vol.28, No.4, pp.309-312 (1993).

64. Devanathan, M.A.V., Stachurski, Z., "The Adsorption and Diffusion of Electrolytic Hydrogen in Palladium", Proceedings of Royal Society, Vol.A270, pp.90-102 (1962).

65. Devanathan, M.A.V., Stachurski, Z., "A Technique for the Evaluation of Hydrogen Embritlement Characteristics of Electroplating Baths", Journal of Electrochemical Society, Vol.110, pp.886-890 (1963).

66. Boes, N., Zuchner, H., "Electrochemical Methods for Studying Diffusion, Permeation, and Solubility of Hydrogen in Metals", Journal of Less-Common Materials, Vol.49, pp.223-240 (1976).

67. Casanova, T., Crousier, J., "The Influence of An Oxide Layer on Hydrogen Permeation Through Steel", Corrosion Science, Vol.38, No.9, pp.1535-1544 (1996).

68. Casanova, T., Crousier, J., "Study of the Passive Layer on Steel by Hydrogen Permeation", http://www.intercorr.com/intercorr/techsess/papers/session4/abstracts/casanova.html.

69. Shaw, W.J.D. et.al., "Parameters Affecting Electrochemical Hydrogen Permeation Measurements", paper no. 392, Proceedings NACE Corrosion '98 Conference, San-Diego, USA, pp.392/1-392/11, March (1998).

70. Shaw, W.J.D. et.al., "Required Environmental Test Procedures for Making Representative Materials Service Evaluations", Materials Performance: Sulphur and Energy, CIM, pp.195-208 (1992).

71. Shaw, W.J.D. et.al., "A Permeable Hydrogen Measurement Calibration Method", paper presented at NACE Western Regional Conference, Victoria, Canada, February (1998).

72. Shaw, W.J.D., Standard for Hydrogen Permeation Measurements, first draft, The University of Calgary, Calgary, Canada, May (1996).

73. Shaw, W.J.D., Matei, D.G., Fundamental and Applied Studies of Hydrogen Embritlement, special report, The University of Calgary, Calgary, Canada, September (1998).

74. Pressouyre, G.M., "The Role of Trapping on Hydrogen Transport and Embrittlement", Ph.D. Thesis, Carnegie-Mellon University, Pittsburgh, USA (1977).

75. "Hydrogen Embrittlement", http://www.intercorr.com/testing/he.html.

76. "Hydrogen Permeation Monitoring", http://www.bakerhughes.com/bapt/ref.hcp.html.

77. Manolatos, P. et.al., "The Electrochemical Permeation of Hydrogen in Palladium. Boundary Conditions During a Galvanostatic Charging Under Low Charging Current Densities", Corrosion Science, Vol.31, No.11, pp.1797-1807 (1995).

78. Surkein, M., Heidersbach, R., "Hydrogen Permeation in Iron at Low Temperatures", Advanced Techniques for Characterizing Hydrogen in Metals, N.F. Fiore, B.J. Berkowitz eds., Metallurgical Society of AIME, Warrendale, USA, pp.119-131 (1982).

79. Berman, D.A. et.al., "The Determination of Hydrogen in High-Strength Steel Structures by an Electrochemical Technique", Hydrogen in Metals, I.M. Bernstein, A.W. Thompson eds., ASM, Warrendale, USA, pp.595-607 (1974).

80. Berman, D.A., Agarwala, V.S., "The Barnacle Electrode Method to Determine Diffusible Hydrogen in Steels", Hydrogen Embrittlement: Prevention and Control, L. Raymond ed., ASTM, Philadelphia, USA, pp.98-104 (1988).

81. Lucas, K.A., Robinson, M.J., "The Influence of Lattice Hydrogen Content on the Hydrogen-Assisted Cracking of High-Strength Steel", Corrosion Science, Vol.26, no.9, pp.705-717 (1986).

82. Mansfeld, F: Final Report, Contract N62268-77-c-0351, Naval Air Development Center, Warminster, USA, pp.2-3 (1979).

83. Brown, G.K., "External Hydrogen Sensor Monitors Internal Pipe Corrosion- Part 3", Pipe Line & Gas Industry, pp.29-32, June (1996).

84. Beta Foil Operating Manual, Beta Corporation, Calgary, Canada, January (1995).

85. Shaw, W.J.D., Matei, D.G., "Hydrogen Flux Measurements and Relationships to Corrosion", paper presented at International Pipeline Conference, IPC'98, Calgary, Canada, June (1998).

86. Betalogger Software, Beta Corporation, Calgary, Canada (1996).

87. Brown, G.K., "Traditional Corrosion Monitors Have Their Uselfulness- Part 2", Pipe Line & Gas Industry, pp.53-56, April (1996).

88. Shaw, W.J.D., Bizon, A., Fundamental and Applied Studies of Hydrogen Embrittlement, special report, The University of Calgary, Calgary, Canada, (1996).

89. Shaw, W.J.D., Jayasinghe, D.M., Matei, D.G., "Correlations Between Corrosion, Electrochemical Hydrogen Flux and A Vacuum Foil Technique", Proceedings at NACE Corrosion '98 Conference, San-Diego, USA, pp.391/1-391/12, March (1998).

90. Shaw, W.J.D., Jayasinghe, D.M., Matei, D.G., "Correlations Between Corrosion, Electrochemical Hydrogen Flux and A Vacuum Foil Technique", http://www.dvcorp.com/dc_frame.html?ongoing_research.

91. Shaw, W.J.D., Matei, D.G., Jayasinghe, D.M., "Effects of Various Parameters on Vacuum Induced Hydrogen Flux", paper presented at NACE Western Region Conference, Victoria, Canada, February 16-19 (1998).

92. Shaw, W.J.D., Matei, D.G., Limits and Correlations of Vacuum Induced Hydrogen Flux in Corrosive Environments, Final Report, The University of Calgary, Calgary, Canada, July (1998).

93. Cutnell, J.D., Johnson,K.W., Physics, 3rd ed.,Vol.1, p.426, John Wiley & Sons, New-York, USA (1995).

94. Hydrogen: Its Technology and Implications, Vol.IV, Utilization of Hydrogen, CRC Press Inc., Boca Raton, USA (1979).

95. Sistemul International de Unitati (SI), Editura Tehnica, Bucuresti, Romania (1965).

96. "Conversion Tables", http://www.economatics.co/uk/sprint/textversion1.html.

97. "SNIP SI Unit Conversion Factors", http://www.snip.com/brodes/sysinter/factors.html.

98. "Useful Conversions",
http://www.webug.physics.uiuc.edu/courses/phys100/conversion.html.
99. "Units and Conversion Factors", http://www/pxpower.com/convers.html.
100. Yepez, O., et.al., "A Comparison Between An Electrochemical And A Vacuum Loss Technique As Hydrogen Probes for Corrosion Monitoring", Corrosion/97, paper no.272, NACE International, Houston, USA (1997).